5
Molecular Gels – Nanostructured Soft Materials

David K. Smith

5.1
Introduction to Molecular Gels

It seems increasingly likely that *nanochemistry* will underpin manufacturing technology in the 21st century, with the ability to control structure and morphology at the nanometer level allowing the synthesis of a new generation of smart materials [1]. As such, the use of organic building blocks, which can *self-assemble* into nanoscale architectures, offers a simple approach to the spontaneous generation of nanomaterials. Of particular interest in this regard has been the rapid development of *gel-phase materials* constructed via the hierarchical assembly of molecular building blocks; indeed, over the past 15 years, there has been an explosion of publications dealing with the self-assembly of organic molecules into nanostructured gels in a variety of solvents [2]. In 2006, an excellent book, edited by Terech and Weiss, was published dealing with the topic in a comprehensive manner [3]. This chapter makes no attempt to reproduce a comprehensive coverage of the topic, but instead intends to provide a "primer" which will act as an accessible overview and summarize the following issues:

- What is a molecular gel?
- How can molecular gels be prepared?
- How can molecular gels be studied?
- What kind of molecules assemble into molecular gels and why?
- What are the applications, both real and potential, of molecular gels?

By answering these questions, it is hoped that this chapter will provide a useful overview for the non-specialist reader, in addition to offering new insights for those well acquainted with the field.

Gels are a well-known colloidal state of matter and are familiar to us in everyday life (hair gel, toothpaste, cleaning products, air fresheners, contact lenses, foodstuffs, etc.). However, perhaps surprisingly, an accurate definition of the gel state remains

Organic Nanostructures. Edited by Jerry L. Atwood and Jonathan W. Steed

ISBN: 978-3-527-31836-0

somewhat elusive. In the simplest terms, Dorothy Jordan Lloyd's definition from the 1920s (paraphrased as "if it looks like 'Jell-O' – it must be a gel") is easy to use on a macroscopic level [4]. However, more useful in terms of visualizing the structure of a gel on a molecular level was her additional statement ". . . they must be built up from two components, one of which is a liquid at the temperature under consideration and the other of which, the gelling substance proper . . . is a solid". Indeed, it is usually argued that in gels, a "solid-like" network is able to "immobilize" the flow of bulk "liquid-like" solvent [5].

Most of the gels familiar from everyday life are constructed from polymers and as such are not strictly "molecular" gels. In polymer gels, crosslinking between polymer chains (either covalent or noncovalent) gives rise to an entangled network, which constitutes the "solid-like" phase. The "liquid-like" solvent is primarily located in pores within the crosslinked network, in addition to solvating the polymer chains. It is worth noting that on the *molecular level*, the solvent is mobile within the gel-phase network [4]; flow of the bulk solvent is only prevented as a consequence of capillary forces and some solvent–gelator interactions. This leads to one of most striking visual properties of gels – when placed in an inverted vial, liquid is unable to flow out of the material under the force of gravity, in spite of the high liquid content (Figure 5.1). Indeed, this simple test is one of the best ways of rapidly identifying a new gelator in addition to performing basic characterization (see Section 5.3.1).

It is relatively straightforward to see how entangled polymer chains can yield gel-phase materials, but it is more difficult to understand how low molecular weight molecules can achieve gelation – so-called molecular gels. The concept of low molecular weight compounds causing viscosity modification is not new – molecular gels based on simple organic building blocks (e.g. fatty acid salts) were first recognized in the 19th century [6]. However, the recent academic interest has

Figure 5.1 Photograph of a typical gel.

coincided with the ready availability of imaging techniques able to visualize objects on the nanometer length scale. Electron microscopy in particular has allowed researchers to observe gel-phase materials on the nanoscale. In turn, this has enhanced the understanding of the way in which low molecular weight systems can achieve gelation and improved the ability of researchers to study the effect of molecular structural change on the gelation process.

It has recently become well understood that self-assembly processes underpin the formation of molecular gel-phase materials. Intermolecular interactions, such as *hydrogen bonding*, *π–π stacking*, *van der Waals interactions* and *solvophobicity* are able to encourage the assembly of molecular building blocks in a one-dimensional manner. Such a process can be considered as a *supramolecular polymerization* [7], i.e. the polymers formed are held together solely by noncovalent interactions between building blocks. These supramolecular polymers may then be able to form entangled networks and hence give rise to gelation. The process of gelation is often described as *hierarchical* and depends on a number of steps:

1. Molecule interacts with adjacent molecule to form a dimer.
2. Dimers interact to form oligomers.
3. Oligomers extend into supramolecular polymer *fibrils*, which have approximately the same width as the molecular building block (e.g. 1–2 nm wide).
4. Fibrils bundle together to form *fibers* (often ca. 20–50 nm wide).
5. Fibers interact to form an *interconnected sample spanning network*. These fiber–fiber interactions are one of the least well-characterized and understood aspects of molecular gels.
6. Sample spanning network "immobilizes" solvent.

It should be noted that in different cases, the levels of hierarchical assembly may be expressed slightly differently; however, some degree of hierarchy is always assumed – two examples from the literature are illustrated in Figure 5.2. One of the most fascinating features of molecular gels is that very small amounts of gelator often achieve complete solvent "immobilization" and this demonstrates the power of hierarchical assembly. Typically, molecular gels contain $<2\%$ w/v gelator. Molecules which achieve gelation at concentrations $<1\%$ w/v are sometimes described as "*supergelators*".

There is clearly a relationship between gelation and *crystallization*, as in both cases a solid-like component assembles in a liquid-like phase as a consequence of multiple noncovalent interactions. However, in gelation, the solid-like network is compatible with the solvent and remains solvated and hence does not fully phase-separate. As such, gelation can be considered to be a competition between solubilization and phase separation. Furthermore, in gelation, the assembly process is *directional* – i.e. unlike a crystallization process, aggregation does not occur in three dimensions; in gels the growth of the supramolecular polymer is usually one dimensional.

Perhaps one of the key advantages of materials based on low molecular weight building blocks is their *reversibility*. Unlike a covalently crosslinked polymer network, molecular gels can be broken down into their individual molecular building blocks

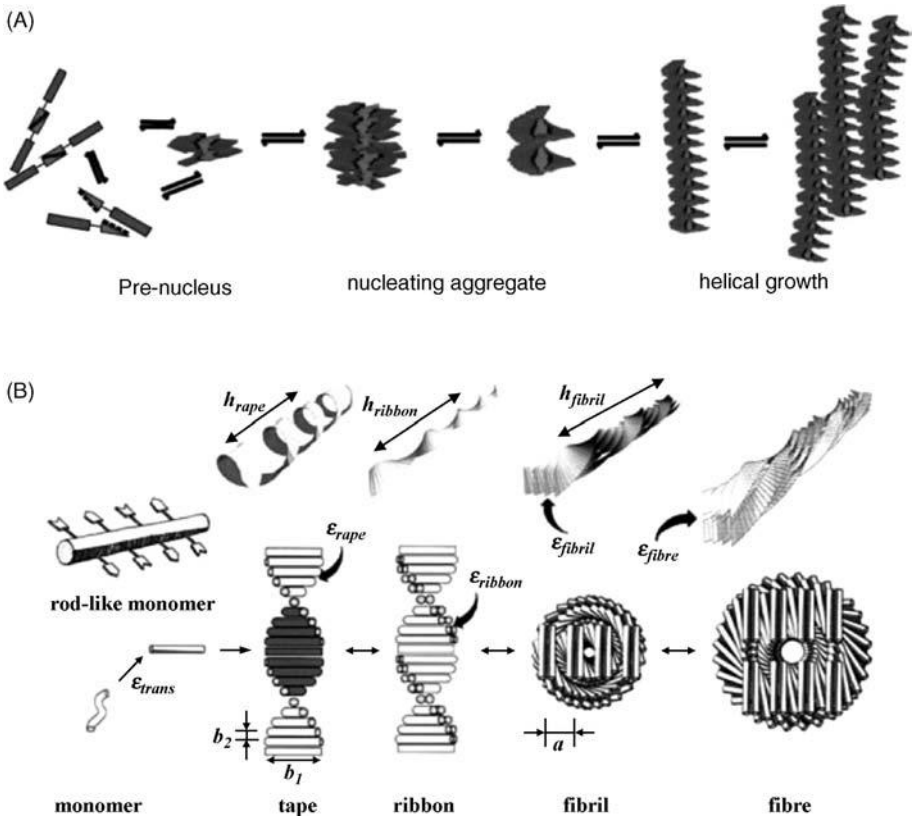

Figure 5.2 Hierarchical assembly of gel-phase materials as illustrated for synthetic systems developed by (A) Meijer's group and (B) Aggeli and coworkers. Ref. [8] adapted with permission of Science and Ref. [9] adapted with permission of National Academy of Sciences.

and this makes molecular gels highly tunable, responsive materials. For example, raising the *temperature* has a profound effect on the assembly process due to the entropy term ($\Delta G = \Delta H - T\Delta S$) and encourages disassembly of the gel into the less ordered "sol" state. Molecular gel formation is also *concentration* dependent; at low concentration, the interaction between molecules is unable to yield supramolecular polymers. Such effects are now well understood in supramolecular polymer chemistry [7] and can be applied to gel-phase materials.

5.2 Preparation of Molecular Gels

Molecular gels are often formed by *heating* the solid low molecular mass gelator in an appropriate solvent, with *sonication* sometimes being applied to the sample [10].

This process results in the solubilization of the gelator. In the isotropic solution, the gelator molecules have a relatively low degree of aggregation – insufficient to support a sample spanning network. On cooling, preferably at a controlled rate, the sol transforms into a gel. In general terms, the higher the concentration of gelator used, the higher is the temperature of the gel–sol boundary. On some occasions, a gel forms instantly on dispersing a gelator in the appropriate liquid [11]. This would imply that in this case, the activation energy required for solubilization and subsequent molecular assembly is lower than that in those cases where a heat–cool cycle (or sonication) is required for gelation. It is essential that the method of gel preparation is accurately reported, as gel properties can vary depending on the precise details of preparation (e.g. rapid cooling versus slow cooling, heating versus sonication).

One key recent study provided a detailed insight into a one-dimensional aggregation process, in which molecules aggregated into dimers, which formed helical fibrils, that then assembled further into fibers and bundles (Figure 5.2A) [8]. It was concluded that the basic model of aggregation described above to form gels was accurate, but that solvent molecules played an unexpected explicit role in forming an ordered shell capable of rigidifying the aggregates and guiding them towards assembly into bundles/gels. This analysis is consistent with the observation that gelation is highly (and sometimes unpredictably) solvent dependent [12]. Understanding these nucleation and assembly mechanisms in more detail will hopefully enable the important goal of extending *rational synthesis into the nanoscale regime* in a more controllable way.

5.3
Analysis of Molecular Gels

Perhaps one of the most interesting features of gels is the ability to gain an understanding of the connection between *molecular structure*, *nanoscale self-assembled morphology* and *macroscopic materials properties*. In the following sections, we discuss the ways in which gels can be analyzed across the full range of length scales. It should be noted that a full discussion of each of these techniques is beyond the scope of this chapter, which will instead try to focus on the key points of each method and direct the reader to useful references in the literature.

5.3.1
Macroscopic Behavior – "Table-Top" Rheology

Quick and simple ways of visually assessing the physical (i.e. macroscopic) behavior of the gels are referred to as "table-top" rheology [13] and can be readily carried out in any laboratory without sophisticated equipment. These techniques, discussed in further detail below, are particularly useful for exploring the *gel–sol phase boundary*, as the conversion of the material from a gel to a sol can be readily assessed in a visual manner. There are two simple parameters which are widely used to define the

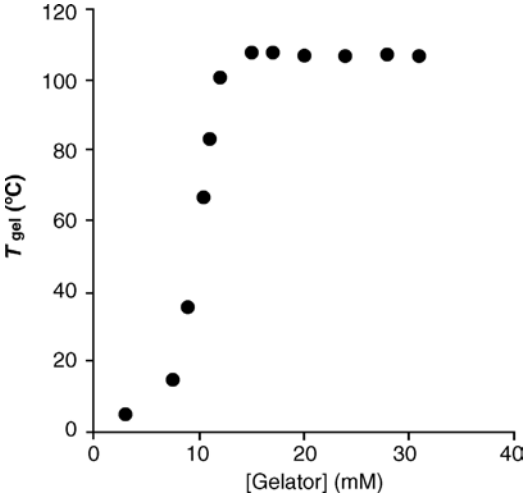

Figure 5.3 Example of a phase diagram for gelation. Reproduced from Ref. [14] with permission of the American Chemical Society.

macroscopic properties of molecular gels:

1. *Minimum gelation concentration* (MGC) – the minimum concentration of gelator required to form a sample-spanning self-supporting gel at a given temperature (usually 25°C).
2. *Gel–sol transition temperature* (T_{gel}) – this value can be determined by monitoring gelation with the use of a high-precision thermoregulated heating–cooling bath. It is concentration dependent and determining T_{gel} values at different concentrations allows the construction of a "phase diagram" (e.g., Figure 5.3).

5.3.1.1 Tube Inversion Methodology

The simplest method of monitoring the gel–sol transition involves inverting a vial of the gel and watching to see whether any flow occurs (for example, the gel shown in Figure 5.1 would satisfy the tube inversion test) [15]. It is essential to use the same sample mass and vial type when performing comparative studies, to ensure that the yield stress exerted on the gel remains constant. This ensures that the gel–sol transition in each case is determined under the same conditions of stress and hence meaningful comparative results can be obtained. However, this limitation means that it can sometimes be difficult to compare results recorded in different laboratories in a quantitative way.

5.3.1.2 Dropping Ball Method

In this method, a small metal ball is placed on the gel and the dropping of the ball through the gel is observed [16]. In the ideal scenario, the ball should be immobile in the gel, but drop rapidly in the sol. In this way, the T_{gel} value at any given concentration of gelator can be determined. In this case, the yield stress is dependent

on the density of the ball and its radius. Therefore, the ball must be kept constant across experiments in order to ensure that data can be compared in a meaningful way. The sample tube should also be significantly larger than the ball, otherwise the presence of the nearby walls can affect the motion of the ball (wall effects can never be completely eliminated).

It is possible to analyze the phase diagrams constructed from "table-top" rheology methods in order to estimate thermodynamic parameters associated with gelation. Schrader's relationship can be used to generate plots of ln[gelator] against $1/T_{gel}$, in which the gradient is $-\Delta H/R$, where ΔH can be approximated to the enthalpy associated with the gel–sol transition [17]. This value can therefore provide some insight into the thermodynamics of the interactions between molecular-scale building blocks, although the assumptions inherent in this treatment probably mean that the data are best used to compare the behavior of related gelators. It should also be noted that many gels apparently exhibit a plateau region in T_{gel} above a certain concentration (see Figure 5.3) – corresponding to a point at which the presence of additional gelator does not appear to enhance the thermal macroscopic properties of the gel, presumably because the formation of a sample-spanning network is complete. This behavior cannot be fitted to Schrader's relationship.

5.3.2
Macroscopic Behavior – Rheology

As soft materials, gels can ideally be explored using *rheological methods* [18], although this requires the use of specialist equipment. In typical experiments, the magnitudes and ratios of the elastic (G') and loss (G'') moduli are determined under oscillatory shear. The elastic modulus (G') indicates the ability of a deformed material to regain its shape, whereas the loss modulus (G'') represents the ability of the material to flow under stress. For a gel, the elastic modulus should be independent of oscillatory frequency and G' should exceed G'' by about one order of magnitude. Measurements of viscosity also provide a useful method for comparing gel-phase materials in a quantitative way and generating structure–activity relationships.

Rheology has been performed on a number of molecular gels [19] and it is increasingly clear, from the relationship between strain and stress tensors, that the choice of theoretical model is not straightforward. Molecular gels can be classified rheologically as cellular solids, fractal/colloidal systems or soft glassy materials, depending on their behavior. Evidently, there is the need for continued application of rheological methods to molecular gel materials in order to provide a better insight into the way in which modifying gelator structures on the molecular scale controls the macroscopic rheological properties of the self-assembled material.

5.3.3
Macroscopic Behavior – Differential Scanning Calorimetry

In differential scanning calorimetry (DSC), the difference in the amount of heat required to increase the temperature of a sample and reference is measured as a

function of temperature [13]. When the sample of interest undergoes a physical transformation, such as a gel–sol phase transition, more heat will need to flow to it than the reference in order to maintain both at the same temperature. Observing the difference in heat flow associated with this endothermic phase transition permits the measurement of the amount of heat absorbed or released by integration of the DSC trace. This provides a way of directly measuring the phase-change enthalpy ($\Delta H_{gel-sol}$) and can provide an insight into the thermodynamics of the gelator–gelator interactions. DSC should be performed in both heating and cooling modes in order to assess both endothermic and exothermic transitions and assess the thermoreversibility of the gel–sol phase change.

5.3.4
Nanostructure – Electron Microscopy

Electron microscopy is, perhaps more than any other method, the technique that has opened up the "nanoworld". In the simplest use of electron microscopy to image the nanostructure of gel-phase materials, a gel sample is first allowed to dry on a substrate (either under ambient conditions or *in vacuo*). The sample is coated under vacuum with a thin (ca. 2 nm) metallic layer and then imaged by scanning electron microscopy (SEM). The SEM image obtained in this way therefore depicts a *dried and treated sample*. Usually the network structure of the gel "collapses" on to itself during drying to yield a *xerogel* (if "collapse" does not occur, the structure is referred to as an *aerogel*). It should be noted that changes in the nanostructure other than "collapse" may also occur during drying; however, it is often assumed that such effects are minor.

A range of morphologies are observed for gel-phase materials using SEM (Figure 5.4). In general, transparent gels exhibit nanoscale structuring, whereas opaque gels, which scatter light, have microscale features. Typically assembled *nanofibers* are observed, as might be expected for supramolecular polymers. Other types of "one-dimensional" objects such as *tapes/ribbons* have also been reported. In some cases nanoscale chirality of these objects can be observed – usually in the form of *helicity*. Transmission electron microscopy (TEM) can also be applied to gel imaging, although it is often necessary to apply a heavy metal staining agent to enhance image contrast.

Cryo-electron microscopy techniques are used to try and minimize disruption to the self-assembled network [20]. This method uses a rapid freezing step to prevent thermal motion of the assembled gelator network. In some cases solvent is then sublimed from the sample by freeze-drying (although this may modify the gelator structure, the low temperatures make gelator reorganization less likely). Overall, cryo-electron microscopy leads to significantly less disruption of the gelator network and therefore a typical cryo-EM image shows a more expanded and "solvated" network, in which the solvent pockets can be readily visualized as cavities within the network (Figure 5.5).

In some rare examples, *nonfibrillar gel morphologies* have been observed by electron microscopy methods. For example, platelet-type morphologies have been observed in

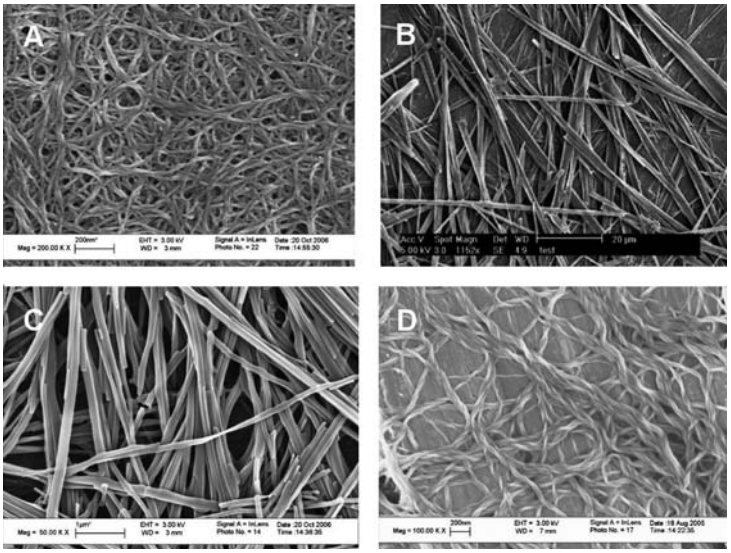

Figure 5.4 SEM images of nanostructured gels synthesized in the author's laboratories showing (A) fibrillar, (B) tape-like, (C) rod-like and (D) helical ribbon morphologies for different gelators.

which interpenetrating networks of platelet-like objects constitute the "solid-like" phase [21]. Figure 5.6 illustrates how a honeycomb network of two-dimensional platelets may lead to the effective "immobilization" of solvent molecules within the nanoscale cavities inherent within the morphology. It has been argued that in these systems, growth of an ordered structure occurs in two dimensions (and is prevented in the third). This would therefore appear to be conceptually related to the more typically observed formation of gel fibers, in which growth is only allowed in one direction and prevented in the other two.

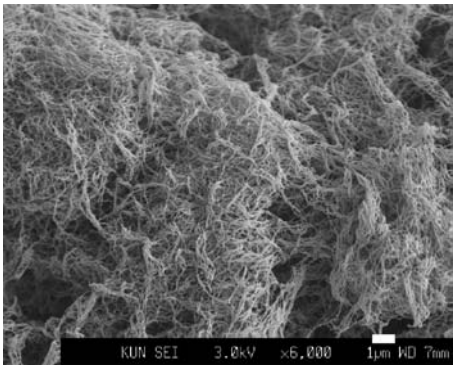

Figure 5.5 Cryo-scanning electron microscopy image of a self-assembled gel. Reproduced from Ref. [12a] with permission from the American Chemical Society.

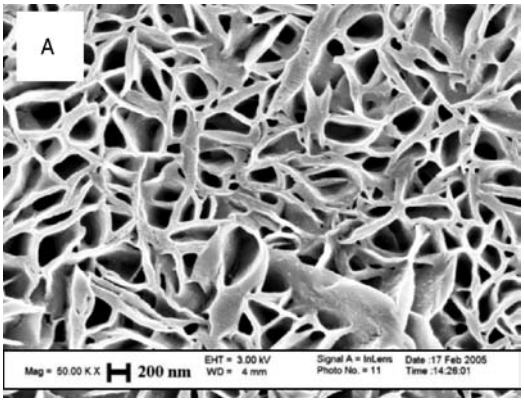

Figure 5.6 SEM image of an unusual nonfibrillar interconnected honeycomb morphology constructed from interlocked platelets underpinning a gel-phase network. Reproduced from Ref. [12d] with permission of Wiley.

5.3.5
Nanostructure – X-Ray Methods

The irregular packing of fibrils and fibers within gel-phase materials means that rather than leading to well-defined diffraction patterns, solvated molecular gels generally scatter X-rays, which can, at low angles of scattering, be fitted to a computer model [22]. For example, the scattering data obtained from a gel can be modeled as a collection of cylinders or tapes. The data can provide useful information about nanoscale dimensions, such as the cylinder diameter. If the model is accurate, this will correspond to the fibril dimensions (e.g. ca. 1–3 nm). This is useful information, as the objects visualized by electron microscopy methods are usually larger fibers and bundles (i.e. not molecular scale) – X-ray scattering analysis therefore provides a way of "visualizing" the *molecular-scale fibrils* present in the gel, which underpin the morphology observed by electron microscopy. X-ray methods can also be used on the dried gels (xerogels), in which case diffraction peaks are generally observed. This can lead to a more precise understanding of the molecular packing within fibrils, although results must be treated with some care, as drying can lead to morphological change [23]. Computer modeling is often an excellent complement to X-ray diffraction (and other) investigations of molecular gels and such approaches can sometimes be used to provide a predictive understanding of fibril/fiber packing [24] and lead to pictorial models such as that illustrated in Figure 5.2B [9].

5.3.6
Molecular Scale Assembly – NMR Methods

NMR spectroscopy provides a useful method to try to understand why, on a molecular level, gelators assemble into fibrillar architectures and to probe the

intermolecular interactions between the molecular building blocks which underpin the self-assembly of fibrillar architectures [25]. It should first be noted that NMR in the "rigid" gel-phase is challenging because the low mobility of the molecular building blocks causes broad peaks. As in solid-phase NMR, magic angle spinning (MAS) could, in principle, be employed to obtain NMR spectra of rigid gels [26], although this has not been widely applied to low molecular weight gelation systems. In some rigid gels, unexpected sharp NMR peaks associated with the gelator have been observed; these have been attributed to gelator molecules *not bound* to the nanoscale network. Such peaks can only be observed if the exchange of gelator molecules from bound to unbound forms is kinetically slow [25]. Usually, the concentration of gelator being observed in the NMR spectrum can be quantified by integration with respect to a reference molecule which does not associate with the "solid-like" gelator network and has sharp NMR peaks.

In order to facilitate the study of molecular gels, NMR experiments are often performed on soft solids/partial gels or on samples just above the T_{gel} value – in this way, spectra with reasonably sharp peaks can be recorded. Under this regime of concentration/temperature, the hierarchical assembly is at the stage of oligomer formation (rather than fully formed network) and NMR therefore provides an ideal way of monitoring the way in which one molecule interacts with another to form an oligomeric assembled structure. Several typical experiments are performed:

1. *Variable concentration* – NMR titration. NMR spectra are recorded at increasing concentration of gelator. As the concentration increases, the NMR spectra should broaden due to gel formation and loss of gelator mobility. However, the NMR peaks should also shift – particularly those that are involved in noncovalent interactions between the molecules. For example, N–H protons are often observed to shift downfield as concentration increases (Figure 5.7) [27]. This indicates that as the concentration increases, these peaks become increasingly involved in hydrogen bond interactions. Alternatively, aromatic peaks may shift upfield – which would be indicative of the aromatic rings becoming involved in the formation of $\pi-\pi$ interactions.

2. *Variable temperature (VT) experiments*. As the temperature of a sample is increased, the gel should gradually become more mobile and interactions between molecules will weaken. Once again, as these interactions weaken, NMR peaks will shift and this can be assigned to breaking hydrogen bonding and $\pi-\pi$ interactions [28].

3. *NOE experiments* [25,27b,29]. NOE experiments can provide information on the way in which one molecule interacts with another through space and this can help uncover the interactions present within a gel.

4. *Relaxation time experiments* [30]. Relaxation time experiments performed on the broadened peaks at known concentrations can be used to estimate the molecular mobility of the aggregated species (diffusion rates can be obtained from such experiments).

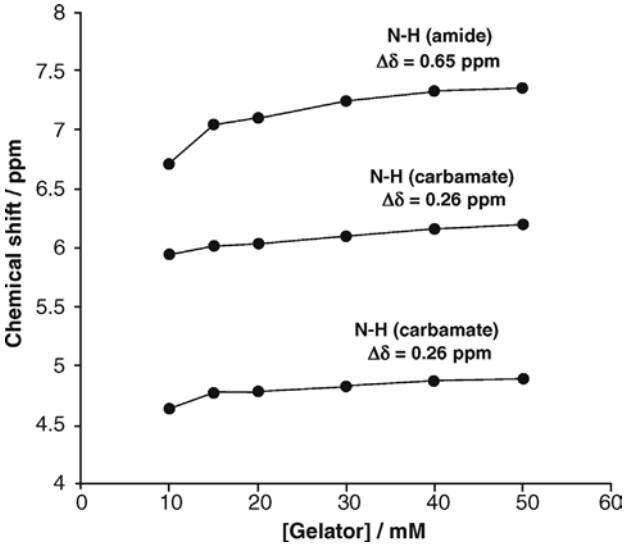

Figure 5.7 Variable concentration NMR experiment indicating downfield shifts of NMR peaks on increasing gelator concentration. Reproduced from Ref. [27c] with permission of the American Chemical Society.

5.3.7
Molecular Scale Assembly – Other Spectroscopic Methods

There are many other spectroscopic methods which can be applied to provide greater insight into the assembly of gel-phase materials. Two illustrative examples are given here:

1. *Infrared (IR) spectroscopy.* This method is very useful for probing hydrogen bond interactions between the molecular building blocks. In particular, O−H, N−H and C=O stretches all show distinctive responses to hydrogen bonding. Van der Waals interactions can also be detected by looking for changes in C−H stretching interactions. Typically, it is necessary to compare IR spectra of the gelator in both the sol and the gel in order to determine the key noncovalent interactions. Variable temperature IR spectra can provide a useful way of probing the response of these interactions to temperature changes [31].

2. *Fluorescence spectroscopy* [32]. Gelators which include fluorophores can exhibit changes in their spectra on aggregation. For example, many fluorophores emit as excimers when in close proximity (such as in a gel fiber) but emit as monomers when present in dilute solution. In one very recent example, excimers were present in the sol, but not in the gel [33]. Fluorescence can also detect smaller changes associated with differences in polarity between the gelator in aggregated and nonaggregated states. Once again, VT fluorescence

can be a useful technique in order to determine which spectral features are responsive to the aggregation process [34].

5.3.8
Chirality in Gels – Circular Dichroism Spectroscopy

Circular dichroism (CD) spectroscopy [35] is an ideal technique which can be used to monitor both molecular and nanoscale chirality [36]. An achiral molecule will exhibit no bands in the CD spectra, whereas a chiral molecule can exhibit a signal (either positive or negative), in the same wavelength region where it has its UV–Vis absorption. In general terms, however, solvated isolated chiral molecules often have relatively small CD signals (unless they have well-organized chromophores inherent within the molecular structure). As individual molecules assemble into a chiral nanostructure, the interaction with polarized light can be significantly enhanced and hence self-assembled nanostructures often exhibit much larger CD bands than their isolated molecular building blocks. The presence of a CD signal therefore provides good evidence for the presence of a chiral nanoscale object. To confirm this assignment, however, it is necessary to carry out a VT experiment or compare the CD spectrum with that observed in a solvent where aggregation does not take place [37]. In VT CD, the CD band should decrease in intensity as the temperature increases, because the nanoscale aggregates break up into their constituent building blocks on heating (Figure 5.8). For well-characterized chromophores, it can sometimes be possible to use CD spectroscopy to predict whether they are packed in a clockwise or an anticlockwise manner within the helical assembly and examples will be discussed later in the chapter.

CD spectroscopy also provides an ideal method for probing the assembly of mixtures of enantiomeric molecular building blocks into gels and can be used to

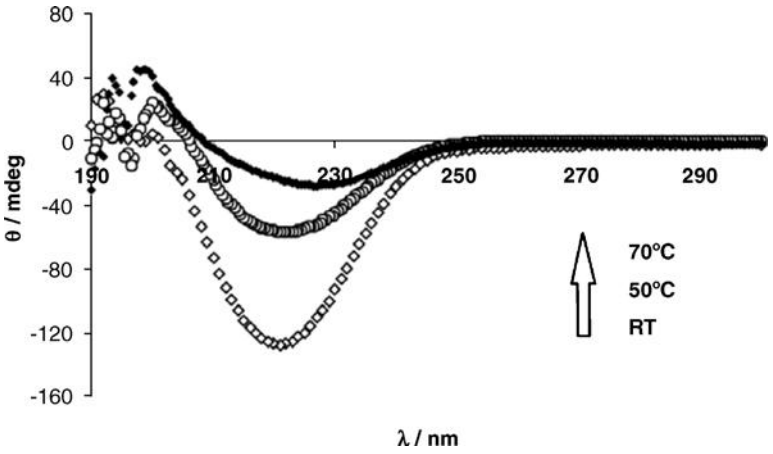

Figure 5.8 VT temperature CD experiment demonstrating disassembly of chiral nanostructure on application of heat. Reproduced from Ref. [37] with permission of the publishers.

distinguish between situations in which:

1. the presence of one enantiomer *disrupts the assembly* of the other and cause a breakdown in chiral order [38];
2. one enantiomer (present in excess) enforces its chirality on to the other enantiomer via a "*majority rules*"-type mechanism – this is well known in supramolecular polymers [39] but not widely explored in gels; or
3. the two enantiomers ignore one another's presence and are able to "*self-sort*" into a proportional mixture of their own homochiral assemblies [37,40].

5.4 Building Blocks for Molecular Gels

Gelation is highly dependent on the choice of solvent – indeed, it is common for researchers to present large tables of data testing gelation behavior across a wide range of solvents. For the purposes of this discussion we will broadly classify gels as either organogels or hydrogels, where *organogels* form in apolar, non-hydrogen-bonding solvents (e.g. hexane, toluene, acetonitrile, food and fuel oils), whereas *hydrogels* form in polar, hydrogen-bonding solvents (e.g. water, methanol, ethanol). The driving forces for gelation in these two classes of solvent are markedly different, as will be discussed below.

The design of a gelator from first principles is a difficult and challenging task. More often than not, gelators are discovered serendipitously. However, there is now sufficient literature available to suggest the following broad conclusions about whether or not a molecule may be expected to gelate:

1. The molecule must be *partly soluble* in the solvent of choice (but not too soluble, otherwise it will simply dissolve).
2. The molecule must be *partly insoluble* in the solvent of choice (but not too insoluble otherwise it will simply precipitate).
3. The molecule must have the potential to form *multiple noncovalent interactions* with itself. Typically, although not exclusively, these might be *hydrogen bonds and/or π–π interactions for organogels* and *hydrophobic and/or donor–acceptor interactions for hydrogels*.
4. *Van der Waals forces* are usually present to support the gelation process and in very rare cases, gelation can occur solely through these very weak interactions.
5. These noncovalent interactions should occur in a *directional manner* (a degree of asymmetry is often advantageous).

The sections that follow highlight the major classes of gelator systems explored in the literature. The examples chosen are highly selective and, for a more comprehensive overview, the interested reader is directed towards relevant review articles at the start of each section.

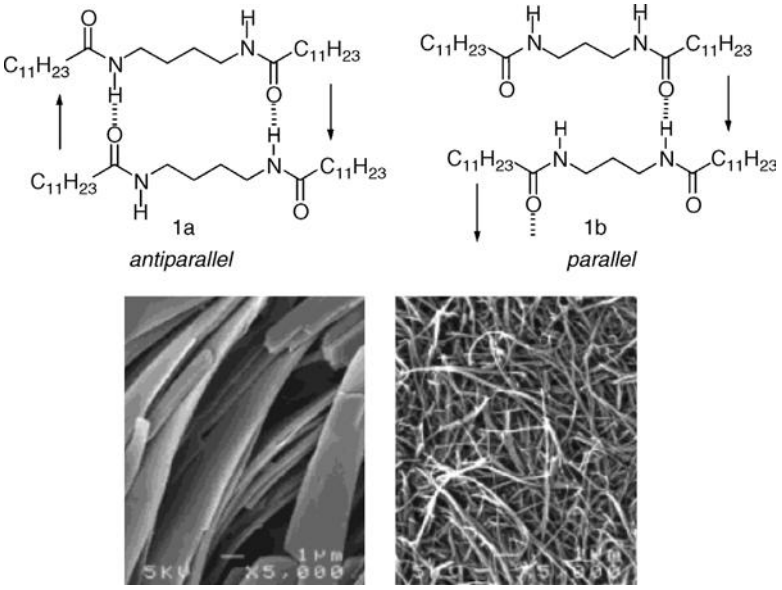

Figure 5.9 Gelators **1a** and **1b** with even and odd spacer chains stack in antiparallel and parallel modes, leading to different gel behavior and nanostructures (SEM images, scale bar = 1 μm). Adapted from Ref. [42a] with permission of the American Chemical Society.

5.4.1
Amides, Ureas, Carbamates (−XCONH− Groups, Hydrogen Bonding)

The −CONH− group has both a hydrogen bond donor (N−H) and a hydrogen bond acceptor (C=O) and, as such, is ideal for the formation of intermolecular hydrogen bonded networks [41]. For example, bisamide compounds **1a** and **1b** (Figure 5.9) form effective gels in aromatic solvents such as mesitylene due to a combination of hydrogen bond and van der Waals interactions [34,42]. Interestingly, the length of the aliphatic spacer chain between the amide groups was observed to exert an *odd/even effect* on gelation. It was argued that the ability of the molecules to assemble in either a parallel or antiparallel manner was dependent on whether the spacer chain had an odd or even number of carbon atoms. Indeed, the gels formed by gelators with odd and even spacer chains had markedly different thermal stabilities and SEM studies indicated that the gels were underpinned by different nanostructures.

Compound **2** (Figure 5.10) is another example of a bisamide gelator [43] and, once again, intermolecular hydrogen bonds and van der Waals forces drive the assembly

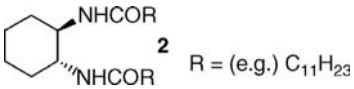

Figure 5.10 Compound **2** – a chiral gelator building block.

process. In this case, the molecular building block is chiral. Racemic mixtures of compound **2** with its enantiomer were observed to form much less stable gels than either pure enantiomer, demonstrating that chirality can play an essential role in controlling the molecular packing. This is consistent with the argument that the supramolecular polymers which underpin molecular gels have nanoscale chirality such as helicity (see Section 5.3.8).

In general, if peptidic molecules are to act as hydrogelators, rather than organogelators, they require slightly *higher polarity* in order to ensure sufficient compatibility with the aqueous solvent medium but they must also have sufficiently large hydrophobic surfaces to provide a thermodynamic driving force for assembly. Consequently, many hydrogelators contain unmasked carboxylic acid groups (or amines) to provide polarity and long alkyl chains to provide a hydrophobic surface for assembly. Amphiphilic structures such as **3** and **4** have therefore been employed (Figure 5.11) [44]. These molecules self-assemble as a consequence of hydrophobic interactions (and van der Waals forces) between the long alkyl chains and hydrogen bond interactions between the peptide groups, with the carboxylic acids/amines ensuring compatibility of the "solid-like" assembled network with the "liquid-like" solvent phase.

Ureas can readily replace the peptide groups and bisurea bola-amphiphilic structures also act as highly efficient hydrogelators. Depending on the choice of spacer chain, compounds such as **5** can have minimum gelation concentrations of $<0.3\%$ w/v (Figure 5.11) [45]. The gelation ability of many hydrogelators is highly *pH dependent*. Compound **5** forms vesicles at low pH and only assembles into fibrillar gel-phase materials when the pH is increased, a process which optimizes the solubility of the bola-amphiphile.

Compound **6** provides an interesting example of a photoswitchable hydrogel (Figure 5.12) [46]. Only the *trans* form of this compound assembles into nanoscale fibrillar objects and acts as a hydrogelator, whereas the *cis* form of the compound assembles into a microspherical morphology. The *cis* form of the gelator can be

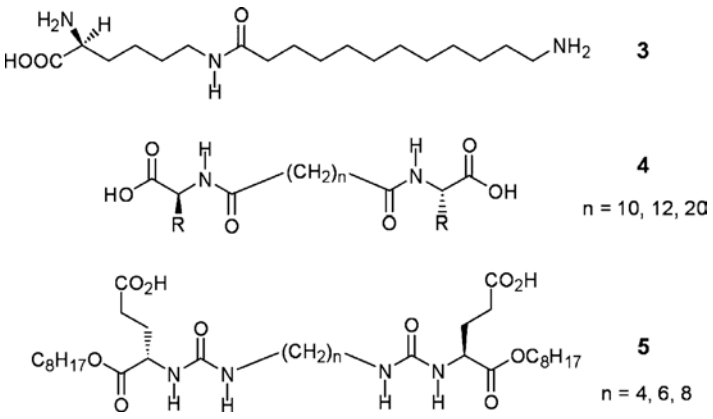

Figure 5.11 Hydrogelators based on peptide (**3** and **4**) and urea (**5**) functional groups.

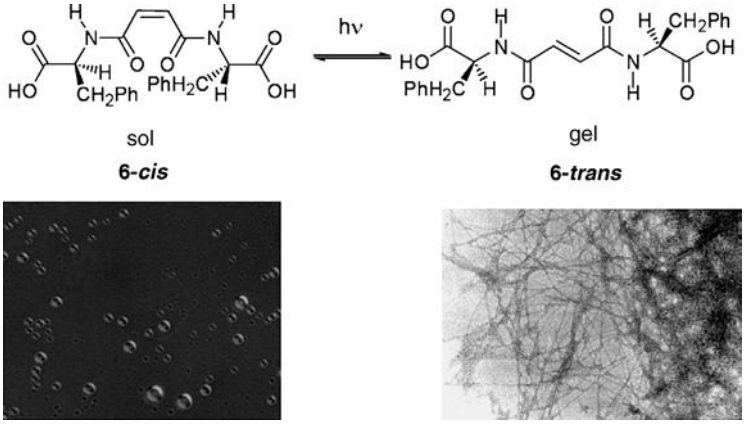

Figure 5.12 Compound **6** – a photoswitchable hydrogelator. Adapted from Ref. [46] with permission of the American Chemical Society.

converted into the *trans* form by photoirradiation and consequently, photoisomerization triggers a morphological transition at the nanoscale level and hence "switches on" gelation. Using *external stimuli* in this way to *trigger* gelation is an important target in controlled release applications such as drug delivery (see Section 5.5.4) and is one of the key ways in which the reversibility of supramolecular gels can be harnessed.

5.4.2
Carbohydrates (Multiple −OH Groups, Hydrogen Bonding)

Like peptides, alcohol groups contain both a *hydrogen bond donor* and an *acceptor*, ideal for setting up intermolecular hydrogen-bonded networks. Carbohydrates are particularly interesting building blocks for gels [47] as this class of molecule has many naturally occurring members which possess multiple −OH groups with subtly different organizations and chiralities, hence providing fertile ground for investigations of *structure–activity relationships* [48]. Normally, for the formation of organogels, some of the sugar alcohol groups will be protected – a completely unprotected sugar would not have the right solubility profile, being too hydrophilic and hence insoluble in organic solvents. Once again, the key appears to be achieving *balanced solubility* combined with the presence of potential self-assembling functional groups.

Chiral molecule **7**, a partly protected version of sorbitol, demonstrates these principles in action and has been extensively studied as a gelator of organic solvents and polymer melts since the first reports, which remarkably appeared as long ago as 1891 (Figure 5.13) [49]. Recently, this molecule has been applied as the matrix gelator in the development of quasi-solid-state dye-sensitized solar cells [50]. A wide range of analogues of this compound have since been investigated as

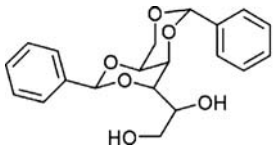

7

Figure 5.13 Carbohydrate-based organogelator **7**.

organogelators and this has led to an understanding of the role of both intra- and intermolecular hydrogen-bonding pathways on controlling the self-assembly of these molecules [51].

Carbohydrates have also been employed as hydrogelators – for example, gels based on unprotected sorbitol are widely employed in personal care products such as toothpaste and shaving gel. Typically, in hydrogelators, the carbohydrate is fully *deprotected* to provide high compatibility with the aqueous phase and the potential for multiple intermolecular hydrogen bond pathways. Furthermore, the carbohydrate is often functionalized with a significant *hydrophobic* surface in order to provide a *thermodynamic driving force* for assembly [52]. An example of this strategy is provided by amphiphilic compound **8**, which assembles into helical nanoscale fibers (Figure 5.14). Hydrogelators based on sugars have also been constructed with bola-amphiphile type architectures. For example, it was reported that compound **9** remarkably formed gels at concentrations as low as 0.05% w/v (Figure 5.14) [53]. The chromophoric azo dye used as the linker in these gelators experienced an induced CD signal due to its incorporation within a chiral nanoscale self-assembled architecture – the stereochemistry of the glucose units drives the chiral assembly process. The exciton coupling bands in these CD spectra could be assigned to the transition dipoles in the azobenzene units being orientated in a clockwise direction – indicating *right-handed helical growth* of the molecular fibrils. SEM observation of the gel fibers showed that this helicity was also manifested in the fibers observed at the nanometer scale. Transcription of chiral information from the molecular scale to the helicity on the nanoscale was therefore unambiguously demonstrated.

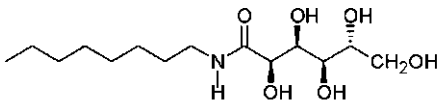

8

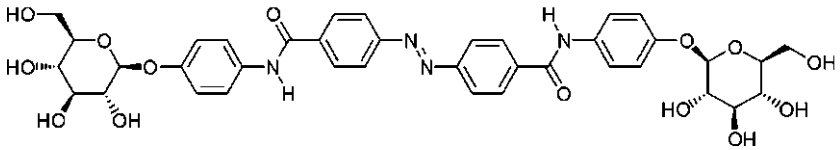

9

Figure 5.14 Carbohydrate hydrogelators **8** and **9**.

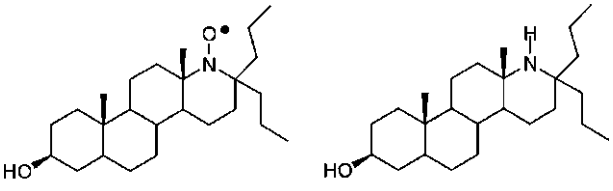

10 **11**

Figure 5.15 Compounds **10** and **11** as simple steroid organogelators.

5.4.3
Steroids/Bile Salts (Hydrophobic Surfaces)

Steroids, such as cholesterol, are naturally occurring lipid molecules which exist in all plants and animals; they have apolar tetracyclic skeletons and relatively planar rigid structures and have been widely explored as gelators [54]. It is well known in biology that steroids can interact with lipid membranes as a consequence of solvophobicity and van der Waals interactions. In gelation, solvophobicity will play the greater role in hydrogel formation whereas van der Waals interactions will be more important in the assembly of organogels. In 1979, it was reported that compounds **10** and **11** could gelate organic solvents and many of the fundamental techniques used to study organogels were developed using these molecules (Figure 5.15) [55]. Interestingly, the free radical on compound **10** meant that this gelator could also be investigated by electron spin resonance (ESR), with this technique even being used to generate a phase diagram.

Steroids modified with aromatic rings can become even more effective gelators due to π–π *stacking*. For example, compound **12** forms gels at concentrations <1% w/v and was described as a "supergelator" (Figure 5.16) [56]. In an elegant study, chiral gelator **13**, a functionalized cholesterol derivative, was investigated by CD spectroscopy (Figure 5.16) [57]. The chromophoric azo dye unit attached to the steroid

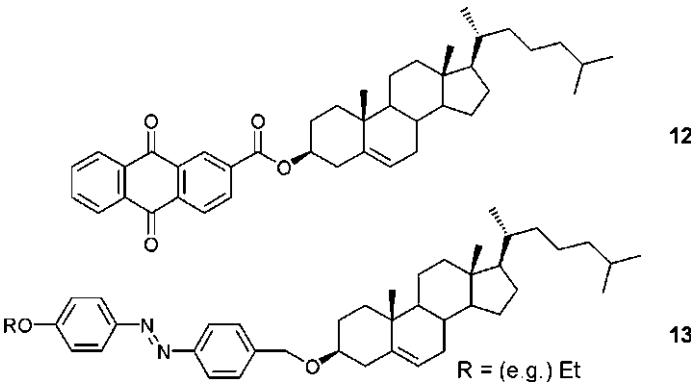

Figure 5.16 Modified steroid gelators **12** and **13**.

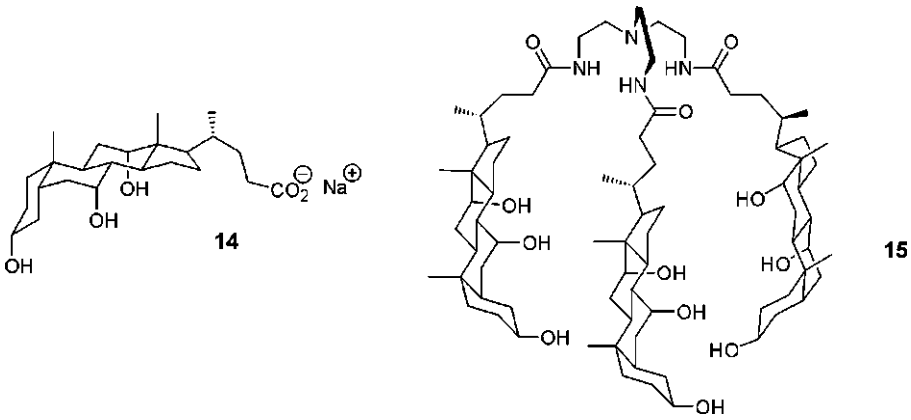

Figure 5.17 Bile acid salt **14** and bile acid derivative **15** both act as hydrogelators.

experienced an induced CD signal due to its incorporation within a nanoscale self-assembled architecture (caused by the presence of the cholesterol, with its high propensity for aggregation). Once again, the directionality of helical stacking within the nanoscale aggregate could be assigned from these CD spectra. In some cases, it was found that the speed of cooling during gel formation could control the 'handedness' of the assembled helical nanostructure – indicating the importance of carefully controlling and reporting the conditions of gel synthesis, as indicated in Section 5.2.

Bile acids, such as **14**, possess a rigid steroid skeleton, but are functionalized with polar −OH groups on the concave α-face and apolar methyl groups on the convex β-face (Figure 5.17). In addition, they contain a carboxylic acid unit which increases water solubility. As such, these molecules have a degree of *facial amphiphilicity* and they might be expected to have higher compatibility with aqueous solvents than simple steroids such as cholesterol – indeed, they are able to act as hydrogelators, with the first observation of this process being made for sodium deoxycholate as long ago as 1913 [58]. As expected for hydrogelators, *hydrophobicity* (between β-faces) drives the assembly process, supported by hydrogen bond interactions. Simple bile acids have also been used to construct more sophisticated gelator architectures. For example, compound **15**, which contains three cholic acid units attached to a triamine scaffold, forms gels at remarkably low concentrations (Figure 5.17) (0.02% w/v) [59]. The formation of hydrophobic "cavities" in the gel was characterized using 8-anilinonaphthalene-1-sulfonic acid (ANS) as a fluorescent probe of polarity.

5.4.4
Nucleobases (Hydrogen Bonding and π–π Stacking)

Nucleobases are substituted heteroaromatic pyrimidines and purines and are primary building blocks in the structures of nucleic acids. They constitute interesting building blocks for gel-phase materials [60] because they can form hydrogen bonding interactions within the plane of the heteroaromatic ring and π–π interactions

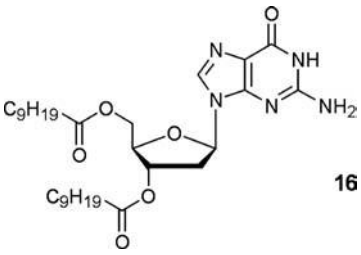

Figure 5.18 Compound **16** is a nucleobase organogelator.

perpendicular to the plane. This allows these molecules to become involved in extended networks of intermolecular interactions.

Compound **16** is a typical organogelator incorporating a guanosine nucleobase (Figure 5.18) [61]. These molecules formed gel-like liquid crystalline phases in hydrocarbon solvents, but fibrillar structures were not observed – instead, a planar tape-like assembly was indicated, with in-depth X-ray diffraction analysis providing evidence that the tapes contained the hydrogen-bonded guanine residues while the hydrocarbon chains and solvent molecules filled the gap between the tapes. Derivatives of thymidine have also been systematically investigated as organogelators [62].

One of the interesting features of nucleobase derivatives is their ability to form *specific interactions* with their *complementary partner nucleobase* – this can modify the self-assembly process and hence the properties of the gel. For example, thymidine derivative **17** (Figure 5.19) forms opaque gels in organic solvents such as benzene, but on mixing with complementary poly(A) (as a complex solubilized by cationic lipid), the opaque gel became transparent [63]. However, adding non-complementary poly (C) had no effect on the optical properties of the gel. SEM demonstrated that the addition of poly(A) changed the morphology of the gel from a *microscale* platelet-like structure (opaque) to an entangled *nanoscale* fibrillar network (transparent). As expected, the addition of poly(C) caused no perturbation of the microscale platelet-like morphology of compound **17**.

Nucleobases have been used to generate bola-amphiphile-type structures such as **18**, with two thymine units attached to either end of a spacer chain. This molecule assembles into hydrogels in a similar manner to the bola-amphiphiles described in previous sections [64]. Stacking of the nucleobases was indicated by a large hypochromicity in the UV–Vis spectrum. This system was demonstrated to respond

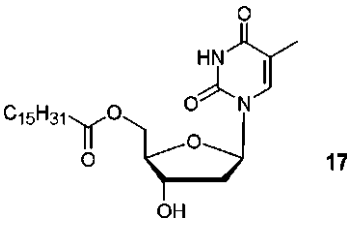

Figure 5.19 Structure of thymidine derivative **17**, the self-assembly of which is modified by the addition of complementary poly(A).

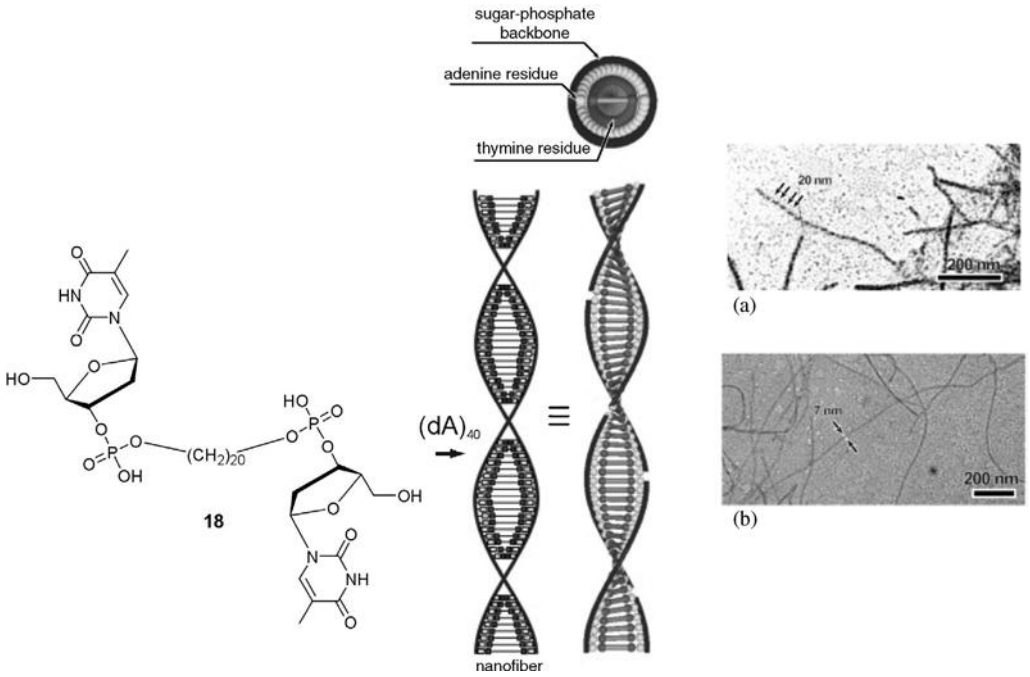

Figure 5.20 Compound **18** based on thymine, self-assembled with oligo(adenine) to yield twisted nanofibers based on complementary A–T interactions. TEM imaging [(a) and (b)] indicated the helical pitch and diameter of these nanoscale assemblies. Adapted from Ref. [65] with permission of Wiley.

to the presence of oligo(adenine) (Figure 5.20) [65]. In the presence of longer strands of oligo(A), helical nanofibers 7–8 nm in width and several hundred nanometers in length were observed. In these nanostructures, the oligo(A) strand had wrapped itself around the fibrillar assembly of compound **18** as a consequence of complementary hydrogen bond interactions between the A and T nucleobases.

Guanosine derivatives are also known to form gels in aqueous solvents as a consequence of G-quartet (**19**) formation (Figure 5.21) – a process which can be templated by Na^+ or K^+ cations (which interact with free lone pairs of the C=O groups pointing into the cavity). These G quartets can assemble into columnar gels, primarily driven by hydrophobic stacking [66].

5.4.5
Long-chain Alkanes (van der Waals Interactions)

Alkyl chains are *widely incorporated* into gelators as they provide a simple way of tuning the solubility of the molecular building blocks – indeed they are near ubiquitous in gelation systems. Alkyl chains can pack together via van der Waals forces and this can enhance gelation by supporting other intermolecular forces, particularly during the formation of organogels. Alkyl chains can also play a role in

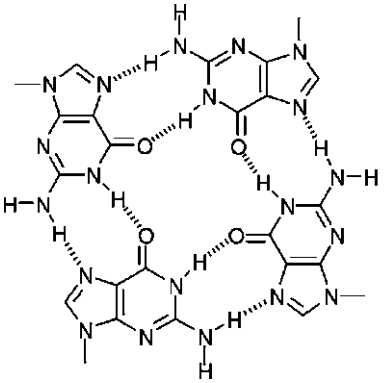

19

Figure 5.21 G quartet structure, **19**.

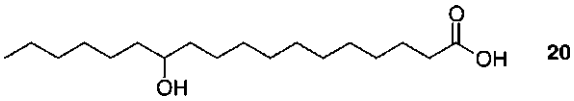

20

Figure 5.22 Fatty acid **20** (12-hydroxystearic acid, HSA) is capable of gelating a wide range of organic solvents and has widespread industrial use in the form of its lithium salt (Section 5.5.1).

ensuring the compatibility of the molecules with organic oil-type solvents and hence preventing phase separation. In hydrogels, alkyl chains often play a key role in driving the aggregation process as a consequence of the hydrophobic effect.

Fatty acids and their salts (e.g. **20**, Figure 5.22) have been widely employed for their gelation potential [6] and are industrially applied in a range of, e.g., cosmetic products. In 1925, Zsigmondy won the Nobel Prize for his investigations of colloidal systems, including fatty acid salts [67]. These systems are all underpinned by fibrillar self-assembled morphologies.

In one unusual example, van der Waals interactions and packing forces alone are sufficient to drive the gelation process. Simple long-chain alkanes such as *n*-hexatriacontane [$H(CH_2)_{36}H$] are able to act as gelators in a variety of hydrocarbon liquids, alcohols, halogenated liquids and a silicone oil [21a]. The extended alkyl chains pack together in a lamellar fashion to form a type of platelet microcrystal, which subsequently forms an interpenetrating network of platelets (Figure 5.23). Interestingly, it is known that this type of aggregation process causes problems in oil pipelines and production equipment, where so-called "waxes" of long-chain alkanes are deposited – understanding and prevention of this aggregation process are therefore of commercial importance.

5.4.6
Dendritic Gels

In recent years, *dendritic* (branched) molecules have been explored as gelators [68]. Dendritic systems possess *multiple functional groups* within the branched structure

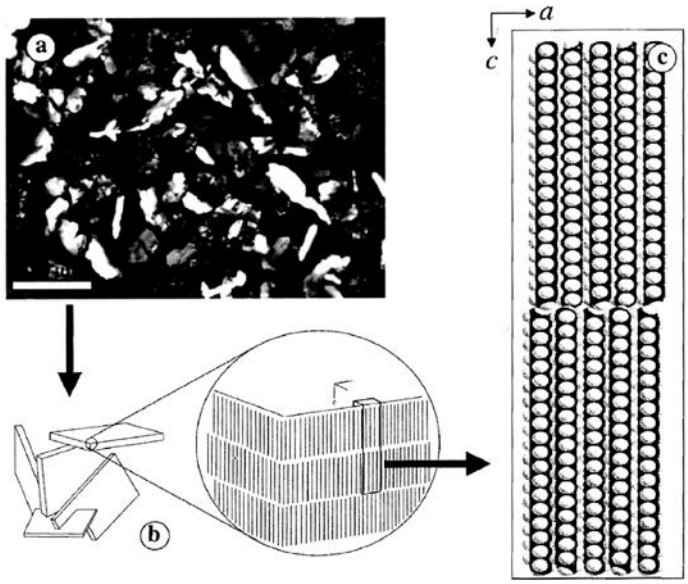

Figure 5.23 (a) Optical micrograph (scale bar 100 μm) of the platelet morphology formed by *n*-hexatriacontane in 1-octanol; (b) proposed model of platelet formation; (c) proposed molecular packing of long-chain hydrocarbons driven by van der Waals forces. Reproduced from Ref. [21a] with permission of the American Chemical Society.

and as such are capable of forming multiple intermolecular interactions, making their self-assembly [69] and gelation properties of considerable interest.

Compound **21** was one of the first dendritic organogelators [70]. In this system, intermolecular hydrogen bond interactions between the peptide groups at the focal point of the dendron were responsible for the self-assembly process (Figure 5.24).

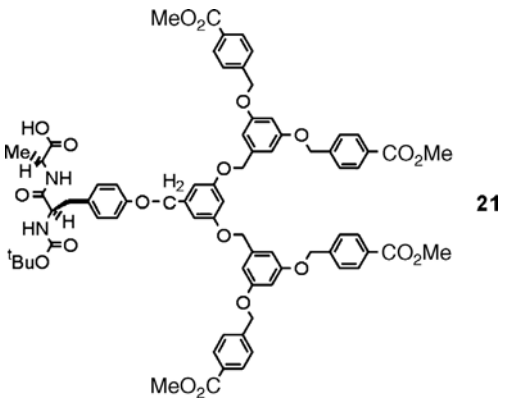

21

Figure 5.24 Compound **21**.

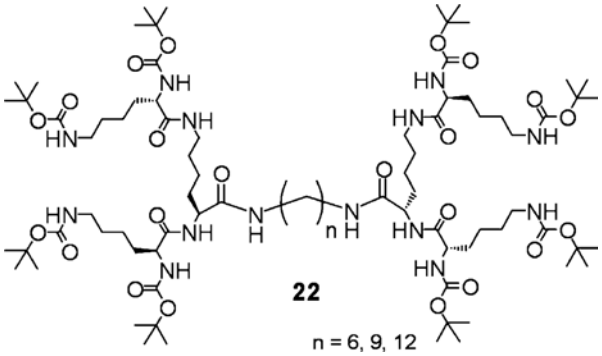

Figure 5.25 Compound **22**.

Lower generation dendritic analogues (with less branching) did not lead to gelation, instead giving precipitate. It seems likely that in this case, the dendritic branching plays a steric role in enforcing the directionality of the assembly process and preventing the formation of "three-dimensional" aggregates.

Compounds such as **22**, with dendritic lysine head groups attached to an alkyl spacer chain, have been investigated in detail as gelators (Figure 5.25) [27c]. These molecules assemble predominantly as a consequence of *hydrogen bond interactions* between the dendritic peptide head groups, as demonstrated by NMR titration and variable temperature experiments. In this case, the highest generation system investigated (third generation) was the most effective gelator. It has been argued [27c] that dendritic effects on gelation are a balance between favorable additional intermolecular interactions and unfavorable steric hindrance and entropic penalties. In this case, therefore, it appears that the additional hydrogen bonds possible on introducing more branching more than compensate for the steric and entropic penalty of assembling more bulky and flexible molecular building blocks.

In a key study [37], the gelation of mixtures of these building blocks has been investigated (Figure 5.26). It was reported that in mixtures where the peptide head groups are different, such as those based on "*size*" or "*chirality*", the dendritic building blocks are able to *self-sort* and form their own independent nanostructures. However, in systems where the dendritic head groups remain the same and only the spacer chain is changed ("*shape*") the molecular recognition pathways between the peptide head groups become confused, self-assembly is disrupted and the nanoscale assemblies which result are constructed from a mixture of the different building blocks.

Amphiphilic dendritic organogelators [*dendron rod-coil* (DRC) molecules] such as **23** have been investigated as gelators (Figure 5.27) [72]. In this case, structure–activity relationship studies indicated that at least four hydrogen bonding O−H groups were required to support gelation, that the rigid aromatic rod became involved in π–π stacking interactions and that a sufficiently long apolar coil was required. These gelators have been widely exploited and some examples will be given in Section 5.5.5.

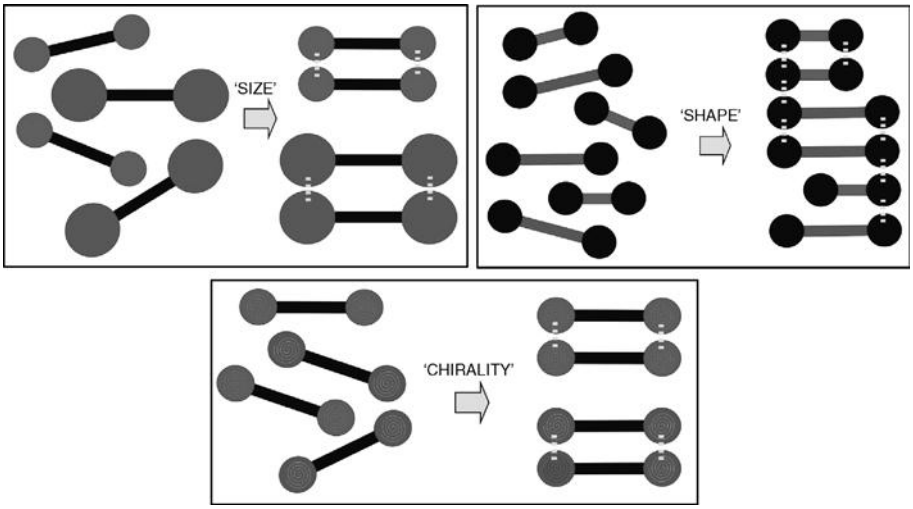

Figure 5.26 Self sorting mixtures – size, shape and chirality. Reproduced from Ref. [37] with permission of Wiley.

Dendritic hydrogelators are also well established. Once again, it is no surprise that some of these structures are bola-amphiphilic in nature, with hydrophobicity driving self-assembly. For example, compounds **24** and **25** form gel-phase materials at concentrations of 1% w/v in water, with fibrous assemblies being visualized by TEM methods (Figure 5.28) [73]. A series of structure–activity relationship experiments were performed and it was reported that there was an *optimum balance* between the length of the spacer chain and the size of the dendritic head group in order for gelation to occur. Indeed, compound **24** will form a gel when the spacer chain contains only eight carbon atoms, whereas compound **25**, which has more extensive polar head groups, requires at least 10 carbon atoms in the spacer chain for gelation to be observed. This hydrophobic/hydrophilic balance reflects the balance in solubility which is required for effective gelation.

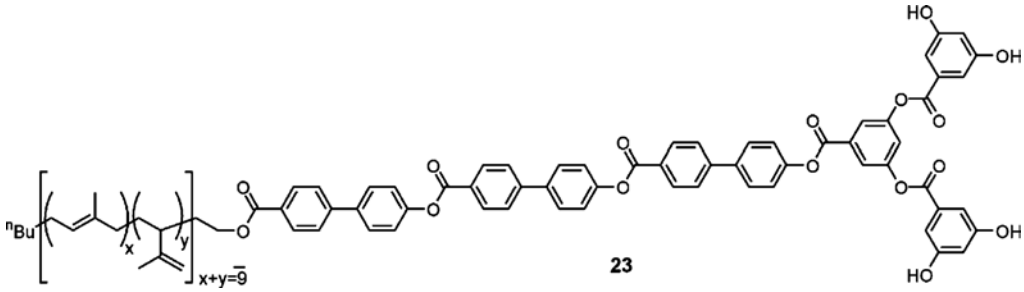

23

Figure 5.27 Dendron rod-coil **23**.

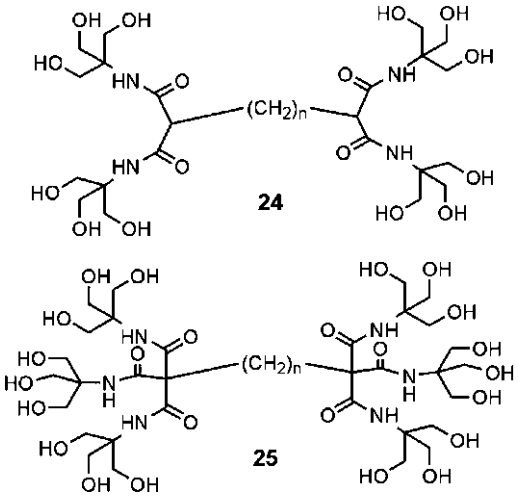

Figure 5.28 Dendritic hydrogelators **24** and **25**.

5.4.7
Two-component Gels

Two-component gelation systems are of rapidly increasing importance [74]. In such systems, two independent components are *both* required to be present in order for gels to form. The two components must first form a *complex*, which subsequently self-assembles into a gel-phase material. This introduces another step into the hierarchical assembly process and consequently provides another level by which the gelation event can be controlled and tuned.

An early example of a two-component gelation process made use of the well-known interaction between barbituric acid (**26**) and pyrimidine (**27**) (Figure 5.29). Appropriate functionalization of these building blocks sterically blocked the formation of a three-dimensional aggregate and encouraged the formation of a linear supramolecular polymer held together by hydrogen bonds [75]. Although this system only formed gels at relatively high concentrations, it demonstrated the principle that two components could act in a synergistic manner to form a gel-phase material.

Extensive studies have been made of a two-component gelation system in which a twin-tailed anionic surfactant, sodium bis(2-ethylhexyl)sulfosuccinate (AOT, **28**) interacts with substituted phenols (**29**) (Figure 5.30) [76]. Gelation is initiated via the formation of a hydrogen bonding interaction (possibly with associated proton transfer) between the phenol and the sulfonate group. Subsequently, the aromatic phenols form a π-stacked architecture. The alkyl chains of the surfactant are then able to contribute van der Waals interactions, in addition to ensuring the compatibility of the fibrillar aggregates with the surrounding solvent. Small-angle X-ray scattering was used to demonstrate that molecular-scale fibrils (diameter ca. 2.1 nm) assemble into fibers (diameter ca. 10 nm), which then aggregate further to yield fiber bundles (diameters 20–100 nm) – a clear example of the *hierarchical assembly process*.

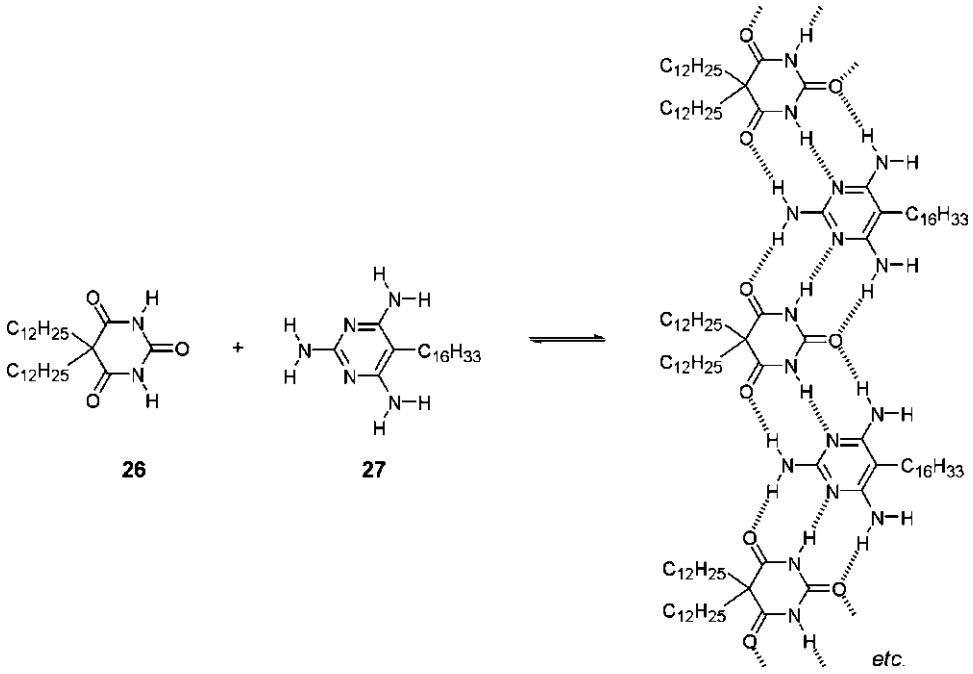

Figure 5.29 Compounds **26** and **27**.

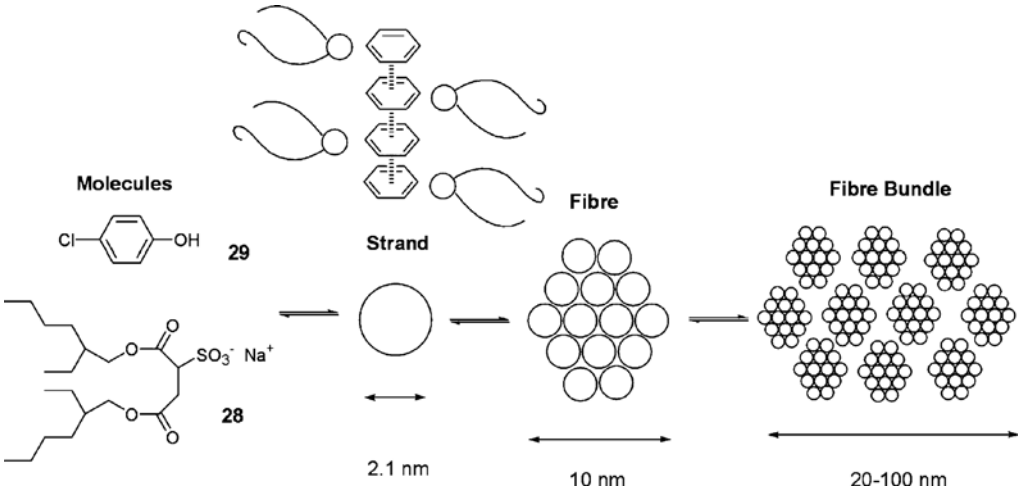

Figure 5.30 Compounds **28** and **29** assemble hierarchically to form strands, fibrils and fibers. Adapted from Ref. [74] with permission of Wiley.

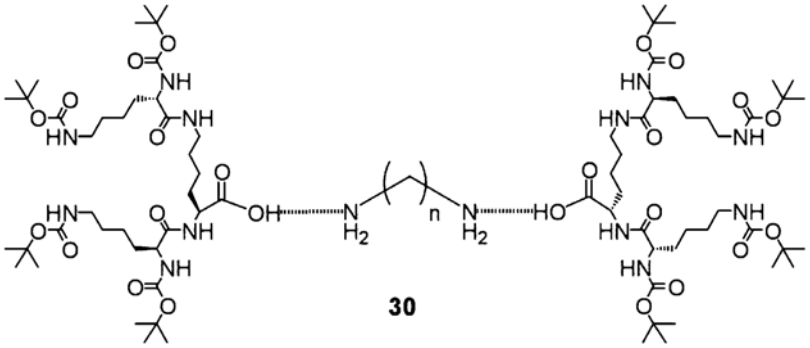

Figure 5.31 Two-component gelation system **30**.

Two-component gels based on dendritic building blocks such as **30** have been reported and fully characterized (Figure 5.31) [12a,14,77]. Intriguingly, it has been demonstrated that the molar ratio of the two components can control the nanoscale morphology into which these molecular-scale building blocks assemble [21d]. A stoichiometric 2 : 1 ratio of dendron to diamine gave rise to well-defined nanofibrillar architectures; however, when the amount of dendron was decreased relative to the diamine (e.g. 1 : 4.5 ratio), the dendron was less able to stabilize this extended fibrillar morphology. Gel-phase materials were still obtained, but it was found that these were underpinned by networks of *micro- or nano-crystalline platelets* (Figure 5.32). It was argued that when sufficient dendron is present, the growth of diamine "crystals" is prevented in two dimensions, giving rise to one-dimensional fibers. However, when the amount of dendron becomes insufficient, it can only prevent growth of diamine "crystals" in one dimension and hence two-dimensional platelets result. Different diamines gave rise to different morphologies (platelet, square, rosette); however, all of them were fundamentally composed of interlocked two-dimensional objects. This demonstrates how two-component gels can provide additional control over nano-fabrication.

Two-component gels have been constructed based on well-known receptors widely used in *molecular recognition*. For example, compound **31** employs a dibenzo-24-

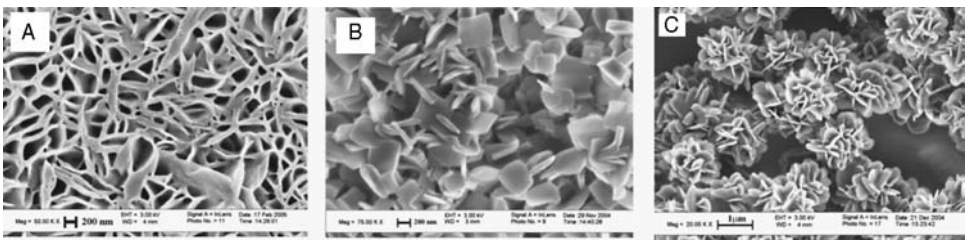

Figure 5.32 SEM images of nanoplatelets formed from different diamines in the case where there is insufficient dendron present to prevent growth of diamine platelet crystals in two dimensions. Adapted from Ref. [21d] with permission of the publishers.

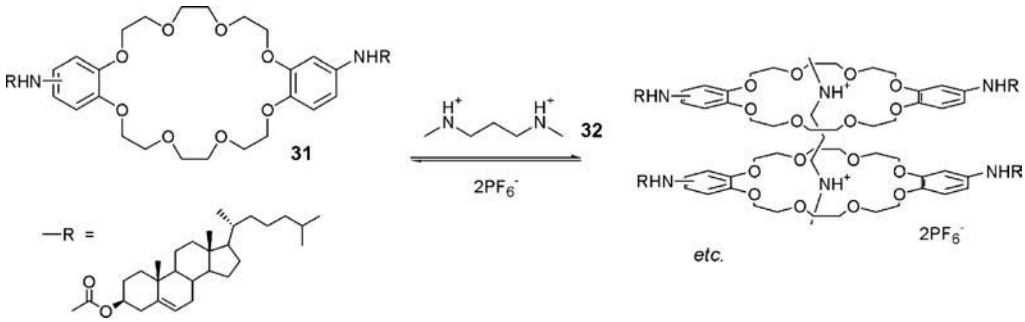

Figure 5.33 Compounds **31** and **32**.

crown-8 building block appended with steroid units [78]. Addition of substrate **32**, capable of binding to the crown ether, was observed to enhance significantly the propensity for gelation (Figure 5.33). It was proposed that molecular recognition induced a conformational change in compound **31** which encouraged the stacking of the steroid units and organization of the hydrogen bonding groups. This indicates how using a two-component approach, gelation can become responsive to specific chemical triggers. Other researchers have also developed gels which respond to the presence of specific ions via a host–guest binding mechanism and such systems have potential in controlled-release applications (Section 5.5.4) [79].

Donor–acceptor π–π interactions have also been employed for the assembly of two-component gels. Bile acid derivative **33**, functionalized with a donor group, formed gels when present in 1:1 stoichiometry with acceptor molecule **34** (Figure 5.34) [80]. UV–Vis spectroscopy indicated the presence of *donor–acceptor interactions*, as the gelation process was accompanied by a substantial increase in the *charge-transfer*

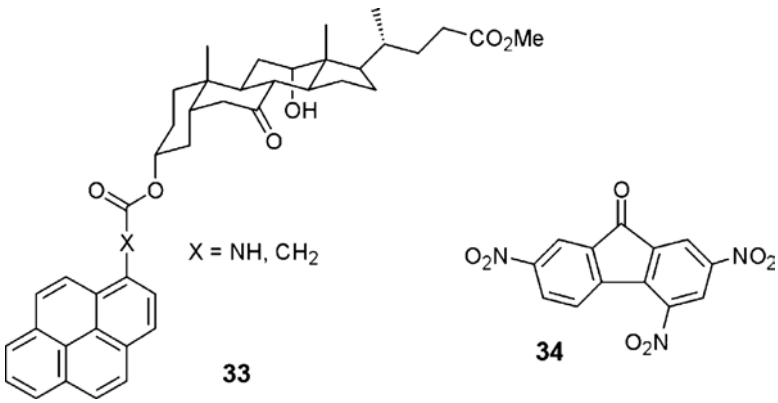

Figure 5.34 Compounds **33** and **34**.

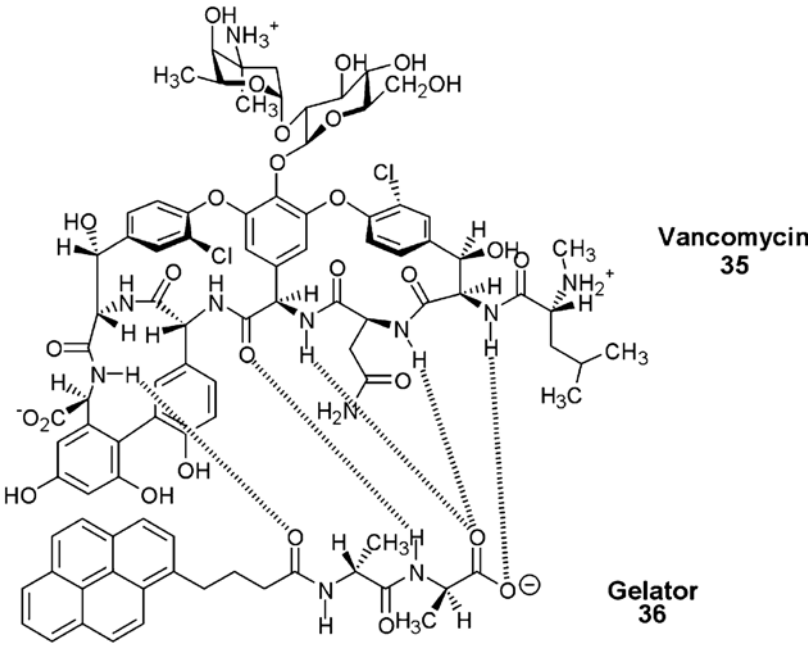

Figure 5.35 Vancomycin **35** triggers the enhanced gelation of compound **36** via host–guest interactions as illustrated.

band. Indeed, whereas the individual components are colorless/pale yellow, the nanostructured assembled gel is brightly colored.

Two-component hydrogels have also been uncovered in recent years. Perhaps one of the most interesting makes use of the medicinally relevant interaction between the antibiotic vancomycin (**35**) and pyrene-functionalized D-Ala,D-Ala derivatives such as **36** (Figure 5.35) [81]. It was demonstrated that the addition of vancomycin to a solution of gelator **36** gave rise to a significant increase in the mechanical strength of the gel – indeed, a dramatic 10^5-fold increase in the storage modulus of the material was reported. SEM investigations demonstrated that vancomycin changed the structure which underpins gelation transforming a self-assembled linear superstructure into a highly crosslinked two-dimensional sheet.

5.5
Applications of Molecular Gels

The endless and subtle synthetic variations which can be made to molecular gelators as illustrated in Section 5.4, means that the resultant materials have vast potential for application in a variety of different areas. The following section aims to provide a brief overview of some current and proposed applications.

5.5.1
Greases and Lubricants

Many *lubricating greases* in everyday commercial use are in fact molecular gels, although perhaps surprisingly, this is not always widely recognized in the recent scientific literature dealing with organogels [82]. In most greases, the "liquid-like" phase or base oil makes up 65–95% of the grease and is composed of hydrocarbons with between 25 and 45 carbon atoms (molecular weights 350–700) and with boiling points between 350 and 500 °C. One of the most commonly applied types of grease, referred to as "lithium grease", is based on a blend of mineral oil and the lithium salt of 12-hydroxystearic acid (HSA) (**20**). Over 50% of the lithium grease market is based on the use of compound **20** as the thickening agent – this compound is obtained from castor oil, with 65% of the world's supply being produced in India. This grease contains a hydrogen bonding OH group, a long alkyl chain (van der Waals interactions) and a charged head group, all of which will assist in the self-assembly process. The fibrillar nature of the self-assemblies formed by these low molecular weight additives is well characterized in the grease literature [83].

5.5.2
Napalm

Unfortunately, napalm, one of the most notorious inventions in the history of mankind, is a gel-phase material [84]. Napalm was originally a mixture of aluminum salts of naphthenic and palmitic acids in petrol and is a *sticky incendiary gel*. Naphthenic acid refers to the mixture of carboxylic acids obtained from crude oil. Palmitic acid is the most common saturated fatty acid found in plants, $C_{15}H_{31}COOH$. Napalm was used in flamethrowers and bombs by the US and Allied forces to increase the effectiveness of flammable liquids by causing them to adhere to materials. When used against human targets, napalm rapidly deoxygenates the available air in addition to creating large amounts of carbon monoxide, causing suffocation. In some cases, napalm incapacitates and kills its victims very quickly, but victims who suffer second-degree burns from splashed napalm will be in significant amounts of pain. Napalm was used in the Second World War by US troops and has also been used in many subsequent military conflicts. Most infamously, napalm was used in the Vietnam war; however, this later version of napalm used a polymer to achieve gelation rather than using low molecular weight compounds.

5.5.3
Tissue Engineering – Nerve Regrowth Scaffolds

On a more positive note, self-assembled gels have recently been of great interest for their ability to act as *biomaterials*. In particular, they can be considered to provide a form of *nanoscaffolding*, which may have uses in tissue engineering [85]. There have been interesting studies investigating nerve growth through gels within animal model systems [86]. In one study, hamsters were surgically blinded by cutting the

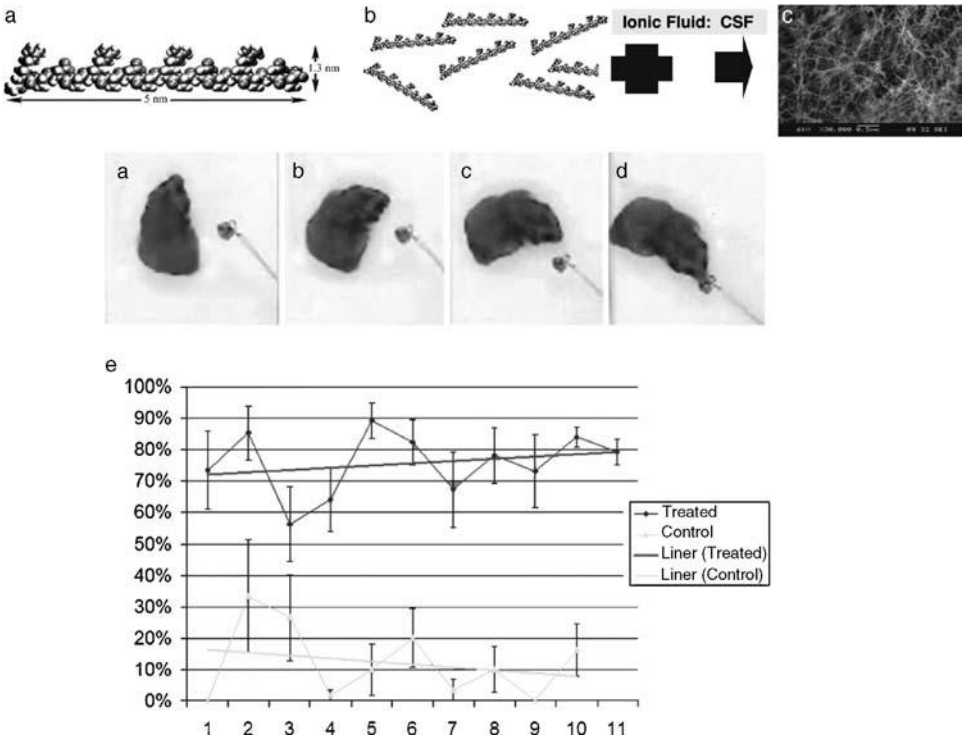

Figure 5.36 Peptide hydrogelator assembles into a fibrillar network as a consequence of hydrophobic and hydrogen bond interactions. When applied to the damaged optic nerve of hamsters with blinding in their right eye, vision is regenerated and the hamster responds to stimulus (a–d). Data (e) indicated that treated hamsters regained ca. 80% of vision, whereas untreated animals regained only 10%. Adapted from Ref. [86] with permission of the National Academy of Sciences of the USA.

optic nerve to one eye. Some of the hamsters then had a self-assembling peptide hydrogel injected in liquid form into the optic nerve – these animals regained ca. 80% of their vision as the nerves regrew through the nanostructured gel matrix (Figure 5.36). Untreated animals remained blind. This demonstrates that this kind of material is compatible with living tissue and has the potential to act as a matrix to encourage the growth of nerve cells.

In a different study, nanofibers have been self-assembled as a result of interactions between synthetic amphiphilic peptide **37** and the polyanionic biopolymer heparin (Figure 5.37) [87]. The nanostructured gel which resulted has been demonstrated to promote the growth of new blood vessels (angiogenesis), a process which is essential in wound healing and will be critical in tissue engineering applications. It is known that heparin binds many of the required angiogenic growth factors. It was argued that immobilization of the heparin as an integral part of the self-assembled nanofiber scaffold should help orient the domains of growth factors, in addition to protecting

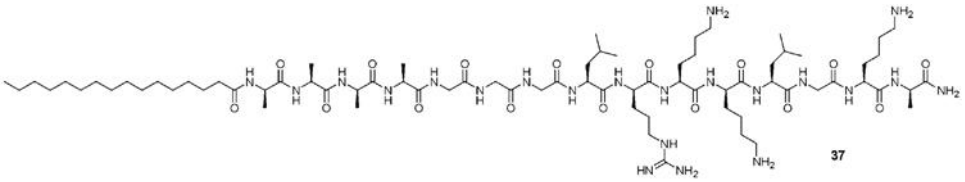

37

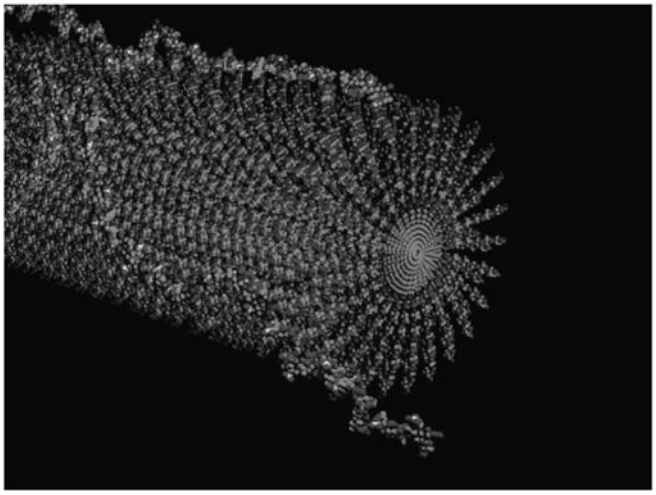

Figure 5.37 Peptide **37** used in tissue engineering studies and a schematic illustration of the way in which heparin can interact with the surface of the self-assembled nano-cylinder. Adapted from Ref. [87] with permission of the American Chemical Society.

them from protease activity – hence promoting angiogenesis – indeed, *in vivo*, these systems stimulated extensive new blood vessel formation. Once again, the fact that the components can self-assemble *in vivo* means that they can easily be delivered by liquid injection.

The fact that molecular hydrogels are based on relatively low molecular weight peptide building blocks means they should be *biocompatible* and furthermore will gradually *degrade in vivo*. Hence, over time, these gels should break down and the degradation products (simple amino acids) are biocompatible. This potential biodegradability is a major advantage of molecular gels over polymeric hydrogels, which are well known in medical applications. Obviously, the long-term stabilities and toxicities of these gels still have to be fully determined, but there is great promise in this area.

5.5.4
Drug Delivery – Responsive Gels

Molecular gels have great potential as drug delivery matrices. Indeed, it is worth noting that a wide range of pharmaceuticals are already *formulated as gels* (normally using

polymeric systems) for oral delivery. Gels can also be subcutaneously injected along with a drug in liquid form and then allowed to gelate *in vivo* [88] for sustained release of a drug by allowing slow diffusion of the drug molecule out of the gel. The rate of release could be controlled depending on whether the drug molecule itself has any *specific interactions* with the gelator fibers (which would inhibit release of the drug). Alternatively, responsive molecular gels can achieve rapid ("burst") delivery of encapsulated drugs as a consequence of going through a gel–sol transition. As has been discussed above, molecular gels can be responsive to a wide range of different *stimuli* – temperature, pH, photoirradiation, ionic and molecular triggers, etc., and as such, the design of responsive drug delivery scaffolds is an area of considerable interest [89].

5.5.5
Capturing (Transcribing) Self-assembled Architectures

Although gels are soft materials, it is possible to try and capture the structures into which they assemble in a more rigid form. In this way, the self-assembled organic nanoarchitecture can be considered to act as a *template* for the formation of an inorganic material. One of the first examples of this approach was the use of compound **38** in the synthesis of nanostructured silica (Figure 5.38) [90]. A gel was formed in a mixture of acetic acid, tetraethyl orthosilicate (TEOS) and water. After 10 days, the solidified material was dried and calcined and was shown to consist of tubular silica. The charged quaternary ammonium salt was essential for encouraging the deposition of the silica onto the gel fibers.

Since this initial report, there have been numerous reports of transcription of organic gel morphologies into silica. Particularly eye-catching has been the generation of spiral/helical silica morphologies using different gelator structures (Figure 5.39) [91]. It has been hypothesized that these nanostructured inorganic or hybrid materials may have applications in enantioselective catalysis or separation.

This approach is not limited to the generation of silica-type materials. Dendron rod-coil molecules have been transcribed into CdS nanohelices [92]. These gelators self-assemble into one-dimensional tape-like objects with a uniform width of 10 nm and lengths up to 10 μm. When these dendron rod-coils were present during the

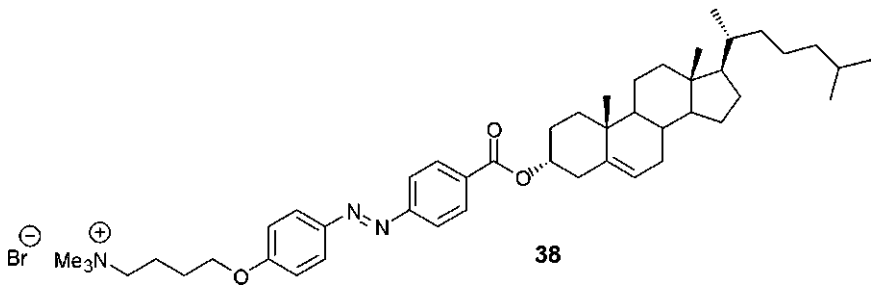

38

Figure 5.38 Compound **38** m used for transcription into silica.

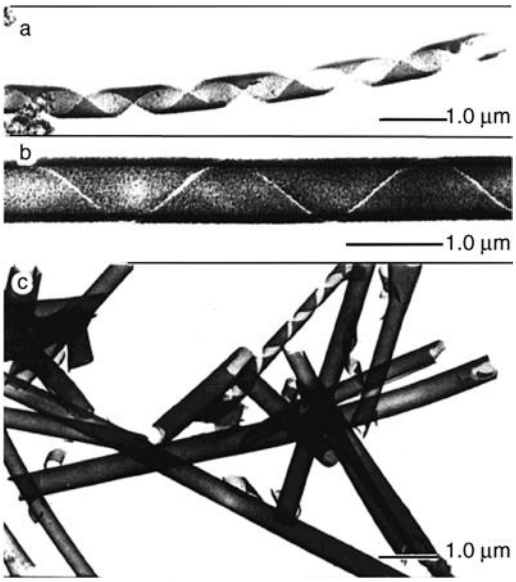

Figure 5.39 Spiral and tubular silica structures created by silica synthesis in the presence of a self-assembled gelator, as imaged by TEM. Reproduced from Ref. [91c] with permission of the American Chemical Society.

synthesis of CdS, they had a direct impact on the morphology of the product – TEM analysis indicated the formation of right- and left-handed helices of CdS, which had been templated on the nanoribbon architecture assembled by the dendron rod-coil. ZnO nanocrystals have also been generated using dendron rod-coils in a similar approach [93]. When these organic–inorganic hybrid assemblies were placed in an electric field, a degree of alignment occurred and these aligned nanocomposites had a lower threshold for lasing behavior than pure ZnO nanocrystals. These results indicate how self-assembly nanofabrication methods can be used to generate *hybrid nanomaterials* with potential photonic applications.

In related studies, gelators have been present during the polymerization of monomers such as styrene or methyl methacrylate. It has been demonstrated that polymerization of these gelated monomers leads to materials which have embedded nanostructures [94]. These *embedded nanostructures* can have a direct impact on the materials properties of the resultant polymer, leading to toughening/hardening effects and, in general terms, this approach may yield new advanced functional materials, in particular if functional gelators can be embedded within the polymer network. Subsequent washing of these nanoembedded polymers can often remove the self-assembled fibers and generate materials that are effectively imprinted by the memory of the nanoscale self-assembled networks [95]. Such *nanoimprinted polymers* have potential applications in catalysis and separation science.

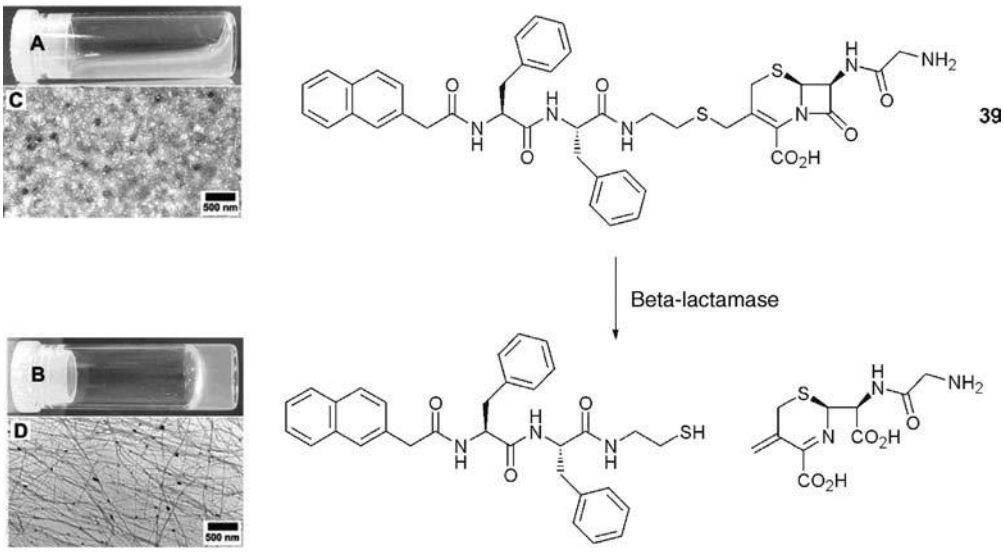

Figure 5.40 Compound **39**, which reacts with β-lactamase enzymes, present in penicillin-resistant bacteria, to generate a more effective gelator. Adapted from Ref. [96] with permission of the American Chemical Society.

5.5.6
Sensory Gels

A recent study has demonstrated the potential of hydrogel materials to act as sensors [96]. Compound **39** is not a gelator in its own right, but can be considered as a latent gelator. This compound includes a β-lactam unit; such structures are important in penicillin-type antibiotic drugs (Figure 5.40). One of the key mechanisms of bacterial resistance to penicillin-type drugs is caused by hydrolysis of the β-lactam ring by β-lactamase enzymes. Compound **39** is therefore also susceptible to β-lactamase enzymes and, in their presence, a chemical conversion takes place which activates the gelator, making it able to form a self-supporting network.

This system, therefore, is capable of *detecting the presence of penicillin-resistant bacteria* by undergoing a sol–gel transition – a clear and easily monitored *sensory response*. It was demonstrated that this system could operate in biological cell lysates and therefore clearly illustrates how gelation can be a useful detection event which can be incorporated into biosensors. The ability to modify the structure of gelators in a precise manner using organic synthesis means that their potential in this field is very high.

5.5.7
Conductive Gels

Given that gel-phase materials are usually underpinned by fibrillar objects, the analogy of these nanoscale structures with "*wires*" is evident. There has therefore

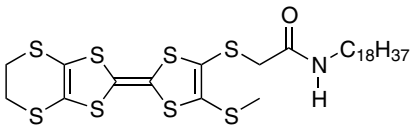

Figure 5.41 Compound **40**.

been considerable interest in the incorporation of conjugated molecular building blocks into gel-phase materials. This can be considered as a bottom-up approach to the construction of well-defined nanoscale wires. Recently, compound **40** has been demonstrated to form gel-phase materials in hexane (Figure 5.41) [97]. Drying the gel on a TEM grid to give the aerogel, followed by doping with iodine vapor and annealing, gave rise to an *electrically conducting thin film*. The hydrogen bond interactions which underpin gelation were essential for organizing the molecular-scale building blocks in order to generate nanowires, which could be visualized by TEM. The self-assembly approach to nanofabrication has considerable potential in the development of *molecular-scale electronics*.

5.6 Conclusions

Gel-phase materials are one of the most intriguing classes of self-assembled material and one of the few systems in which the impact of *synthetic changes made on the molecular level* is clearly evident on the *nanoscale* and furthermore has direct control over *macroscopic materials behavior* visible to the naked eye. This chapter has aimed to provide a "primer" to the area and tried to *highlight key principles* and *emerging themes* in terms of gelator design and applications. There is no doubt that over the coming years, the simplicity of *nanofabrication* using a *self-assembly strategy* will ensure that gel-phase materials are increasingly widely explored. In particular, it seems likely that materials incorporating ever increasing degrees of functional behavior will be developed and for this reason it is predicted that nanochemistry and nanofabrication methods will become dominant themes of new manufacturing industries in the 21st century.

References

1 Whitesides, G.M. (2005) *Small*, **1**, 172–179.

2 For reviews, see (a) Low Molecular Mass Gelators – Design, Self Assembly, Function, F. Fages (ed.), *Top. Curr. Chem.* (2005) p. 256. (b) Terech, P. and Weiss, R.G. (1997) *Chem. Rev.*, **97**, 3133–3159. (c) Gronwald, O., Snip, E. and Shinkai, S. (2002) *Curr. Opin. Colloid Interface Sci.*, **7**, 148–156. (d) Shimizu, T. (2003) *Polym. J.*, **35**, 1–22. (e) Sangeetha, N.M. and Maitra, U. (2005) *Chem. Soc. Rev.*, **34**,

821–836. (f) Smith, D.K. (2007) *Tetrahedron*, **63**, 7283–7284.

3 R.G. Weiss and P. Terech (eds) (2006) *Molecular Gels, Materials with Self-Assembled Fibrillar Networks*, Springer, Dordrecht.

4 Jordan Lloyd, D. (1926) *Colloid Chemistry* (ed. J. Alexander), Chemical Catalog Co., New York, vol. 1, pp. 767–782.

5 (a) Graham, T. (1861) *Philos. Trans. R. Soc. London*, **151**, 183–224. (b) Dean, R.B. (1948) *Modern Colloids*, Van Nostrand, New York, p.2. (c) Hermans, P.H. (1949) *Colloid Science* (ed. H.R. Kruyt), Elsevier, Amsterdam, vol. II, p. 484. (d) Ferry, J.D. (1961) *Viscoelastic Properties of Polymers*, Wiley, New York, p. 391. (e) Flory, P. (1974) *Discuss. Faraday Soc.*, **57**, 7–18. (f) Gelbart, W.M. and Ben-Shaul, A. (1996) *J. Phys. Chem.*, **100**, 13169–13189.

6 (a) Zsigmondy, R. and Batchmann, W. (1912) *Z. Chem. Ind. Kolloide*, **11**, 145–157, this paper indicates that this phenomenon had been recognized since the 19th century. (b) Hatschek, F. (1912) *Z. Chem. Ind. Kolloide*, **11**, 158–165. (c) Hardy, W.B. (1900) *Proc. R. Soc. London*, **66**, 95–109.

7 (a) Brunsveld, L., Folmer, B.J.B., Meijer, E.W. and Sijbesma, R.P. (2001) *Chem. Rev.*, **101**, 4071–4097. (b) Ciferri, A. (ed.) (2005) *Supramolecular Polymers*, Taylor and Francis, Boca Raton, FL.

8 Jonkheijm, P., van der Schoot, P., Schenning, A.P.H.J. and Meijer, E.W. (2006) *Science*, **313**, 80–83.

9 Aggeli, A., Nyrkova, I.A., Bell, M., Harding, R., Carrick, L., McLeish, T.C.B., Semenov, A.N. and Boden, N. (2001) *Proc. Natl. Acad. Sci. USA*, **98**, 11857–11862.

10 Li, Y., Wang, T. and Liu, M. (2007) Tetrahedron, **63**, 7468–7473.

11 For an example, see Trivedi, D.R. and Dastidar, P. (2006) *Chem. Mater.*, **18**, 1470–1478.

12 (a) Hirst, A.R. and Smith, D.K. (2004) *Langmuir*, **20**, 10851–10857. (b) Zhu, G. and Dordick, J.S. (2006) *Chem. Mater.*, **18**, 5988–5995.

13 Raghavan, S.R. and Cipriano, B.H. (2006) 'Gel Formation: Phase Diagrams using Tabletop Rheology and Calorimetry', in *Molecular Gels, Materials with Self-Assembled Fibrillar Networks* (eds. R.G. Weiss and P. Terech), Springer, Dordrecht, Chapter 8.

14 Hirst, A.R., Smith, D.K., Feiters, M.C. and Geurts, H.P.M. (2003) *J. Am. Chem. Soc.*, **125**, 9010–9011.

15 Macosko, C.W. (1994) *Rheology: Principles, Measurements and Applications*, VCH, New York.

16 Takahashi, A., Sakai, M., Kato, T. and Polym, J. (1980) **12**, 335–341.

17 Murata, K., Aoki, M., Suzuki, T., Hanada, T., Kawabata, H., Komori, T., Ohseto, F., Ueda, K. and Shinkai, S. (1994) *J. Am. Chem. Soc.*, **116**, 6664–6676.

18 Sollich, P. (2006) 'Soft Glassy Rheology', in *Molecular Gels, Materials with Self-Assembled Fibrillar Networks* (eds. R.G. Weiss and P. Terech), Springer, Dordrecht, Chapter 5.

19 For an excellent recent example, see Terech, P. and Friol, S. (2007) *Tetrahedron*, **63**, 7366–7374.

20 Wade, R.H., Terech, P., Hewat, E.A., Ramasseul, R. and Volino, F. (1986) *J. Colloid Interface Sci.*, **114**, 442–451.

21 (a) Abdallah, D.J., Sirchio, S.A. and Weiss, R.G. (2000) *Langmuir*, **16**, 7558–7561. (b) Ashbaugh, H.S., Radulescu, A., Prud'homme, R.K., Schwahn, D., Richter, D. and Fetters, L.J. (2002) *Macromolecules*, **35**, 7044–7055. (c) Schmidt, R., Adam, F.B., Michel, M., Schmutz, M., Decher, G. and Mésini, P.J. (2003) *Tetrahedron Lett.*, **44**, 3171–3174. (d) Hirst, A.R., Smith, D.K. and Harrington, J.P. (2005) *Chem. Eur. J.*, **11**, 6552–6559.

22 (a) Anne, M. (2006) 'X-Ray Diffraction of Poorly Organized Systems and Molecular Gels', in *Molecular Gels, Materials with Self-Assembled Fibrillar Networks* (eds R.G. Weiss and P. Terech), Springer, Chapter 11. (b) Glatter, O. and Kratky, O. (eds) (1982) *Small*

Angle X-ray Scattering, Academic Press, London.

23 Kumar, D.K., Jose, D.A. and Das, A. (2004) *Langmuir*, **20**, 10413–10418.

24 For selected examples, see (a) Terech, P., Ostuni, E. and Weiss, R.G. (1996) *J. Phys. Chem.*, **100**, 3759–3766. (b) Jeong, Y., Friggeri, A., Akiba, I., Masunaga, H., Sakurai, K., Sakurai, S., Okamoto, S., Inoue, K. and Shinkai, S. (2005) *J. Colloid Interface Sci.*, **283**, 113–122.

25 Escuder, B., Llusar, M. and Miravet, J.F. (2006) *J. Org. Chem.*, **71**, 7747–7752.

26 Schnell, I. (2005) *Curr. Anal. Chem.*, **1**, 3–27.

27 For a general overview of NMR titration methods in molecular recognition, see (a) Fielding, L. (2000) *Tetrahedron*, **56**, 6151–6170. For examples applied to gels, see (b) Schoonbeek, F.S., van Esch, J.H., Hulst, R., Kellogg, R.M. and Feringa, B.L. (2000) *Chem. Eur. J.*, **6**, 2633–2643. (c) Huang, B., Hirst, A.R., Smith, D.K., Castelletto, V. and Hamley, I.W. (2005) *J. Am. Chem. Soc.*, **127**, 7130–7139.

28 Hirst, A.R., Smith, D.K., Feiters, M.C. and Geurts, H.P.M. (2004) *Langmuir*, **20**, 7070–7077.

29 (a) Becerril, J., Burguette, M.I., Escuder, B., Galindo, F., Gavara, R., Miravet, J.F., Luis, S.V. and Peris, G. (2004) *Chem. Eur. J.*, **10**, 3879–3890. (b) Makarević, J., Jokić, M., Raza, Z., Stefanic, Z., Kojic-Prodic, B. and Žinić, M. (2003) *Chem. Eur. J.*, **9**, 557–5580.

30 (a) Capitani, D., Rossi, E., Segre, A.L., Giustini, M. and Luisi, P.L. (1993) *Langmuir*, **9**, 685–689. (b) Capitani, D., Segre, A.L., Dreher, F., Walde, P. and Luisi, P.L. (1996) *J. Phys. Chem.*, **100**, 15211–15217. (c) Duncan, D.C. and Whitten, D.G. (2000) *Langmuir*, **16**, 6445–6452.

31 Suzuki, M., Nanbu, M., Yumoto, M., Shirai, H. and Hanabusa, K. (2005) *New J. Chem.*, **29**, 1439–1444.

32 (a) Terech, P., Furman, I. and Weiss, R.G. (1995) *J. Phys. Chem.*, **99**, 9558–9566. (b) Geiger, C., Stanescu, M., Chen, L. and Whitten, D.G. (1999) *Langmuir*, **15**, 2241–2245. (c) Ajayaghosh, A. and George, S.J. (2001) *J. Am. Chem. Soc.*, **123**, 5148–5149. (d) Ikeda, M., Takeuchi, M. and Shinkai, S. (2003) *Chem. Commun.*, 1354–1355. (e) Sugiyasu, K., Fujita, N. and Shinkai, S. (2004) *Angew. Chem. Int. Ed.*, **43**, 1229–1233. (f) Desvergne, J.-P., Brotin, T., Meerschaut, D., Clavier, G., Placin, F., Pozzo, J.-L. and Bouas-Laurent, H. (2004) *New J. Chem.*, **28**, 234–247.

33 Kamikawa, Y. and Kato, T. (2007) *Langmuir*, **23**, 274–278.

34 Coates, I.A., Hirst, A.R. and Smith, D.K. (2007) *J. Org. Chem.*, **72**, 3937–3940.

35 Berova, N., Nakanishi, K. and Woody, R.W. (1994) *Circular Dichroism: Principles and Applications*, 2nd edn. Wiley-VCH, Weinheim.

36 Mateos-Timoneda, M.A., Crego-Calama, M. and Reinhoudt, D.N. (2004) *Chem. Soc. Rev.*, **33**, 363–372.

37 Hirst, A.R., Castelletto, V., Hamley, I.W. and Smith, D.K. (2007) *Chem. Eur. J.*, **13**, 2180–2188.

38 (a) Hirst, A.R., Smith, D.K., Feiters, M.C. and Geurts, H.P.M. (2004) *Chem. Eur. J.*, **10**, 5901–5910. (b) Fuhrhop, J.-H., Schnieder, P., Rosenberg, J. and Boekema, E. (1987) *J. Am. Chem. Soc.*, **109**, 3387–3390. (c) Fuhrhop, J.-H., Bedurke, T., Hahn, A., Grund, S., Gatzmann, J. and Riederer, M. (1994) *Angew. Chem. Int. Ed. Engl.*, **33**, 350–351. (d) Jokić, M., Makarević, J. and Žinić, M. (1995) *J. Chem. Soc., Chem. Commun.*, 1723–1724. (e) Bhattacharya, S., Acharya, S.N.G. and Raju, A.R. (1996) *Chem. Commun.*, 2101–2102. (f) Mamiya, J.I., Kanie, K., Hiyama, T., Ikeda, T. and Kato, T. (2002) *Chem. Commun.*, 1870–1871. (g) Boettcher, C., Schade, B. and Fuhrhop, J.-H. (2001) *Langmuir*, **17**, 873–877. (h) Becerril, J., Escuder, B., Miravet, J.F., Gavara, R. and Luis, S.V. (2005) *Eur. J. Org. Chem.*, 481–485. (i) Koga, T., Matsuoka, M. and Higashi, N. (2005) *J. Am. Chem. Soc.*, **127**, 17596–17597.

39 (a) van Gestel, J. (2004) *Macromolecules*, **37**, 3894–3898. (b) van Gestel, J., Palmans,

A.R.A., Titulaer, B., Vekemans, J.A.J.M. and Meijer, E.W. (2005) *J. Am. Chem. Soc.*, **127**, 5490–5494.

40 (a) Singh, A., Burke, T.G., Calvert, J.M., Georger, J.H., Herendeen, B., Price, R.R., Schoen, P.E. and Yager, P. (1988) *Chem. Phys. Lipids*, **47**, 135–148. (b) Yamada, N., Sasaki, T., Murata, H. and Kunitake, T. (1989) *Chem. Lett.*, 205–208. (c) Gulik-Krzywicki, T., Fouquey, C. and Lehn, J.-M. (1993) *Proc. Natl. Acad. Sci. USA*, **90**, 163–167. (d) Messmore, B.W., Sukerkar, P.A. and Stupp, S.I. (2005) *J. Am. Chem. Soc.*, **127**, 7992–7993. (e) Terech, P., Rodriguez, V., Barnes, J.D. and McKenna, G.B. (1994) *Langmuir*, **10**, 3406–3418. (f) Spector, M.S., Selkinger, J.V., Singh, A., Rodriguez, J.M., Price, R.R. and Schnur, J.M. (1998) *Langmuir*, **14**, 3493–3500.

41 Fages, F., Vögtle, F. and Žinić, M. (2005) *Top. Curr. Chem.*, **256**, 77–131.

42 (a) Tomioka, K., Sumiyoshi, T., Narui, S., Nagaoka, Y., Iida, A., Miwa, Y., Taga, T., Nakano, M. and Handa, T. (2001) *J. Am. Chem. Soc.*, **123**, 11817–11818. (b) Hanabusa, K., Tanaka, R., Suzuki, M., Kimura, M. and Shirai, H. (1997) *Adv. Mater.*, **9**, 1095–1097; (c) Luo, X., Li, C. and Liang, Y. (2000) *Chem. Commun.*, 2091–2092. (d) van Gorp, J.J., Vekemans, J.A.J.M. and Meijer, E.W. (2002) *J. Am. Chem. Soc.*, **124**, 14759–14769.

43 Hanabusa, K., Yamada, M., Kimura, M. and Shirai, H. (1996) *Angew. Chem. Int. Ed. Engl.*, **35**, 1949–1951.

44 (a) Fuhrhop, J.-H., Spiroski, D. and Boettcher, C. (1993) *J. Am. Chem. Soc.*, **115**, 1600–1601. (b) Franceschi, S., de Viguerie, N., Riviere, M. and Lattes, A. (1999) *New J. Chem.*, **23**, 447–452. (c) D'Aléo, A., Pozzo, J.-L., Fages, F., Schmutz, M., Mieden-Gundert, G., Vögtle, F., Caplar, V. and Žinić, M. (2004) *Chem. Commun.*, 190–191. (d) Nakashima, T., Kimizuka, N. (2002) *Adv. Mater.*, **14**, 1113–1116. (e) Suzuki, M., Yumoto, M., Kimura, M., Shirai, H. and Hanabusa, K. (2003) *Chem. Eur. J.*, **9**, 348–354.

45 Estroff, L.A. and Hamilton, A.D. (2001) *Angew. Chem. Int. Ed.*, **39**, 3447–3450.

46 Frkanec, L., Jokić, M., Makarević, J., Wolsperger, K. and Žinić, M. (2002) *J. Am. Chem. Soc.*, **124**, 9716–9717.

47 Fujita, N. and Shinkai, S. (2006) Design and Function of Low Molecular-Mass Organic Gelator (LMOGs) Bearing Steroid and Sugar Groups, in *Molecular Gels, Materials with Self-Assembled Fibrillar Networks* (eds R.G. Weiss and P. Terech), Springer, Dordrecht, Chapter 15.

48 (a) Kiyonaka, S., Sugiyasu, K., Shinkai, S. and Hamachi, I. (2002) *J. Am. Chem. Soc.*, **124**, 10954–10955. (b) Kiyonaka, S., Shinkai, S. and Hamachi, I. (2003) *Chem. Eur. J.*, **9**, 976–983.

49 (a) Meunier, M.J. (1891) *Ann. Chim. Phys.*, **22**, 412. (b) Yamamoto, S. (1942) *Kogyou Kagaku Zasshi*, **45**, 695. (c) Yamamoto, S. (1943) *J. Chem. Soc. Jpn., Ind. Chem. Sect.*, **46**, 779.

50 Mohmeyer, N., Wang, P., Schmidt, H.-W., Zakeeruddin, S.M. and Grätzel, M. (2004) *J. Mater. Chem.*, **14**, 1905–1909.

51 See, for example, (a) James, T.D., Murata, K., Harada, T., Ueda, K. and Shinkai, S. (1994) *Chem. Lett.*, 273–276. (b) Amanokura, N., Yoza, K., Shinmori, H. and Shinkai, S. (1998) *J. Chem. Soc., Perkin Trans.*, **2**, 2585–2591. (c) Yoza, K., Amanokura, N., Ono, Y., Akao, T., Shinmori, H., Takeuchi, M., Shinkai, S. and Reinhoudt, D.N. (1999) *Chem. Eur. J.*, **5**, 2722–2729. (d) Luboradzki, R., Gronwald, O., Ikeda, M., Shinkai, S. and Reinhoudt, D.N. (2000) *Tetrahedron*, **56**, 9595–9599.

52 (a) Pfannemuller, B. and Welte, W. (1985) *Chem. Phys. Lipids*, **37**, 227–240. (b) Fuhrhop, J.-H., Schnieder, P., Rosenberg, J. and Boekema, E. (1987) *J. Am. Chem. Soc.*, **109**, 3387–3390. (c) Bhattacharya, S. and Acharya, S.N.G. (1999) *Chem. Mater.*, **11**, 3504–3511.

53 Kobayashi, H., Friggeri, A., Koumoto, K., Amaike, M., Shinkai, S. and Reinhoudt, D.N. (2002) *Org. Lett.*, **4**, 1423–1426.

54 Žinić, M., Vögtle, F. and Fages, F. (2005) *Top. Curr. Chem.*, **256**, 39–76.

55 (a) Martin-Borret, O., Ramasseul, R. and Rassat, R. (1979) *Bull. Soc. Chim. Fr.*, **7–8**, II-401. (b) Terech, P., Ramasseul, R. and Volino, F. (1983) *J. Colloid Interface Sci.*, **91**, 280–282. (c) Terech, P. (1985) *J. Colloid Interface Sci.*, **107**, 244–255.

56 (a) Lin, Y.-c. and Weiss, R.G. (1987) *Macromolecules*, **20**, 414–417. (b) Lin, Y.-c., Kachar, B. and Weiss, R.G. (1989) *J. Am. Chem. Soc.*, **111**, 5542–5551. (c) Mukkamala, R. and Weiss, R.G. (1995) *J. Chem. Soc., Chem. Commun.*, 375–376. (d) Mukkamala, R. and Weiss, R.G. (1996) *Langmuir*, **12**, 1474–1482.

57 Murata, K., Aoki, M., Suzuki, T., Harada, T., Kawabata, H., Komori, T., Ohseto, F., Ueda, K. and Shinkai, S. (1994) *J. Am. Chem. Soc.*, **116**, 6664–6676.

58 (a) Schryver, S.B. (1914) *Proc. R. Soc. London, Ser. B*, **87**, 366–374. (b) Sobotka, H. and Czeczowiczka, N. (1958) *J. Colloid Sci.*, **13**, 188–191. (c) Rich, A. and Blow, D.M. (1958) *Nature*, **182**, 423–426.(d) Blow, D.M. and Rich, A. (1960) *J. Am. Chem. Soc.*, **82**, 3566–3571.

59 Maitra, U., Mukhopadhyay, S., Sarkar, A., Rao, P. and Indi, S.S. (2001) *Angew. Chem. Int. Ed.*, **40**, 2281–2283.

60 Araki, K. and Yoshikawa, I. (2005) *Top. Curr. Chem.*, **256**, 133–165.

61 (a) Gottarelli, G., Masiero, S., Mezzina, E., Spada, G.P., Mariani, P. and Recanatini, M. (1998) *Helv. Chim. Acta*, **81**, 2078–2092. (b) Giorgi, T., Grepioni, F., Manet, I., Mariani, P., Masiero, S., Mezzina, E., Pieraccini, S., Saturni, L., Spada, G.P. and Gottarelli, G. (2002) *Chem. Eur. J.*, **8**, 2143–2152. (c) Sato, T., Seko, M., Takasawa, R., Yoshikawa, I. and Araki, K. (2001) *J. Mater. Chem.*, **11**, 3018–3022.

62 Yun, Y.J., Park, S.M. and Kim, B.H. (2003) *Chem. Commun.*, 254–255.

63 Sugiyasu, K., Numata, M., Fujita, N., Park, S.M., Yun, Y.J., Kim, B.H. and Shinkai, S. (2004) *Chem. Commun.*, 1996–1997.

64 (a) Shimizu, T., Iwaura, R., Masuda, M., Hanada, T. and Yase, K. (2001) *J. Am. Chem. Soc.*, **123**, 5947–5955. (b) Shimizu, T. (2002) *Macromol. Rapid Commun.*, **23**, 311–331. (c) Iwaura, R., Yoshida, K., Masuda, M., Yase, K. and Shimizu, T. (2002) *Chem. Mater.*, **14**, 3047–3053.

65 Iwaura, R., Yoshida, K., Masuda, M., Ohnishi-Kameyama, M., Yoshida, M. and Shimizu, T. (2003) *Angew. Chem. Int. Ed.*, **42**, 1009–1012.

66 For a review of G quartets, see (a) Davis, J.T. (2004) *Angew. Chem. Int. Ed.*, **43**, 668–698. For examples, see (b) Ghoussoub, A. and Lehn, J.-M. (2005) *Chem. Commun.*, 5763–5765. (c) Sreenivasachary, N. and Lehn, J.-M. (2005) *Proc. Natl. Acad. Sci. USA*, **102**, 5938–5943.

67 http://nobelprize.org/nobel_prizes/chemistry/laureates/1925/zsigmondy-lecture.pdf.

68 For reviews, see (a) Hirst, A.R. and Smith, D.K. (2005) *Top. Curr. Chem.*, **256**, 237–273. (b) Smith, D.K. (2006) *Adv. Mater.*, **18**, 2773–2778.

69 Smith, D.K., Hirst, A.R., Love, C.S., Hardy, J.G., Brignell, S.V. and Huang, B. (2005) *Prog. Polym. Sci.*, **30**, 220–293.

70 (a) Jang, W.-D., Jiang, D.-L. and Aida, T. (2000) *J. Am. Chem. Soc.*, **122**, 3232–3233. (b) Jang, W.-D. and Aida, T. (2003) *Macromolecules*, **36**, 8461–8469.

71 Love, C.S., Hirst, A.R., Chechik, V., Smith, D.K., Ashworth, I. and Brennan, C. (2004) *Langmuir*, **10**, 6580–6585.

72 (a) Zubarev, E.R., Pralle, M.U., Sone, E.D. and Stupp, S.I. (2001) *J. Am. Chem. Soc.*, **123**, 4105–4106. (b) Zubarev, E.R. and Stupp, S.I. (2002) *J. Am. Chem. Soc.*, **124**, 5762–5773. (c) de Gans, B.J., Wiegand, S., Zubarev, E.R. and Stupp, S.I. (2002) *J. Phys. Chem. B*, **106**, 9730–9736.

73 (a) Newkome, G.R., Baker, G.R., Saunders, M.J., Russo, P.S., Gupta, V.K., Yao, Z.Q., Miller, J.E. and Bouillion, K. (1986) *J. Chem. Soc., Chem. Commun.*, 752–753. (b) Newkome, G.R., Baker, G.R., Arai, S., Saunders, M.J., Russo, P.S., Theriot, K.J., Moorefield, C.N., Rogers, L.E., Miller, J.E., Lieux, T.R., Murray, M.E., Phillips, B. and

Pascal, L. (1990) *J. Am. Chem. Soc.*, **112**, 8458–8465. (c) Newkome, G.R., Moorefield, C.N., Baker, G.R., Behera, R.K., Escamilla, G.H. and Saunders, M.J. (1992) *Angew. Chem. Int. Ed. Engl.*, **31**, 917–919. (d) Yu, K.H., Russo, P.S., Younger, L., Henk, W.G., Hua, D.W., Newkome, G.R. and Baker, G. (1997) *J. Polym. Sci., Polym. Phys. Ed.*, **35**, 2787–2793. (e) Newkome, G.R., Lin, X.F., Yaxiong, C. and Escamilla, G.H. (1993) *J. Org. Chem.*, **58**, 3123–3129.

74 For a review, see Hirst, A.R. and Smith, D.K. (2005) *Chem. Eur. J.*, **11**, 5496–5508.

75 Hanabusa, K., Miki, T., Taguchi, Y., Koyama, T. and Shirai, H. (1993) *J. Chem. Soc., Chem. Commun.*, 1382–1384.

76 (a) Xu, X., Ayyagari, M., Tata, M., John, V.T. and McPherson, G.L. (1993) *J. Phys. Chem.*, **97**, 11350–11353. (b) Tata, M., John, V.T., Waguespack, Y.Y. and McPherson, G.L. (1994) *J. Am Chem. Soc.*, **116**, 9464–9470. (c) Tata, M., John, V.T., Waguespack, Y.Y. and McPherson, G.L. (1994) *J. Phys. Chem.*, **98**, 3809–3817. (d) Simmons, B.A., Taylor, C.E., Landis, F.A., John, V.T., McPherson, G.L., Schwartz, D.K. and Moore, R. (2001) *J. Am. Chem. Soc.*, **123**, 2414–2421. (e) Simmons, B., Li, S.C., John, V.T., McPherson, G.L., Taylor, C., Schwartz, D.K. and Maskos, K. (2002) *Nano Lett.*, **2**, 1037–1042.

77 (a) Partridge, K.S., Smith, D.K., Dykes, G.M. and McGrail, P.T. (2001) *Chem. Commun.*, 319–320. (b) Hirst, A.R., Smith, D.K., Feiters, M.C. and Geurts, H.P.M. (2003) *J. Am. Chem. Soc.*, **125**, 9010–9011. (c) Hirst, A.R. and Smith, D.K. (2004) *Org. Biomol. Chem.*, **2**, 2965–2971. (d) Hardy, J.G., Hirst, A.R., Smith, D.K., Ashworth, I. and Brennan, C. (2005) *Chem. Commun.*, 385–387.

78 Kawano, S., Fujita, N. and Shinkai, S. (2003) *Chem. Commun.*, 1352–1353.

79 (a) Brignell, S.V. and Smith, D.K. (2007) *New J. Chem.*, **31**, 1243–1249. (b) Sohna, J.E.S. and Fages, F. (1997) *Chem. Commun.*, 327–328. (c) Amanokura, N., Kanekiyo, Y., Shinkai, S. and Reinhoudt, D.N. (1999) *J. Chem. Soc., Perkin Trans.*, **2**, 1999–2005. (d) Stanley, C.E., Clarke, N., Anderson, K.M., Elder, J.A., Lenthall, J.T. and Steed, J.W. (2006) *Chem. Commun.*, 3199–3201.

80 (a) Maitra, U., Kumar, P.V., Chandra, N., D'Souza, L.J., Prasanna, M.D. and Raju, A.R. (1999) *Chem. Commun.*, 595–596. (b) Babu, P., Sangeetha, N.M., Vijaykumar, P., Maitra, U., Rissanen, K. and Raju, A.R. (2003) *Chem. Eur. J.*, **9**, 1922–1932.

81 (a) Zhang, Y., Gu, H., Yang, Z. and Xu, B. (2003) *J. Am. Chem. Soc.*, **125**, 13680–13681. (b) Zhang, Y., Yang, Z., Yuan, F., Gu, H., Gao, P. and Xu, B. (2004) *J. Am. Chem. Soc.*, **126**, 15028–15029.

82 For an accessible overview, see Donahue, C.J. (2006) *J. Chem. Educ.*, **83**, 862–869.

83 Dresel, W. and Heckler, R. (2001) Lubricating Greases, in *Lubricants and Lubrications* (eds T. Mang and W. Dresel), Wiley-VCH, Wenheim, Chapter 16.

84 (a) Fieser, L.F., Harris, G.C., Hershberg, E.B., Morgana, M., Novello, F.C. and Putnam, S.T. (1946) *Ind. Eng. Chem.*, **38**, 768–773. (b) Mysels, K.J. (1949) *Ind. Eng. Chem.*, **41**, 1435–1438.

85 (a) Woolfson, D.N. and Ryadnov, M.G. (2006) *Curr. Opin. Chem. Biol.*, **10**, 559–567. (b) Levenberg, S. and Langer, R. (2004) *Curr. Top. Dev. Biol.*, **61**, 113–134.

86 Ellis-Behnke, R.G., Liang, Y.-X., You, S.-W., Tay, D.K.C., Zhang, S., So, K.-F. and Schneider, G.E. (2006) *Proc. Natl. Acad. Sci. USA*, **103**, 5054–5059.

87 Rajangam, K., Behanna, H.A., Hui, M.J., Han, X., Hulvat, J.F., Lomasney, J.W. and Stupp, S.I. (2006) *Nano Lett.*, **6**, 2086–2090.

88 Chitkara, D., Shikanov, A., Kumar, N. and Domb, A.J. (2006) *Macromol. Biosci.*, **6**, 977–990.

89 de Jong, J.J.D., Feringa, B.L. and van Esch, J. (2006) Responsive Molecular Gels, in *Molecular Gels, Materials with Self-Assembled Fibrillar Networks* (eds R.G. Weiss and P. Terech), Springer, Dordrecht, Chapter 26.

90 Ono, Y., Nakashima, K., Sano, M., Kanekiyo, Y., Inoue, K., Hojo, J. and Shinkai, S. (1998) *Chem. Commun.*, 1477–1478.

91 (a) Ono, Y., Nakashima, K., Sano, M., Hojo, J. and Shinkai, S. (1999) *Chem. Lett.*, 1119–1120. (b) Jung, J.H., Ono, Y. and Shinkai, S. (2000) *Angew. Chem. Int. Ed.*, **39**, 1862–1865. (c) Jung, J.H., Kobayashi, H., Masuda, M., Shimizu, T. and Shinkai, S. (2001) *J. Am. Chem. Soc.*, **123**, 8785–8789. (d) Sugiyasu, K., Tamaru, S., Takeuchi, M., Berthier, D., Huc, I., Oda, R. and Shinkai, S. (2002) *Chem. Commun.*, 1212–1213. (e) Kawano, S.-i., Tamaru, S.-i., Fujita, N. and Shinkai, S. (2004) *Chem. Eur. J.*, **10**, 343–351.

92 Sone, E.D., Zubarev, E.R. and Stupp, S.I. (2002) *Angew. Chem. Int. Ed.*, **41**, 1705–1709.

93 Li, L., Beniash, E., Zubarev, E.R., Xiang, W., Rabatic, B.M., Zhang, G. and Stupp, S.I. (2003) *Nature Mater.*, **2**, 689–694.

94 (a) Zubarev, E.R., Pralle, M.U., Sone, E.D. and Stupp, S.I. (2002) *Adv. Mater.*, **14**, 198–203. (b) Stendahl, J.C., Li, L.M., Zubarev, E.R., Chen, Y.-R. and Stupp, S.I. (2002) *Adv. Mater.*, **14**, 1540–1543. (c) Stendahl, J.C., Zubarev, E.R., Arnold, M.S., Hersam, M.C., Sue, H.J. and Stupp, S.I. (2005) *Adv. Funct. Mater.*, **15**, 487–493.

95 (a) Hafkamp, R.J.H., Kokke, B.P.A., Danke, I.M., Geurts, H.P.M., Rowan, A.E., Feiters, M.C. and Nolte, R.J.M. (1997) *Chem. Commun.*, 545–546. (b) Gu, W., Lu, L., Chapman, G.B. and Weiss, R.G. (1997) *Chem. Commun.*, 543–545. (c) Beginn, U., Keinath, S. and Möller, M. (1998) *Macromol. Chem. Phys.*, **199**, 2379–2384. (d) Beginn, U., Sheiko, S. and Möller, M. (2000) *Macromol. Chem. Phys.*, **201**, 1008–1015. (e) Tan, G., Singh, M., He, J., John, V.T. and McPherson, G.L. (2005) *Langmuir*, **21**, 9322–9326.

96 Yang, Z., Ho, P.-L., Liang, G., Chow, K.H., Wang, Q., Cao, Y., Guo, Z. and Xu, B. (2007) *J. Am. Chem. Soc.*, **129**, 266–267.

97 Puigmartí-Luis, J., Laukhin, V., Pérez del Pino, A., Vidal-Gancedo, J., Rovira, C., Laukhina, E. and Amabilino, D.B. (2007) *Angew. Chem. Int. Ed.*, **46**, 238–241.

6
Nanoporous Crystals, Co-crystals, Isomers and Polymorphs from Crystals

Dario Braga, Marco Curzi, Stefano L. Giaffreda, Fabrizia Grepioni, Lucia Maini, Anna Pettersen, and Marco Polito

6.1
Introduction

Molecules have nanometric dimensions, hence crystal engineering, the intelligent and purposeful assembly of molecules in crystalline structures, falls in the burgeoning field of nanochemistry [1–3]. Crystal engineering [4] is at the intersection of supramolecular chemistry [5,6] (molecular aggregates of higher complexity, "supermolecules") with materials chemistry [7–11] (materials made of molecules, i.e. "molecular materials"). Research in supramolecular chemistry has demonstrated that molecules are convenient nanometer-scale building blocks that can be used, in a bottom-up approach, to construct larger aggregates, whether supermolecules or crystalline materials. The controlled assembly and manipulation of three-dimensional nanostructures with well-defined shapes, profiles and functionalities present a significant challenge to nanotechnology. Since chemists know how to synthesize, characterize and exploit molecular aggregation, the molecular approach to functional nanostructures is a natural development of progress in the field.

Making crystals by design is the paradigm of crystal engineering [12,13], the main goal being that of obtaining *collective* properties from the convolution of the physical and chemical properties of the individual building blocks with crystal periodicity and symmetry. This is also the main objective of nanotechnology because the aggregation via *intermolecular* bonds of the component units (molecules or ions) will determine the nature of the *collective* properties and potential applications. Moreover, if "holes", "channels" or "cavities" are present in the crystalline materials because of the way in which the crystalline scaffold is organized, the size of these empty spaces will have, necessarily, nanometric dimensions. The "bottom-up" construction of such materials requires a crystal engineering approach. This will be the focus of this chapter.

One can envisage two main sub-areas of crystal engineering, namely that of coordination frameworks [14–27] or *periodical coordination chemistry* and that of molecular materials [28–39]. This is a practical subdivision, however, and all possible

Organic Nanostructures. Edited by Jerry L. Atwood and Jonathan W. Steed

ISBN: 978-3-527-31836-0

intermediate situations are possible. The possibility of exploiting metal–organic coordination frameworks (MOFs) for practical applications (such as absorption of molecules and reactions in cavities) critically depends on whether the networks contain large empty spaces [40–46] or are close packed because of interpenetration and self-entanglement. [27,47–50] The possibility of a sponge-like behavior to accommodate/release guest molecules is of paramount importance if applications of coordination networks as molecular reservoirs, traps and sensors are sought [24,51–54].

Whereas in periodical coordination chemistry it is useful to focus on the *knots* and *spacers* in order to describe the topology of the network, when dealing with molecular materials what matters most are the characteristics of the component molecules or ions and the type of interactions (van der Waals, hydrogen bonds, π-stacking, ionic interactions, ion pairs, etc.) holding building blocks together [54–72]. The self-assembly of "zeotype" coordination compounds is an extremely active area of research, especially for the synthesis of metal–organic coordination networks, whether finite (triangles, squares, etc.) [73–76] or infinite networks [27,77–83]. The reader is referred to the many relevant books and reviews on this subject [84–96].

This chapter is devoted to the progress made in our research group in the "bottom-up" construction of crystalline aggregates. In particular, we will describe recent results obtained in the construction of (i) nanoporous coordination network crystals able to uptake/release small molecules, (ii) hybrid organic–organometallic and inorganic–organometallic co-crystals and (iii) isomers and polymorphs of crystals obtained from preformed crystalline materials. In the last section we will discuss the dynamic behavior of crystalline systems under the effect of changing temperature.

6.2
Nanoporous Coordination Network Crystals for Uptake/Release of Small Molecules

As mentioned above, the construction of MOFs takes the "lion's share" of the current efforts in the preparation and exploitation of nanoporous materials. Recently, it has been shown that, in addition to traditional solution chemistry or more forcing hydrothermal conditions, coordination framework structures can also be easily prepared by mechanical methods, i.e. by simple grinding of the component units in the air.

Mechanochemical methods pertain to the domain of organic solid-state chemistry. Pioneering work has been carried out by the groups of Rastogi, Etter, Curtin and Paul [97–103]. More recently, there has been an upsurge of interest in solventless methods as it has become apparent that these methods could be used successfully to prepare supramolecular aggregates, crystalline materials, co-crystals and new crystal forms of a same species (polymorphs and solvates). Remarkable results have also been obtained by Steed, Batten, Raston and coworkers [104–107].

We have explored the preparation of 1-D network structures by co-grinding of transition metal salts and organic dinitrogen base that could be used as *divergent* ligands. In particular *trans*-1,4-diaminocyclohexane, $H_2NC_6H_{10}NH_2$ (dace)

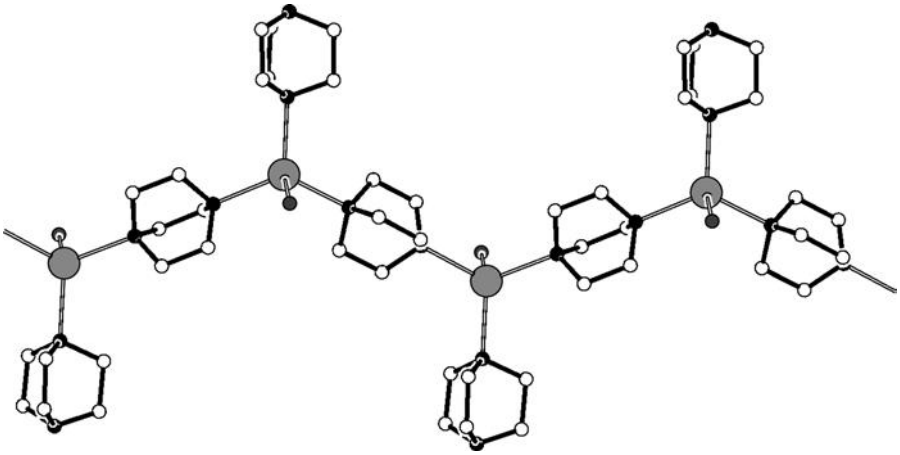

Figure 6.1 The coordination network in Ag[N$(CH_2CH_2)_3N]_2[CH_3COO]\cdot 5H_2O$. Note the chain of $Ag^{(+)}$–[N$(CH_2CH_2)_3N]$–$Ag^{(+)}$–[N$(CH_2CH_2)_3N]$–$Ag^{(+)}$ with each silver cation carrying an extra pendant [N$(CH_2CH_2)_3N]$ ligand and a coordinated water molecule in tetrahedral coordination geometry. H atoms not shown for clarity.

and 1,4-diazabicyclo[2.2.2]octane, $N(CH_2CH_2)_3N$ (dabco), coordination polymer [40–46,108,109], $Ag[N(CH_2CH_2)_3N]_2[CH_3COO]\cdot 5H_2O$, has been prepared by co-grinding of silver acetate and dabco in a 1 : 2 ratio (Figure 6.1).

When $ZnCl_2$ is used instead of $AgCOOCH_3$ in the equimolar reaction with dabco, different products are obtained from the solution and solid-state reactions. Figure 6.2 shows that the structure of $Zn[N(CH_2CH_2)_3N]Cl_2$ is based on a one-dimensional coordination network constituted of alternating $[N(CH_2CH_2)_3N]$ and $ZnCl_2$ units, joined by Zn−N bonds.

More recently, we have applied the same procedure to the solid-state co-grinding of $AgCOOCH_3$ and dace in a 1 : 1 ratio, resulting in the preparation of a crystalline powder tentatively formulated as $Ag[dace][CH_3COO]\cdot xH_2O$ [110]. We have ascertained the formation of different isomers of the same coordination network depending on the preparation and crystallization conditions. The relationship between supramolecular isomerism and network topology has been discussed [6]. Crystallization of the same compound from anhydrous MeOH yields two types of products depending on the solvent evaporation conditions: crystals of $Ag[dace][CH_3COO][MeOH]\cdot 0.5H_2O$ are obtained by crystallization under an argon flow, whereas slow evaporation in the air results in crystals of $Ag[dace][CH_3COO]\cdot 3H_2O$. Structural analysis shows that both of these compounds contain two isomeric forms of the coordination network $\{Ag[dace]^+\}_\infty$. If the same reaction between $AgCOOCH_3$ and dace is carried out directly in MeOH–water solution, a third crystalline material is obtained, namely the tetrahydrate $Ag[dace][CH_3COO]\cdot 4H_2O$. In all cases, correspondence between bulk powder and single crystals was ascertained by comparing computed and observed powder diffractograms. In terms of chemical composition,

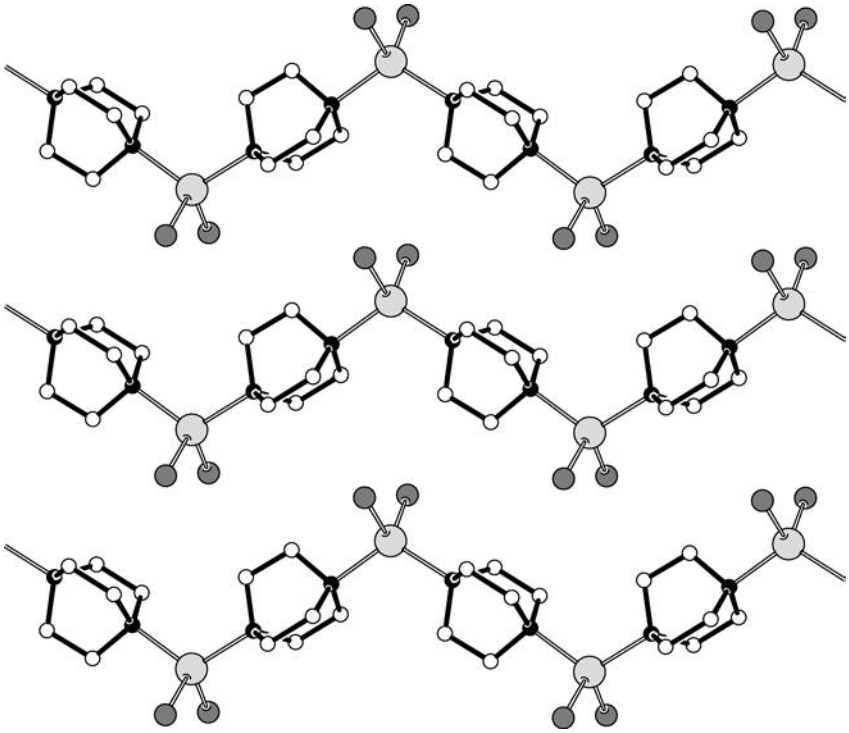

Figure 6.2 The one-dimensional coordination network present in crystals of $Zn[N(CH_2CH_2)_3N]Cl_2$. H atoms not shown for clarity.

the three compounds differ only in the degree and nature of solvation. The differences in topology are, however, much more dramatic and the three compounds must be regarded as isomers of the same basic coordination network. The crystal structure of $Ag[dace][CH_3COO][MeOH]\cdot 0.5H_2O$ is constituted of a two-dimensional coordination network (Figure 6.3) formed by the divergent bidentate dace ligand and two silver atoms, which are joined together by an Ag···Ag bond of length 3.323(1) Å and are asymmetrically bridged by two methanol molecules. There is a close structural relationship between the coordination networks in the $Ag[dace][CH_3COO][MeOH]\cdot 0.5H_2O$ and in the trihydrated compound. This latter structure is built around a zig-zag chain $Ag^{(+)}\cdots[dace]\cdots Ag^{(+)}\cdots[dace]\cdots Ag^{(+)}$ units as shown in Figure 6.3. The Ag atom is coordinated in a linear fashion. A projection perpendicular to the dace planes shows how the zig-zag chains extend in parallel fashion. The $Ag^{(+)}\cdots[dace]\cdots Ag^{(+)}\cdots[dace]\cdots Ag^{(+)}$ chains are bridged together via hydrogen bonds involving the N–H donors, the water molecules and the acetate anions. The tetrahydrated species $Ag[dace][CH_3COO]\cdot 4H_2O$, contains an isomeric form of the coordination networks present in the two former compounds. In the trihydrated compound, two ligands are in a cisoid relative orientation with respect to the silver atom, whereas in the tetrahydrated compound the two ligands adopt a transoid conformation. This is made possible by the different orientation of the N

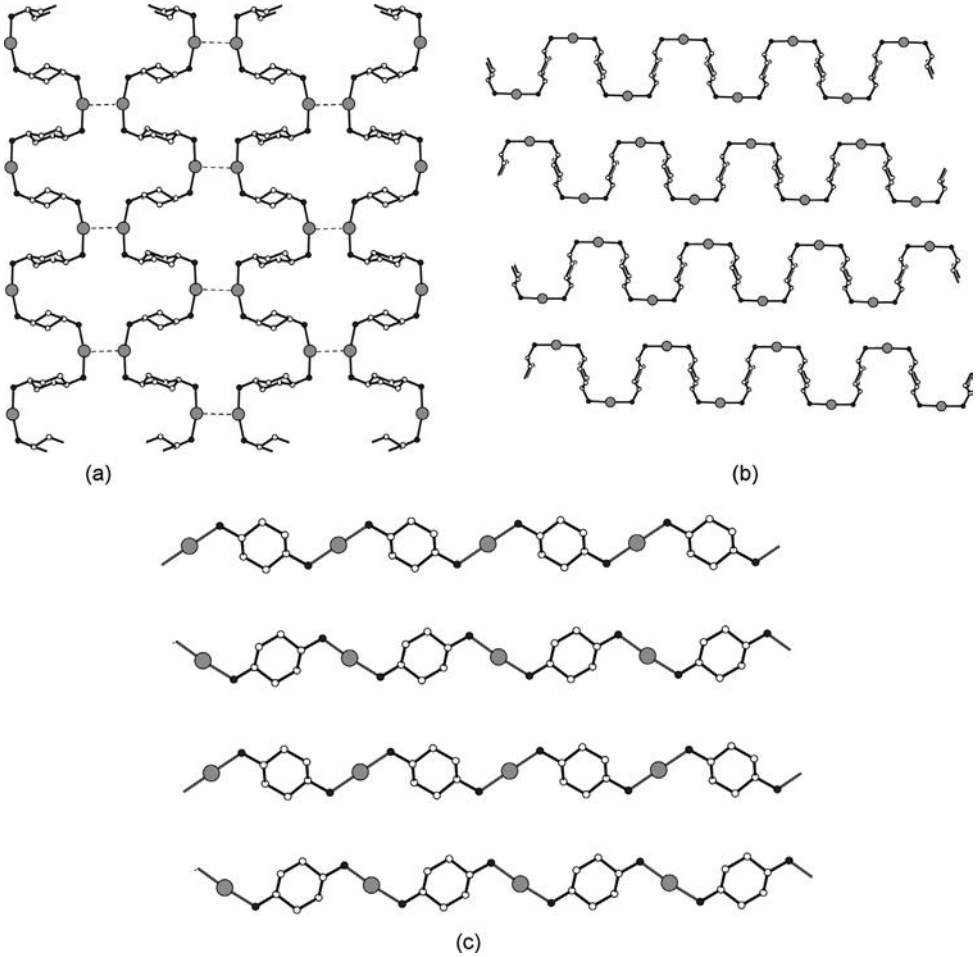

Figure 6.3 Comparison between the isomeric $\{Ag[H_2NC_6H_{10}NH_2]^+\}_\infty$ chains in (a) $Ag[dace][CH_3COO][MeOH]\cdot 0.5H_2O$, (b) $Ag[dace][CH_3COO]\cdot 3H_2O$ and (c) $Ag[dace][CH_3COO]\cdot 4H_2O$.

atom lone pairs in the dace ligand. The acetate anions form a hydrated network and interact with the base and the water molecules.

In a further study of the mechanochemical utilization of dace, we have reported that the compound $[CuCl_2(dace)]_\infty$ can be obtained by thermal treatment of the hydrated compound $[CuCl_2(dace)(H_2O)]_\infty$, which is prepared by *kneading* of solid $CuCl_2$ and dace in the presence of a small amount of water [111]. The structure of $[CuCl_2(dace)]_\infty$ is not known, since it is insoluble in most organic solvents, which does not permit the growth of single crystals of X-ray quality. However, the DMSO adduct $[CuCl_2(dace)(DMSO)]_\infty$ has been fully characterized by single-crystal X-ray diffraction, which gives some insight into the structure of $[CuCl_2(dace)]_\infty$. The DMSO adduct can also be easily obtained by kneading solid $CuCl_2$ and dace in the

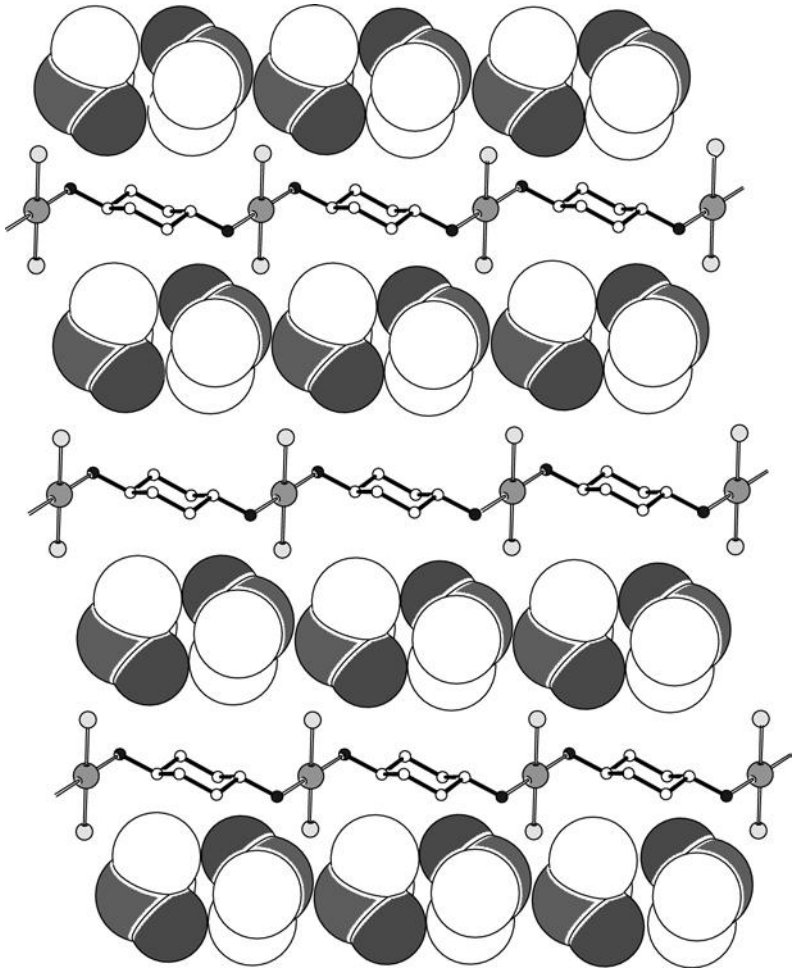

Figure 6.4 A perspective view of the packing of $[CuCl_2(dace)(DMSO)]_\infty$, showing the layers formed by parallel 1D networks of alternating $CuCl_2$ and dace units. H atoms omitted for clarity.

presence of a small amount of DMSO. This compound is formed of 1-D coordination networks, constituted of an alternate sequence of $CuCl_2$ and dace ligands (Figure 6.4). Parallel 1-D $CuCl_2$-dace networks form layers and between the layers, the co-crystallized DMSO is intercalated.

The compound $[CuCl_2(dace)(DMSO)]_\infty$ is interesting in view of its behavior upon thermal treatment. When $[CuCl_2(dace)(DMSO)]_\infty$ is heated to 130°C it converts to $[CuCl_2(dace)]_\infty$, as is easily ascertained by comparing X-ray diffraction powder diffractograms. From the structure of $[CuCl_2(dace)(DMSO)]_\infty$ and from the knowledge of its thermal behavior, it is possible to infer that the structure of $[CuCl_2(dace)]_\infty$ is based on the stacking sequence of layers as in $[CuCl_2(dace)(DMSO)]_\infty$, but "squeezed" at a shorter inter-layer separation as a consequence of DMSO removal.

When a guest molecule enters between the layers, the spacing between the $CuCl_2$–dace chains is expanded and the layers are shifted back in position. A series of small molecules can be taken up/released depending on the preparation method, i.e. kneading, suspension in the liquid guest or kneading followed by suspension. The last approach is the most productive; when suspended in the desired liquid guest the $[CuCl_2(dace)]_\infty$ only takes up relatively small molecules (DMSO, acetone, water, methanol, etc.) whereas in kneading other guest molecules are also taken up. However, if $[CuCl_2(dace)]_\infty$ is first kneaded with a small amount of the desired liquid and then left stirring in the same liquid for 12 h, partial or complete filling of the compound is observed, independently on the guest molecule.

6.3
Hybrid Organic–organometallic and Inorganic-organometallic Co-crystals

Co-crystals are heteromolecular crystals, i.e. molecular crystals constituted of two or more molecular components that are solid at room temperature (to distinguish co-crystals from solvates). The existence of co-crystals is well known, but only recently have they begun to be considered in debates concerning molecular materials mainly because of the claims of their potential interest as pharmaceutical novelties [27].

The formation of co-crystals is possible only when the heteromolecular assembly is more stable than the homomolecular crystals. For this reason, co-crystals are often formed with hydrogen-bonded systems, where the intermolecular hydrogen bonds may afford the additional stabilization required for the co-crystals to form. In fact, the most common way to prepare heteromolecular hydrogen bonded crystals is by mixing (whether in solution of by solid-state grinding) a hydrogen bonding "donor" (usually an acidic species) and a hydrogen bond "acceptor" (usually a base). The mixing of an acid and a base may imply proton transfer from the acid to the base, i.e. protonation, when the pK_a and pK_b values are sufficiently close.

We have exploited the mechanical mixing of solid reactants to prepare novel molecular crystals containing ferrocenyl moieties. It is useful to remember that reactions involving solid reactants or occurring between solids and gases avoid the recovery, storage and disposal of solvents, hence they are of interest in the field of "green chemistry", where environmentally friendly processes are actively sought [112]. Furthermore, solventless reactions often lead to very pure products and reduce the formation of solvate species. In spite of these investigations, solid-state processes involving organometallic systems have only recently begun in a systematic way [113–118].

Manual grinding of the ferrocenyldicarboxylic acid complex $[Fe(\eta^5\text{-}C_5H_4COOH)_2]$ with solid nitrogen-containing bases, namely 1,4-diazabicyclo[2.2.2]octane, 1,4-phenylenediamine, piperazine, *trans*-1,4-cyclohexanediamine and guanidinium carbonate, generates quantitatively the corresponding organic–organometallic adducts (Figure 6.5) [119,120]. The case of the adduct $[HC_6N_2H_{12}][Fe(\eta^5\text{-}C_5H_4COOH)(\eta^5\text{-}C_5H_4COO)]$ is particularly noteworthy, because the same product can be obtained in three different ways: (i) by reaction of solid $[Fe(\eta^5\text{-}C_5H_4COOH)_2]$ with vapor of 1,4-diazabicyclo[2.2.2]octane (which possesses a small but significant vapor

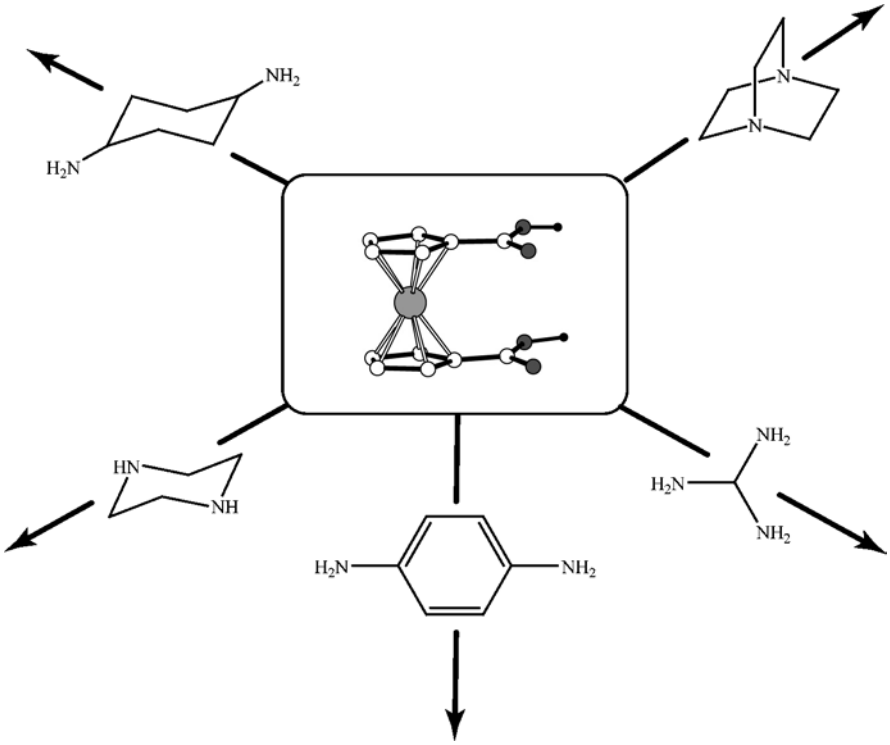

Figure 6.5 Grinding of the organometallic complex [Fe(η^5-$C_5H_4COOH)_2$] as a solid polycrystalline material with the solid bases 1,4-diazabicyclo[2.2.2]octane, guanidinium cation, 1,4-phenylenediamine, piperazine and *trans*-1,4-cyclohexanediamine generates quantitatively the corresponding adducts [$HC_6H_{12}N_2$][Fe(η^5-C_5H_4COOH) (η^5-C_5H_4COO)], [$C(NH_2)_3$]$_2$[Fe(η^5-$C_5H_4COO)_2$]·$2H_2O$, [$HC_6H_8N_2$][Fe(η^5-C_5H_4COOH) (η^5-C_5H_4COO)], [$H_2C_4H_{10}N_2$][Fe (η^5-$C_5H_4COO)_2$] and [$H_2C_6H_{14}N_2$][Fe(η^5-$C_5H_4COO)_2$]·$2H_2O$.

pressure), (ii) by reaction of solid [Fe(η^5-$C_5H_4COOH)_2$] with solid 1,4-diazabicyclo [2.2.2]octane, i.e. by co-grinding of the two crystalline powders, and (iii) by reaction in MeOH solution of the two reactants. It is also interesting to note that the base can be removed by mild treatment, regenerating the structure of the starting dicarboxylic acid.

Bis-substituted pyridine/pyrimidine ferrocenyl complexes have also been obtained by a mechanically induced Suzuki coupling reaction [121] in the solid state starting from the complex ferrocene-1,1′-diboronic acid, [Fe(η^5-C_5H_4-$B(OH)_2)_2$] [122]. The ligand [Fe(η^5-C_5H_4-1-$C_5H_4N)_2$] (**1**), obtained by both solution and solid-state methods, was then used to prepare a whole family of hetero-bimetallic metallomacrocycles by reaction with $AgNO_3$, $Cd(NO_3)_2$, $Cu(CH_3COO)_2$, $Zn(CH_3COO)_2$ and $ZnCl_2$; the complexes [Fe(η^5-C_5H_4-1-$C_5H_4N)_2]_2Ag_2(NO_3)_2$·$1.5H_2O$, [Fe($\eta^5$-$C_5H_4$-1-$C_5H_4N)_2]_2$ $Cu_2(CH_3COO)_4$·$3H_2O$, [Fe(η^5-C_5H_4-1-$C_5H_4N)_2]_2Cd_2(NO_3)_4$· CH_3OH·$0.5C_6H_6$, [Fe (η^5-C_5H_4-1-$C_5H_4N)_2]_2Zn_2(CH_3COO)_4$ and [Fe(η^5-C_5H_4-1-$C_5H_4N)_2]_2Zn_2Cl_4$ were obtained (examples are shown in Figure 6.6) [121]. Reaction of mechanochemically

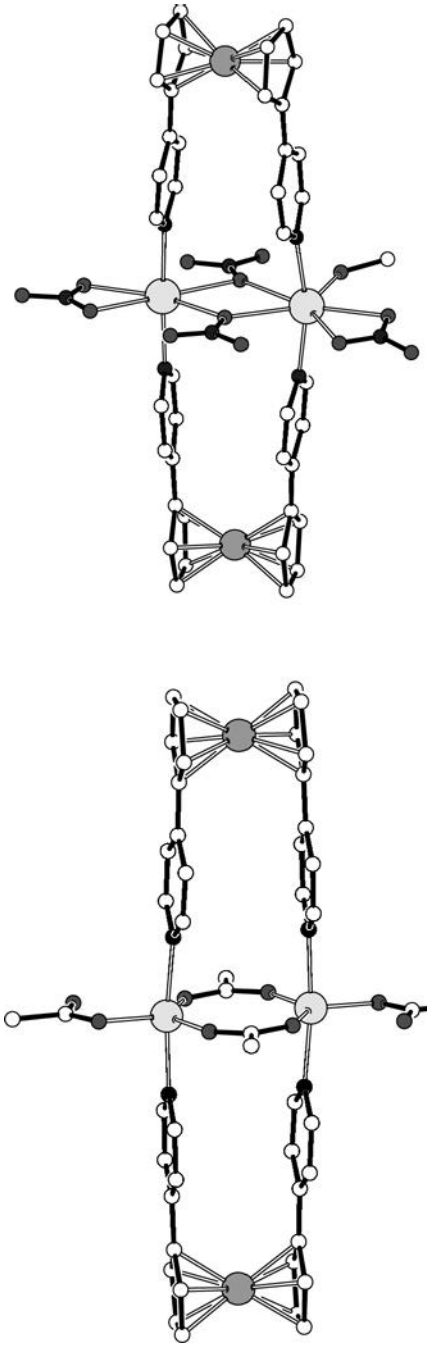

Figure 6.6 The metallomacrocycles produced by reaction of $[Fe(\eta^5\text{-}C_5H_4\text{-}1\text{-}C_5H_4N)_2]$ and the salts $Zn(CH_3COO)_2$ (left) and $Cd(NO_3)_2$ (right). The starting material was obtained by a Suzuki coupling reaction in the solid state starting from the complex ferrocene-1,1′-diboronic acid $[Fe(\eta^5\text{-}C_5H_4\text{-}B(OH)_2)_2]$.

prepared [Fe(η^5-C_5H_4-1-C_5H_4N)$_2$] with the ferrocenyl dicarboxylic acid complex [Fe(η^5-C_5H_4COOH)$_2$] led to the formation of the supramolecular adduct [Fe(η^5-C_5H_4-1-C_5H_4N)$_2$][Fe(η^5-C_5H_4COOH)$_2$] [121].

More recently, the same building block has been used in the preparation of supramolecular metallomacrocycles with dicarboxylic acids of variable aliphatic chain length [123].

The supramolecular macrocyclic adducts of general formula {[Fe(η^5-C_5H_4-C_5H_4N)$_2$]·[HOOC(CH_2)$_n$COOH]}$_2$ with $n = 4$ (adipic acid), $n = 6$ (suberic acid), $n = 7$ (azelaic acid) and $n = 8$ (sebacic acid) have been obtained quantitatively by *kneading* powdered samples of the crystalline organometallic and organic reactants with drops of MeOH (for $n = 4$, 6, 7) and by direct crystallization from MeOH for $n = 8$ (sebacic), whereas the adduct with $n = 5$ (pimelic) represents an isomeric open-chain alternative to the macrocycle. All complexes, with the exception of **1**·pimelic(5), share a common structural feature, namely the formation of supramolecular macrocycles constituted of two organometallic and two organic units linked in large tetramolecular units by O−H···N hydrogen bonds between the –COOH groups of the dicarboxylic acids and the N atom of the ferrocenyl complex. Figure 6.7 shows the structures of **1**·adipic(4), **1**·suberic(6), **1**·azelaic(7) and **1**·sebacic(8). It can be appreciated how the even–odd alternation of carbon atoms in the organic spacers is accommodated by the twist of the cyclopentadienyl-pyridyl groups and by the eclipsed or staggered juxtaposition of the organic moieties

The compounds depicted in Figure 6.7 allow speculation on the *semantics* of these crystal structures: being finite aggregates they cannot be considered as co-crystals but rather as supramolecular systems. On the other hand, they possess a chemical identity and a crystal structure on their own as separate molecules, therefore their solid-state assembly (via *grinding*, incidentally) into the aggregates falls under the broad definition of co-crystals provided above.

The cationic bisamide [Co(η^5-$C_5H_4CONHC_5H_4NH$)$_2$] has been used in the formation of a co-crystal with [Fe(η^5-C_5H_4COOH)$_2$] [124]. In crystalline [Co(η^5-$C_5H_4CONHC_5H_4N$)$_2$][Fe(η^5-C_5H_4COOH)$_2$][PF_6] the two moieties are linked by an O−H···N hydrogen bond forming a sort of dimer (Figure 6.8) reminiscent of that observed in crystalline [Co(η^5-$C_5H_4CONHC_5H_4NH$) (η^5-C_5H_4COO)] [PF_6].

The zwitterion sandwich complex [Co^{III}(η^5-C_5H_4COOH)(η^5-C_5H_4COO)] [86], thanks to its amphoteric behavior, undergoes reversible gas–solid reactions with the hydrated vapors of a variety of acids (e.g. HCl [125], CF_3COOH, CCl_3COOH, CHF_2COOH, HBF_4 and HCOOH) [126–128] and bases (e.g. NH_3, NMe_3 and NH_2Me) [125] and also solid–solid reactions with crystalline alkali metal and ammonium salts of formula MX (M=K^+, Rb^+, Cs^+, NH_4^+; X=Cl^-, Br^-, I^-, PF_6^-) [126]. These products could also be obtained by solution methods, as discussed earlier.

Similar behavior is shown towards other volatile acids. Exposure of the zwitterion to vapors of CF_3COOH and HBF_4, for instance, quantitatively produces the corresponding salts of the cation [Co(η^5-C_5H_4COOH)$_2$]$^+$, viz. [Co(η^5-C_5H_4COOH)$_2$][CF_3COO] and [Co(η^5-C_5H_4COOH)$_2$][BF_4]. Exposure of the solid zwitterion to vapor of CHF_2COOH quantitatively produces the corresponding salts of the cation [Co(η^5-C_5H_4COOH)$_2$][CHF_2COO].

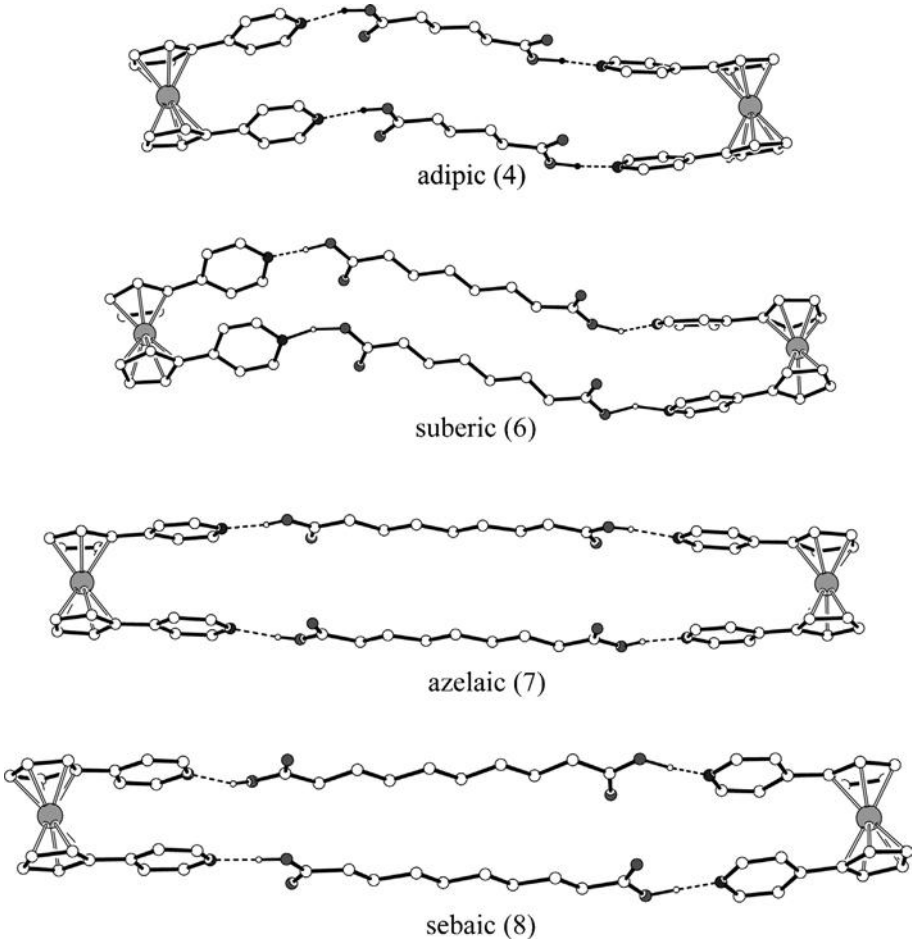

Figure 6.7 The supramolecular structures of the macrocycles **1**·adipic(4), **1**·suberic(6), **1**·azelaic(7) and **1**·sebacic(8) showing the hydrogen bond links between the two outer organometallic molecules and the inner organic spacers.

The zwitterion also reversibly absorbs formic acid from humid vapors, forming selectively a 1 : 1 co-crystal, $[Co(\eta^5\text{-}C_5H_4COOH)(\eta^5\text{-}C_5H_4COO)][HCOOH]$ (Figure 6.9), from which the starting material can be fully recovered by mild thermal treatment. Contrary to the other compounds of this class, no proton transfer from the adsorbed acid to the organometallic moiety has been observed (Figure 6.9). Hence the reaction between $[Co(\eta^5\text{-}C_5H_4COOH)(\eta^5\text{-}C_5H_4COO)]$ (solid) and HCOOH (vapor) would be more appropriately described as a special kind of solvation rather than as a heterogeneous acid–base reaction, as also confirmed by ^{13}C CP/MAS NMR spectroscopy [128].

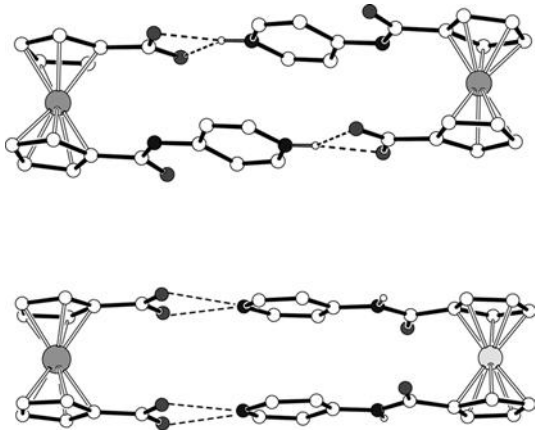

Figure 6.8 (Top) the dimers of $[Co^{III}(\eta^5\text{-}C_5H_4CONHC_5H_4NH)(\eta^5\text{-}C_5H_4COO)][PF_6]$ formed via bifurcate $N-H^{(+)}\cdots O^{(-)}$ hydrogen-bonding interactions [N···O 2.84(2) and 2.88(2) Å]. (Bottom) the ferrocenedicarboxylic acid molecule and the diamido molecule $[Co^{III}(\eta^5\text{-}C_5H_4CONHC_5H_4NH)_2]$ in $[Co^{III}(\eta^5\text{-}C_5H_4CONHC_5H_4N)_2][Fe(\eta^5\text{-}C_5H_4COOH)_2][PF_6]$ are linked via O−H···N hydrogen bonds [N···O 2.52(3) Å].

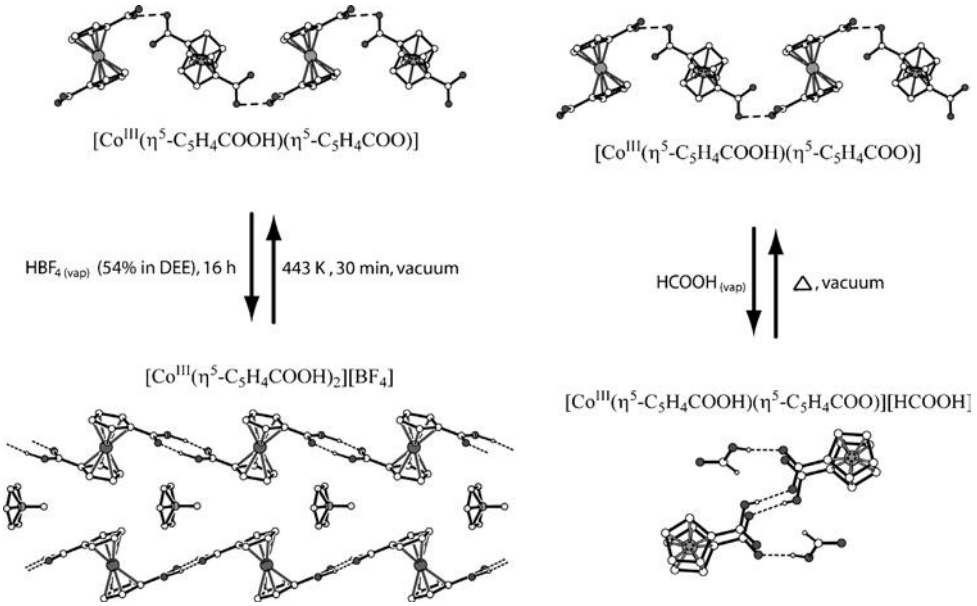

Figure 6.9 (Left) exposure of the solid zwitterion $[Co^{III}(\eta^5\text{-}C_5H_4COOH)(\eta^5\text{-}C_5H_4COO)]$ to vapor of HBF_4 quantitatively produces the corresponding salt $[Co(\eta^5\text{-}C_5H_4COOH)_2][BF_4]$, whereas (right) exposure to vapor of HCOOH yields the co-crystalline material $[Co(\eta^5\text{-}C_5H_4COOH)(\eta^5\text{-}C_5H_4COO)]$ [HCOOH]. Both products revert back to the solid zwitterion after mild thermal treatment.

6.4
Crystal Isomers and Crystal Polymorphs

The phenomenon of polymorphism, viz. the existence of more than one crystal structure for a given compound, is well known and has been widely studied [129,130]. However, the structural, thermodynamic and kinetic factors associated with the nucleation and crystallization of molecular compounds are not yet fully understood. The experimental investigation of crystal polymorphism is still mainly based on a systematic, and sometimes tedious, exploration of all possible crystallization and interconversion conditions [129–131] ("polymorph screening"), while theoretical polymorph prediction is still embryonic [132,133]. The screening of different crystal forms of a compound is not only an academic challenge but also is becoming one of the most important goals in the pharmaceutical industries, since the majority of drugs are administered as solids and solid-state properties significantly influence the bioavailability and stability of the final product. When two or more polymorphs occur, a full characterization of these forms and of the relationship among the different solid phases should be studied, which is best achieved by using complementary techniques such as X-ray diffraction and differential scanning calorimetry combined with IR, Raman and solid-state NMR (SSNMR) spectroscopy.

In the context of this chapter, it is worth discussing a classical case of crystal polymorphism, namely that of the compound 3,4-dicarboxypyridine, also known as cinchomeronic acid [134].

3,4-Dicarboxypyridine is one of the six isomers of the acid pyridinedicarboxylic. All these isomers are widely utilized in the construction of coordination networks, since their metal coordination modes make possible different architectures [135–137]. Furthermore, some of these isomers are biologically active and the acid has been studied for its ability to promote the growth of radishes [138,139].

The structural relationship between the two crystal forms of cinchomeronic acid has been investigated by single-crystal X-ray diffraction, IR, Raman and solid-state NMR spectroscopy, showing that the two polymorphs form a monotropic system, with the orthorhombic form I being the thermodynamically stable form, whereas the monoclinic form II is unstable. In both forms cinchomeronic acid crystallizes as a zwitterion and decomposes before melting. The crystal structure and spectroscopic analysis indicate that the difference in stability can be ascribed to the strength of the hydrogen bonding patterns established by the protonated N atom and the carboxylic/carboxylate O atoms.

Although cinchomeronic acid has been known for almost a century [139] and the presence of two forms has been reported in the PDF-2 [140] database since 1971, no scientific report seems to mention the existence of these two polymorphs. The crystal structure of form **I** (according to the name in PDF-2) was described by Takusagawa et al. in 1973 [141,142].

The molecule is present as a zwitterion both in the solid state and in solution [143], with one acid hydrogen on the ring nitrogen. The presence of different kinds of acceptor and donor groups for hydrogen bonding makes it a worthy candidate for a study of the competition among of different supramolecular synthons that can be

formed [144]. We have fully characterized both forms **I** and **II** by single-crystal X-ray diffraction and spectroscopic methods. Both forms were initially obtained as concomitant [145] polymorphs from an ethanol–water solution.

In a further study, we investigated the behavior of the different crystal forms of barbituric acid ($C_4H_4N_2O_3$) towards basic vapors [146]. The two known crystalline polymorphic forms of barbituric acid ($C_4H_4N_2O_3$) (**I** and **II**) [147,148] and the dihydrate form [$(C_4H_4N_2O_3)\cdot 2H_2O$] [149,150] have been reacted with vapors of ammonia, methylamine and dimethylamine and the crystalline products investigated by means of single-crystal and powder X-ray diffraction, thermogravimetric analysis, differential scanning calorimetry and infrared spectroscopy. It has been shown that forms **I** and **II** and the dihydrate form of barbituric acid react with ammonia leading to the same crystalline ammonium barbiturate salt, $NH_4(C_4H_3N_2O_3)$ (**1a**), whereas the gas–solid reactions of form **II** with methylamine and dimethylamine yield the corresponding crystalline salts, $CH_3NH_3(C_4H_3N_2O_3)$ (**1b**) and $(CH_3)_2NH_2(C_4H_3N_2O_3)$ (**1c**). Thermal desorption of the bases at ca. 200°C leads to formation of a new crystal form of barbituric acid, form **III**, as confirmed by ^{1}H NMR spectroscopy and by its chemical behavior. Dehydration of the dihydrate form has also been investigated, showing that it releases water to yield exclusively crystals of form **II**.

Polymorphism within the barbiturate family is widespread and well studied also in view of the pharmaceutical interest [151–154].

The three crystal forms are easily prepared separately and could thus be used independently in the reaction with gases. A similar experiment has been carried out before by Stowell's group [155] in the course of the investigation of the reactivity of indomethacin amorphous and crystal forms with ammonia. In the case of barbituric acid, the main idea was not only to check whether different crystal forms of the same acidic molecular species reacted in a different way with vapors of the same base but also whether the reverse reactions, namely ammonia desorption, would lead to one of the known crystal form or to the formation of a new polymorph [129,130].

In the first instance, we have discovered that the dihydrate form exclusively transforms upon dehydration into form **II** of barbituric acid. Second, we have shown that all three forms, whether as anhydrous crystals or as the dihydrated form, react in the same way, yielding the same anhydrous barbiturate ammonium salt, **1a**. This analogy in behavior may be taken as an indication that the gas–solid reactions require destruction and reconstruction of the crystal phases and are, therefore, not selective. Form **II** has beeen used in subsequent reactions with vapors of ammonia, methylamine and dimethylamine. In all cases it has been possible to ascertain the rapid formation of the corresponding anhydrous salts in the form of polycrystalline powders. The structures of the salts **1a**, **1b** and **1c** have been investigated by X-ray diffraction experiments on single crystals grown by carrying out the acid–base reaction in solution. In addition to ascertaining the detailed structural features of the salts, the data were used to calculate theoretical powder diffraction patterns for comparison. In all cases, the structures determined by single-crystal X-ray diffraction experiments have been shown to coincide with those of the bulk products.

A related situation has been observed on reacting solid malonic acid, $HOOC(CH_2)COOH$, with solid $N(CH_2CH_2)_3N$ in a 1 : 2 molar ratio [156]. Two different crystal forms of the salt $[HN(CH_2CH_2)_3NH][OOC(CH_2)COOH]_2$ are obtained, depending on the preparation technique (grinding or solution) and crystallization rate. Form **I**, containing monohydrogenmalonate anions forming conventional intramolecular O−H···O hydrogen bonds and interionic N−H···O hydrogen bonds, is obtained by solid-state co-grinding or by rapid crystallization, whereas form **II**, containing *both* intermolecular and intramolecular O−H···O hydrogen bonds, is obtained by slow crystallization (Figure 6.10). Forms **I** and **II** do not interconvert, and form **I** undergoes an order–disorder phase transition on cooling. One can envisage the two crystalline forms as *hydrogen bond isomers* of the same *solid supermolecule*.

Proton transfer along a hydrogen bond poses an interesting question about polymorph definition. In fact, proton mobility along a hydrogen bond [say from

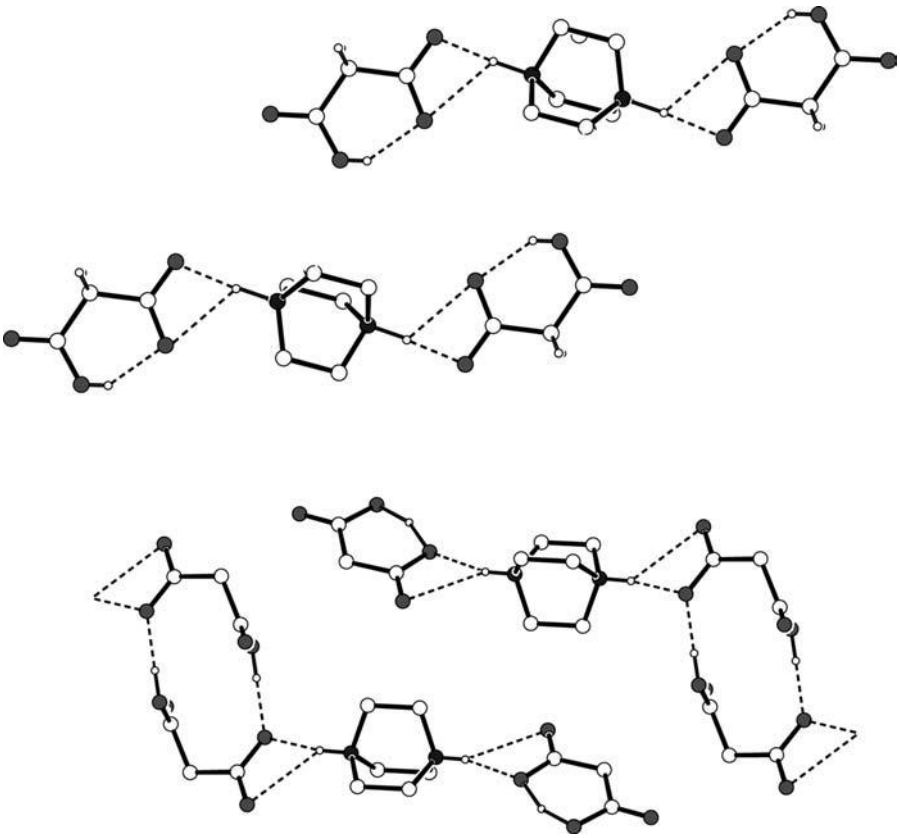

Figure 6.10 Forms **I** (top) and **II** (bottom) of $[HN(CH_2CH_2)_3NH][OOC(CH_2)COOH]_2$ and the hydrogen-bonded anion···cation chains present in their crystals. Form **I** is obtained by solid-state co-grinding or by rapid crystallization, whereas form **II** is obtained by slow crystallization.

O−H···N to $^{(-)}$O···H−N$^{(+)}$] may not be associated with a phase transition, even though it implies the formal transformation of a molecular crystal into a molecular salt. This situation has been observed, for instance, for the proton migration along an O−H···O bond in a co-crystal of urea–phosphoric acid (1 : 1) as a function of temperature [157]. Wiechert and Mootz, on the other hand, have isolated two co-crystals of pyridine and formic acid: in the 1 : 1 co-crystal proton transfer from formic acid to pyridine does not take place, whereas in the 1 : 4 co-crystal N−H$^{(+)}$···O$^{(-)}$ interactions are present [158]. Examples of this kind are rare, but serve to stress how the phenomenon of polymorphism can be, at times, full of ambiguity.

An intriguing case of interconversion between unsolvate and solvate crystals is observed when N(CH$_2$CH$_2$)$_3$N is reacted with maleic acid, HOOC(HC=CH)COOH. The initial product is the anhydrous salt [HN(CH$_2$CH$_2$)$_3$N][OOC(HC=CH)COOH], which contains chains of $^{(+)}$N−H···N$^{(+)}$-bonded [HN(CH$_2$CH$_2$)$_3$N]$^+$ cations and "isolated" [OOC(HC=CH)COOH]$^-$ anions [159]. On exposure to humidity, the anhydrous salt converts within a few hours into the hydrated form [HN(CH$_2$CH$_2$)$_3$N][OOC(HC=CH)COOH]·0.25H$_2$O, which contains more conventional "charge-assisted" $^{(+)}$N−H···O$^{(-)}$ hydrogen bonds between the anion and cation (Figure 6.11). This latter form can also be obtained by co-grinding.

6.5 Dynamic Crystals – Motions in the Nano-world

In a further exploration of the use of mechanochemical methods to prepare hydrogen-bonded nanometric adducts, we have used crown ethers to capture alkali metal cations and the ammonium cation in extended hydrogen-bonded networks formed by hydrogensulfate and dihydrogenphosphate anions [160]. Crown ether complexes have been the subject of a large number of studies because of the interest in ion recognition, complexation and self-assembly processes [6,161–164]. The hydrogensulfate and dihydrogenphosphate salts, on the other hand, have found applications in a number of devices such as H_2 and H_2O sensors, fuel and steam cells and high-energy density batteries [165–168]. Manual co-grinding of solid 18-crown-6 and solid [NH$_4$][HSO$_4$] in air leads to the formation of the crown ether complex 18-crown-6·[NH$_4$][HSO$_4$]·2H$_2$O, the water molecules being taken up from ambient humidity during grinding. In the complex the ammonium cation is trapped via O$_{crown}$···H−N hydrogen bonds by the crown ethers, whereas on the exposed side it interacts with the hydrogensulfate anion (Figure 6.12). The sulfate anion and the water molecules also interact via hydrogen bonding, forming a ribbon that is sandwiched between 18-crown-6·[NH$_4$]$^+$ units. Hydrogen bonds are also observed between water molecules and oxygen atoms in the crown ether. Analogous behavior is shown by the potassium complex 18-crown-6·K[HSO$_4$]·2H$_2$O, which converts into 18-crown-6·K[HSO$_4$] on dehydration and which undergoes, on further heating, enantiotropic solid–solid transitions associated with the onset of a solid-state dynamic process [169].

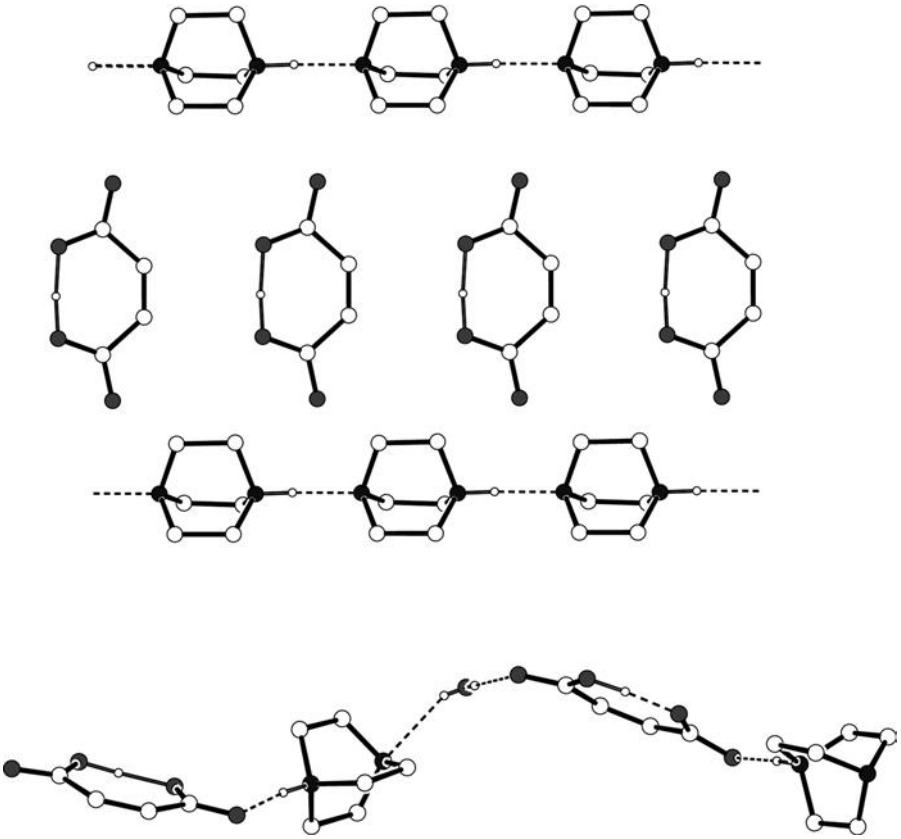

Figure 6.11 Views of the packing and hydrogen bonding in the anhydrous salt $[HN(CH_2CH_2)_3N]$ $[OOC(HC{=}CH)COOH]$ (top) and of the hydrated salt $[HN(CH_2CH_2)_3N][OOC(HC{=}CH)COOH]H_2O_{0.25}$ (bottom).

The crown ether 15-crown-5 is a liquid in room temperature, so when it is kneaded instead of ground, with ammonium hydrogensulfate, a similar reaction as for 18-crown-6 takes place. The product, (15-crown-5)$_3$·$[NH_4]_2[HSO_4]_3$·H_2O, also fully structurally determined by single-crystal X-ray analysis, is also obtained when the reaction takes place in solution. (15-Crown-5)$_3$·$[NH_4]_2[HSO_4]_3$·H_2O is reminiscent of 18-crown-6 because of the formation of hydrogen-bonded ribbons intercalated between the crown ether layers. The difference between the two adducts is, however, the two different types of interactions between the ammonium cation and the crown ether that is present in the 15-crown-5 adduct. One ammonium cation is sandwiched between two crown ether units, whereas the other is linked to the hydrogensulfate anion by N−H···O hydrogen bonds. In the 15-crown-5 adduct a hydrogen-bonded $[H_3O]^+$ ion is also needed to neutralize the overall charge.

More recently, this chemistry has been extended to encompass the investigation of the behavior under thermal treatment of the transition metals complexes 15-crown-5·

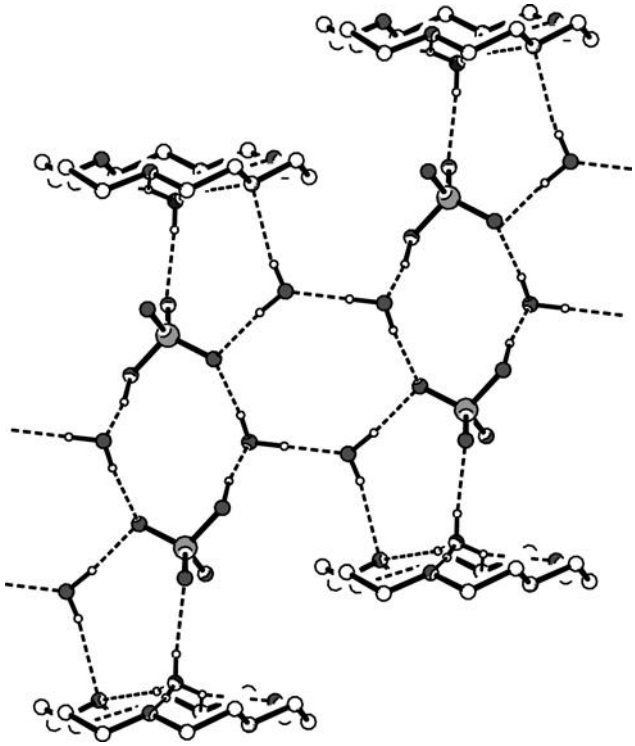

Figure 6.12 The solid-state structure of 18-crown-6·$[NH_4][HSO_4]\cdot 2H_2O$. Note how the crown ether molecules interact via $O_{crown}\cdots H-N$ hydrogen bonds with the ammonium cations, which, in turn, form hydrogen bonds with the hydrogensulfate anions. Two water molecules (per formula unit) contribute to the formation of the central hydrogen-bonded ribbon.

$[Mn(H_2O)_2(HSO_4)_2]$, 15-crown-5·$[Cd(H_2O)_2(HSO_4)_2]$, 15-crown-5·$[(H_7O_3)(HSO_4)_2]\cdot H_2O$, 18-crown-6·$[Pb(HSO_4)_2]$ and 18-crown-6·$[(H_5O_2)(HSO_4)]$, obtained by mechanical mixing or from solution crystallization. It has been shown that the Mo and Cd complexes undergo reversible water release–uptake processes, accompanied by a change in coordination at the metal centers [170].

6.6 Conclusions

In this chapter, we have illustrated, by means of examples coming mainly from our own work, that the basic ideas of crystal engineering belong also to the expanding field of nanochemistry. The possibility of rationally designing and exploring experimentally the construction of nanoporous materials is a valid example. Many research groups world-wide are applying crystal design principles to construct materials for

applications such as sensors, traps and reservoirs. Another area, which we have not touched upon, is that related to nanocomputing, i.e. the use of self-assembly processes to construct addressable nanoarrays based on molecules.

Dealing with molecules, ligands and ions naturally "brings in" the nanometer scale to the scientific strategy, if for no other reason because these chemical entities have nanometric dimensions. Under this premise, the construction of a co-crystal, i.e. the heteromolecular assembly of two or more component units denoted by their own chemical and physical identities, is a nanochemical reaction. The nanochemical reaction may be "mediated" by the formation of hydrogen bonds. Polymorphism, on the other hand, may be seen as nanochemical isomerism, viz. the possibility of different arrangements of the same nano-sized building block in space.

Acknowledgments

We acknowledge financial support from MUR and by the University of Bologna. We thank the Swedish Research Council (VR) and PolyCrystalLine s.r.l. for postdoctoral grants to A.P. and M.C., respectively.

References

1 Ball, P. (1996) *Nature*, **381**, 648.
2 Bryce, M. (1999) *J. Mater. Chem.*, **9**, xi.
3 Ozin, G. and Arsenault, A. (2005) *Nanochemistry: a Chemistry Approach to Nanomaterials*, RSC Publishing, Cambridge, U.K.
4 Braga, D., Grepioni, F. and Orpen, A.G. , (1999) Crystal Engineering: from Molecules and Crystals to Materials.Proceedings of the NATO Advanced Study Institute, held 12–23 May 1999, Erice, Italy. *NATO Sci. Ser., Ser.* 538.
5 Lehn, J.M. (1995) *Supramolecular Chemistry: Concepts and Perspectives*, Wiley-VCH, Weinheim, Germany.
6 Steed, J.W. and Atwood, J.L. (2000) *Supramolecular Chemistry: a Concise Introduction*, Wiley, Chichester, U.K.
7 Lehn, J.-M., Singh, A. and Fouquey, C. (1996) *Polym. Prepr. Am. Chem. Soc. Div. Polym. Chem.*, **37**, 476.
8 Wilson, C.C. (2000) *Single Crystal Neutron Diffraction from Molecular Materials*, World Scientific, Singapore.
9 Coronado, E., Galan-Mascaros, J.R., Gimenez-Saiz, C., Gomez-Garcia, C.J. and Ruiz-Perez, C. (2003) *Eur. J. Inorg. Chem*, 2290.
10 Gatteschi, D. and Sorace, L. (2001) *J. Solid State Chem.*, **159**, 253.
11 Alberola, A., Coronado, E., Galan-Mascaros, J.R., Gimenez-Saiz, C., Gomez-Garcia, C.J. and Romero, F.M. (2003) *Synth. Met.*, **133**, 509.
12 Braga, D. and Grepioni, F. (2006) *Making Crystals by Design*, Wiley-VCH, Weinheim.
13 Desiraju, G. (1989) *Crystal Engeneering: The Design of Organic Solids*, Elsevier, Amsterdam.
14 Blake, A.J., Champness, N.R., Hubberstey, P., Li, W.-S., Withersby, M.A. and Schroder, M. (1999) *Coord. Chem. Rev.*, **183**, 117.
15 Batten, S.R., Hoskins, B.F. and Robson, R. (2000) *Chem. Eur. J.*, **6**, 156.
16 Rather, B. and Zaworotko, M.J. (2003) *Chem. Commun.*, 830.
17 Moulton, B., Abourahma, H., Bradner, M.W., Lu, J., McManus, G.J. and

Zaworotko, M.J. (2003) *Chem. Commun.*, 1342.
18 Fujita, M. (1998) *Chem. Soc. Rev.*, **27**, 417.
19 Olenyuk, B., Fechtenkotter, A. and Stang, P.J. (1998) *J. Chem. Soc., Dalton Trans.*, 1707.
20 Pan, L., Sander, M.B., Huang, X., Li, J., Smith, M., Bittner, E., Bockrath, B. and Johnson, J.K. (2004) *J. Am. Chem. Soc.*, **126**, 1308.
21 Ferey, G., Latroche, M., Serre, C., Millange, F., Loiseau, T. and Percheron-Guegan, A. (2003) *Chem. Commun.*, 2976.
22 Cotton, F.A., Lin, C. and Murillo, C.A. (2001) *J. Chem. Soc., Dalton Trans.*, 499.
23 Cotton, F.A., Lin, C. and Murillo, C.A. (2001) *Chem. Commun.*, 11.
24 Mori, W. and Takamizawa, S. (2000) *J. Solid State Chem.*, **152**, 120.
25 Carlucci, L., Ciani, G., Proserpio, D.M. and Rizzato, S. (2002) *CrystEngComm*, **4**, 121.
26 Lu, J., Moulton, B., Zaworotko, M.J. and Bourne, S.A. (2001) *Chem. Commun.*, 861.
27 Moulton, B. and Zaworotko, M.J. (2001) *Chem. Rev.*, **101**, 1629.
28 Bruce, D.W. and O'Hare, D. (1992) *Inorganic Materials*, Wiley, New York.
29 Long, N.J. (1995) *Angew. Chem. Int. Ed. Engl.*, **34**, 21.
30 Kanis, D.R., Ratner, M.A. and Marks, T.J. (1994) *Chem. Rev.*, **94**, 195.
31 Tucker, M.S., Khan, I., Fuchs-Young, R., Price, S., Steininger, T.L., Greene, G., Wainer, B.H. and Rosner, M.R. (1993) *Brain Res.*, **631**, 65.
32 Gatteschi, D. (1994) *Adv. Mater.*, **6**, 635.
33 Ward, M.D. (2003) *Science*, **300**, 1104.
34 Miller, J.S. (2003) *Angew. Chem. Int. Ed.*, **42**, 27.
35 Vos, T.E., Liao, Y., Shum, W.W., Her, J.H., Stephens, P.W., Reiff, W.M. and Miller, J.S. (2004) *J. Am. Chem. Soc.*, **126**, 11630.
36 Vickers, E.B., Giles, I.D. and Miller, J.S. (2005) *Chem. Mater.*, **17**, 1667.
37 Toma, L., Lescouezec, R., Vaissermann, J., Delgado, F.S., Ruiz-Perez, C., Carrasco, R., Cano, J., Lloret, F. and Julve, M. (2004) *Chem. Eur. J.*, **10**, 6130.
38 Anderson, K.M., Kuendig, E.P., Norman, N.C., Orpen, A.G., Pardoe, J.A.J., Smith, D.W. and Timms, P.L. (2001) *Acta Crystallogr., Sect. E: Struct. Rep. Online*, **E57**, m419.
39 Miller, J.S. and Epstein, A.J. (1995) *Chem. Eng. News*, **73**, 30.
40 Rosi, N.L., Eddaoudi, M., Kim, J., O'Keeffe, M. and Yaghi, O.M. (2002) *Angew. Chem. Int. Ed.*, **41**, 284.
41 Yaghi, O.M., Li, H., Davis, C., Richardson, D. and Groy, T.L. (1998) *Acc. Chem. Res.*, **31**, 474.
42 Li, H., Eddaoudi, M., O'Keeffe, M. and Yaghi, O.M. (1999) *Nature*, **402**, 276.
43 Eddaoudi, M., Kim, J., Rosi, N., Vodak, D., Wachter, J., O'Keeffe, M. and Yaghi, O.M. (2002) *Science*, **295**, 469.
44 Rosi, N.L., Eddaoudi, M., Kim, J., O'Keeffe, M. and Yaghi, O.M. (2002) *CrystEngComm*, **4**, 401.
45 Rosi, N.L., Eckert, J., Eddaoudi, M., Vodak, D.T., Kim, J., O'Keeffe, M. and Yaghi, O.M. (2003) *Science*, **300**, 1127.
46 Braun, M.E., Steffek, C.D., Kim, J., Rasmussen, P.G. and Yaghi, O.M. (2001) *Chem. Commun.*, 2532.
47 Batten, S.R. and Robson, R. (1998) *Angew. Chem. Int. Ed.*, **37**, 1461.
48 Carlucci, L., Ciani, G. and Proserpio, D.M. (2003) *CrystEngComm*, **5**, 269.
49 Carlucci, L., Ciani, G. and Proserpio, D.M. (2003) *Coord. Chem. Rev.*, **246**, 247.
50 Barnett, S.A. and Champness, N.R. (2003) *Coord. Chem. Rev.*, **246**, 145.
51 Benmelouka, M., Messaoudi, S., Furet, E., Gautier, R., Le Fur, E. and Pivan, J.Y. (2003) *J. Phys. Chem. A*, **107**, 4122.
52 Laliberte, D., Maris, T. and Wuest, J.D. (2004) *J. Org. Chem.*, **69**, 1776.
53 Saied, O., Maris, T. and Wuest, J.D. (2003) *J. Am. Chem. Soc.*, **125**, 14956.
54 Biradha, K. (2003) *CrystEngComm*, **5**, 374.
55 Nangia, A. (2002) *CrystEngComm*, **4**, 93.
56 Hosseini, M.W. and De Cian, A. (1998) *Chem. Commun.*, 727.

57 Braga, D. and Grepioni, F. (1996) *Chem. Commun.*, 571.

58 Aakeroy, C.B. and Seddon, K.R. (1993) *Chem. Soc. Rev.*, **22**, 397.

59 Roesky, H.W. and Andruh, M. (2003) *Coord. Chem. Rev.*, **236**, 91.

60 Beatty, A.M. (2003) *Coord. Chem. Rev.*, **246**, 131.

61 Bruton, E.A., Brammer, L., Pigge, F.C., Aakeroey, C.B. and Leinen, D.S. (2003) *New J. Chem.*, **27**, 1084.

62 Braga, D., Grepioni, F., Biradha, K., Pedireddi, V.R. and Desiraju, G.R. (1995) *J. Am. Chem. Soc.*, **117**, 3156.

63 Zaworotko, M.J. (1994) *Chem. Soc. Rev.*, **23**, 283.

64 Calhorda, M.J. (2000) *Chem. Commun.*, 801.

65 Braga, D., Maini, L., Polito, M. and Grepioni, F. (2004) *Struct. Bonding*, **111**, 1.

66 Yang, X.J., Wu, B., Sun, W.H. and Janiak, C. (2003) *Inorg. Chim. Acta*, **343**, 366.

67 George, S., Nangia, A., Bagieu-Beucher, M., Masse, R. and Nicoud, J.-F. (2003) *New J. Chem.*, **27**, 568.

68 Nishio, M. (2004) *CrystEngComm*, **6**, 130.

69 Desiraju, G.R. and Hulliger, J. (2002) *Curr. Opin. Solid State Mater. Sci.*, **6**, 107.

70 Brammer, L., Burgard, M.D., Eddleston, M.D., Rodger, C.S., Rath, N.P. and Adams, H. (2002) *CrystEngComm*, **4**, 239.

71 Brammer, L. (2003) *J. Chem. Soc., Dalton Trans.*, 3145.

72 Burrows, A.D. (2004) in: *Crystal Engineering Using Multiple Hydrogen Bonds*, (ed. D.M.P. Mingos), Vol. 108 p. 55, Springer-Verlag, Berlin and Heidelberg.

73 Philp, D. and Stoddart, J.F. (1996) *Angew. Chem. Int. Ed. Engl.*, **35**, 1155.

74 Holliday, B.J., Arnold, F.P. and Mirkin, C.A. (2003) *J. Phys. Chem. A*, **107**, 2737.

75 Leininger, S., Olenyuk, B. and Stang, P.J. (2000) *Chem. Rev.*, **100**, 853.

76 Fujita, M. (2000) in: Molecular Paneling Through Metal-Directed Self-Assembly, (eds M. Fujita), Vol. 96, 177.

77 Saalfrank, R.W., Maid, H., Hampel, F. and Peters, K. (1999) *Eur. J. Inorg. Chem.*, 1859.

78 Robson, R. (2000) *J. Chem. Soc., Dalton Trans.*, 3735.

79 Eddaoudi, M., Moler, D.B., Li, H., Chen, B., Reineke, T.M., O'Keeffe, M. and Yaghi, O.M. (2001) *Acc. Chem. Res.*, **34**, 319.

80 Evans, O.R. and Lin, W. (2002) *Acc. Chem. Res.*, **35**, 511.

81 Chen, B., Eddaoudi, M., Hyde, S.T., O'Keeffe, M. and Yaghi, O.M. (2001) *Science*, **291**, 1021.

82 Biradha, K. and Fujita, M. (2002) *Angew. Chem. Int. Ed.*, **41**, 3392.

83 Desiraju, G.R. (2001) *Nature*, **412**, 397.

84 Tiekink, E.R.T. and Vittal, J.J. (2005) *Frontiers in Crystal Engineering*, Wiley, New York.

85 Braga, D., Grepioni, F. and Desiraju, G.R. (1998) *Chem. Rev.*, **98**, 1375.

86 Braga, D. (2000) *J. Chem. Soc., Dalton Trans.*, 3705.

87 Braga, D., Desiraju, G.R., Miller, J.S., Orpen, A.G. and Price, S.L. (2002) *CrystEngComm*, **4**, 500.

88 Hollingsworth, M.D. (2002) *Science*, **295**, 2410.

89 Oh, M., Carpenter, G.B. and Sweigart, D.A. (2002) *Organometallics*, **21**, 1290.

90 Oh, M., Carpenter, G.B. and Sweigart, D.A. (2001) *Angew. Chem. Int. Ed.*, **40**, 3191.

91 Oh, M., Carpenter, G.B. and Sweigart, D.A. (2002) *Angew. Chem. Int. Ed.*, **41**, 3650.

92 Oh, M., Carpenter, G.B. and Sweigart, D.A. (2002) *Chem. Commun.*, 2168.

93 Oh, M., Carpenter, G.B. and Sweigart, D.A. (2003) *Organometallics*, **22**, 2364.

94 Oh, M., Carpenter, G.B. and Sweigart, D.A. (2003) *Angew. Chem. Int. Ed.*, **42**, 2026.

95 Oh, M., Carpenter, G.B. and Sweigart, D.A. (2004) *Acc. Chem. Res.*, **37**, 1.

96 Braga, D., Chen, S., Filson, H., Maini, L., Netherton, M.R., Patrick, B.O., Scheffer, J.R., Scott, C. and Xia, W. (2004) *J. Am. Chem. Soc.*, **126**, 3511.

97 Paul, I.C. and Curtin, D.Y. (1973) *Acc. Chem. Res.*, **6**, 217.

98 Chiang, C.C., Lin, C.T., Wang, H.J., Curtin, D.Y. and Paul, I.C. (1977) *J. Am. Chem. Soc.*, **99**, 6303.

99 Desiraju, G.R., Paul, I.C. and Curtin, D.Y. (1977) *J. Am. Chem. Soc.*, **99**, 1594.

100 Patil, A.O., Pennington, W.T., Desiraju, G.R., Curtin, D.Y. and Paul, I.C. (1986) *Mol. Cryst. Liq. Cryst.*, **134**, 279.

101 Etter, M.C. (1991) *J. Phys. Chem.*, **95**, 4601.

102 Ojala, W.H. and Etter, M.C. (1992) *J. Am. Chem. Soc.*, **114**, 10288.

103 Etter, M.C., Reutzel, S.M. and Choo, C.G. (1993) *J. Am. Chem. Soc.*, **115**, 4411.

104 Nichols, P.J., Raston, C.L. and Steed, J.W. (2001) *Chem. Commun.*, 1062.

105 Belcher, W.J., Longstaff, C.A., Neckenig, M.R. and Steed, J.W. (2002) *Chem. Commun.*, 1602.

106 Batten, S.R. (2001) *Curr. Opin. Solid State Mater. Sci.*, **5**, 107.

107 Sun, H.-L., Gao, S., Ma, B.-Q., Su, G. and Batten, S.R. (2005) *Cryst. Growth Des.*, **5**, 269.

108 Stark, J.L., Rheingold, A.L. and Maatta, E.A. (1995) *J. Chem. Soc., Chem. Commun.*, 1165.

109 Eddaoudi, M., Kim, J., Rosi, N., Vodak, D., Wachter, J., O'Keeffe, M. and Yaghi Omar, M. (2002) *Science*, **295**, 469.

110 Braga, D., Curzi, M., Grepioni, F. and Polito, M. (2005) *Chem. Commun.*, 2915.

111 Braga, D., Curzi, M., Johansson, A., Polito, M., Rubini, K. and Grepioni, F. (2006) *Angew. Chem. Int. Ed.*, **45**, 142.

112 Anastas, P. and Warner, J. (1998) *Green Chemistry: Theory and Practice*, Oxford University Press, Oxford.

113 Braga, D., Maini, L., Grepioni, F., Elschenbroich, C., Paganelli, F. and Schiemann, O. (2001) *Organometallics*, **20**, 1875.

114 Tanaka, K. and Toda, F. (2000) *Chem. Rev.*, **100**, 1025.

115 Tanaka, K. (2003) *Solvent-Free Organic Synthesis*, Wiley-VCH, Weinheim, Germany.

116 Rotheberg, G., Downie, A.P., Raston, C.L. and Scott, J.L. (2001) *J. Am. Chem. Soc.*, **123**, 8701.

117 Toda, F. (2002) *CrystEngComm*, **4**, 215.

118 Nassimbeni, L.R. (2003) *Acc. Chem. Res.*, **36**, 631.

119 Braga, D., Maini, L., Polito, M., Mirolo, L. and Grepioni, F. (2003) *Chem. Eur. J.*, **9**, 4362.

120 Braga, D., Maini, L., Polito, M., Mirolo, L. and Grepioni, F. (2002) *Chem. Commun.*, 2960.

121 Braga, D., Polito, M., D'Addario, D., Tagliavini, E., Proserpio, D.M., Grepioni, F. and Steed, J.W. (2003) *Organometallics*, **22**, 4532.

122 Braga, D., Polito, M., Bracaccini, M., D'Addario, D., Tagliavini, E., Sturba, L. and Grepioni, F. (2003) *Organometallics*, **22**, 2142.

123 Braga, D., Giaffreda, S.L. and Grepioni, F. (2006) *Chem. Commun.*, 3877.

124 Braga, D., Polito, M. and Grepioni, F. (2004) *Cryst. Grow. Des.*, **4**, 769.

125 Braga, D., Cojazzi, G., Emiliani, D., Maini, L. and Grepioni, F. (2001) *Chem. Commun.*, 2272.

126 Braga, D., Cojazzi, G., Emiliani, D., Maini, L. and Grepioni, F. (2002) *Organometallics*, **21**, 1315.

127 Braga, D., Maini, L., Mazzotti, M., Rubini, K. and Grepioni, F. (2003) *CrystEngComm*, **5**, 154.

128 Braga, D., Maini, L., Mazzotti, M., Rubini, K., Masic, A., Gobetto, R. and Grepioni, F. (2002) *Chem. Commun.*, 2296.

129 Bernstein, J. (2002) *Polymorphism in Molecular Crystals*, Oxford University Press, Oxford.

130 Brittain, H.G. (1999) *Drugs Pharm. Sci.*, **95**, 227.

131 Hilfiker, R. (2006) *Polymorphism*, Wiley-VCH, Weinheim.

132 Day, G.M., Motherwell, W.D.S., Ammon, H.L., Boerrigter, S.X.M., Della Valle, R.G., Venuti, E., Dzyabchenko, A. Dunitz, J.D., Schweizer, B., van Eijck, B.P., Erk, P., Facelli, J.C., Bazterra, V.E., Ferraro, M.B., Hofmann, D.W.M., Leusen, F.J.J., Liang, C., Pantelides, C.C., Karamertzanis, P.G., Price, S.L., Lewis, T.C., Nowell, H., Torrisi, A., Scheraga, H.A., Arnautova, Y.A.,

Schmidt, M.U. and Verwer, P. (2005) *Acta Crystallogr., Sect. B: Struct. Sci.*, **B61**, 511.
133 Datta, S. and Grant David, J.W. (2004) *Nat. Rev. Drug Discov.*, **3**, 42.
134 Michele, L.M.C.F.P.T. and Dario Braga, R.C.R.G. (2007) *Chem. Eur. J.*, **13**, 1222.
135 Tong, M.-L., Wang, J., Hu, S. and Batten, S.R. (2005) *Inorg. Chem. Commun.*, **8**, 48.
136 Tong, M.-L., Wang, J. and Hu, S. (2005) *J. Solid State Chem.*, **178**, 1518.
137 Senevirathna, M.K.I., Pitigala, P.K.D.D.P., Perera, V.P.S. and Tennakone, K. (2005) *Langmuir*, **21**, 2997.
138 Nishitani, H., Nishitsuji, K., Okumura, K. and Taguchi, H. (1996) *Phytochemistry*, **42**, 1.
139 Taguchi, H., Maeda, M., Nishitani, H., Okumura, K., Shimabayashi, Y. and Iwai, K. (1992) *Biosci. Biotechnol. Biochem.*, **56**, 1921.
140 PDF-2 Release (2005) *International Centre for Diffraction Data*, Newtown Square, PA, U.S.A.
141 Griffiths, P.J.F. (1963) *Acta Crystallogr.*, **16**, 1074.
142 Takusagawa, F., Hirotsu, K. and Shimada, A. (1973) *Bull. Chem. Soc. Jpn.*, **46**, 2669.
143 Harmon, K.M. and Shaw, K.E. (1999) *J. Mol. Struct.*, **513**, 219.
144 Vishweshwar, P., Nangia, A. and Lynch, V.M. (2002) *J. Org. Chem.*, **67**, 556.
145 Bernstein, J., Davey, R.J. and Henck, J.-O. (1999) *Angew. Chem. Int. Ed.*, **38**, 3441.
146 Braga, D., Cadoni, M., Grepioni, F., Maini, L. and Rubini, K. (2006) *CrystEngComm*, **8**, 756.
147 Lewis, T.C., Tocher, D.A. and Price, S.L. (2004) *Cryst. Growth Des.*, **4**, 979.
148 Bolton, W. (1963) *Acta Crystallogr.*, **16**, 166.
149 Jeffrey, G.A., Ghose, S. and Warwicker, J.O. (1961) *Acta Crystallogr.*, **14**, 881.
150 Al-Karaghouli, A.R., Abdul-Wahab, B., Ajaj, E. and Al-Asaff, S. (1977) *Acta Crystallogr., Sect. B: Struct. Sci.*, **B33**, 1655.
151 Lewis, T.C., Tocher, D.A. and Price, S.L. (2005) *Cryst. Grow. Des.*, **5**, 983.
152 Cleverley, B. and Williams, P.P. (1959) *Tetrahedron*, **7**, 277.
153 Caillet, J. and Claverie, P. (1980) *Acta Crystallogr., Sect. B: Struct. Sci.*, **B36**, 2642.
154 Bojarski, J.T., Mokrosz, J.L., Barton, H.J. and Paluchowska, M.H. (1985) *Adv. Heterocycl. Chem.*, **38**, 229.
155 Chen, X., Morris, K.R., Griesser, U.J., Byrn, S.R. and Stowell, J.G. (2002) *J. Am. Chem. Soc.*, **124**, 15012.
156 Braga, D. and Maini, L. (2004) *Chem. Commun.*, 976.
157 Wilson, C.C. (2001) *Acta Crystallogr., Sect. B: Struct. Sci.*, **B57**, 435.
158 Wiechert, D. and Mootz, D. (1999) *Angew. Chem. Int. Ed.*, **38**, 1974.
159 Braga, D., Rubini, K. and Maini, L. (2004) *CrystEngComm*, **6**, 236.
160 Braga, D., Curzi, M., Lusi, M. and Grepioni, F. (2005) *CrystEngComm*, **7**, 276.
161 Calleja, M., Mason, S.A., Prince, P.D., Steed, J.W. and Wilkinson, C. (2003) *New J. Chem.*, **27**, 28.
162 Junk, P.C., McCool, B.J., Moubaraki, B., Murray, K.S., Spiccia, L., Cashion, J.D., Steed, J.W. (2002) *J. Chem. Soc., Dalton Trans.*, 1024.
163 Atwood, J.L., Holman, K.T. and Steed, J.W. (1996) *Chem Commun.*, 1401.
164 Steed, J.W. (2001) *Coord. Chem. Rev.*, **215**, 171.
165 Lipkowski, J., Baranowski, B. and Lunden, A. (1993) *Pol. J. Chem.*, **67**, 1867.
166 Haile, S.M. (1999) *Mater. Res. Soc. Symp. Proc.*, **547**, 315.
167 Haile, S.M., Boysen, D.A., Chisholm, C.R.I. and Merle, R.B. (2001) *Nature*, **410**, 910.
168 Chisholm, M.H. and Hollandsworth, C.B. (2005) *Multiple Bonds Between Metal Atoms*, 3rd edn. p. 203, Springer-Verlag, Berlin and Heidelberg.
169 Braga, D., Gandolfi, M., Lusi, M., Paolucci, D., Polito, M., Rubini, K. and Grepioni, F. (2007) *Chem. Eur. J.*, **13**, 5249.
170 Braga, D., Gandolfi, M., Lusi, M., Polito, M., Rubini, K. and Grepioni, F. (2007) *Cryst. Grow. Des.*, **7** (5), 919–924.